Augmenting L1 Adaptive Control of Piecewise Constant Type to Aerial Vehicles

Pettersson, Anders

2013

Document Version:
Publisher's PDF, also known as Version of record

Augmenting L1 Adaptive Control of Piecewise Constant Type to Aerial Vehicles

Anders Pettersson

Department of Automatic Control
Lund University
Lund, Sweden

Department of Automatic Control
Lund University
Box 118
SE-221 00 LUND
Sweden

ISSN 0280-5316
ISRN LUTFD2/TFRT--3262—SE

Printed in Sweden by Media Tryck.
Lund 2013

Abstract

In aerial vehicle control design, the industrial baseline is to use robust control methods together with gain-scheduling to cover the full airspeed and altitude flight envelope. An adaptive controller could possibly add value by increasing performance while keeping robustness to deviation from nominal assumptions.

In this thesis *L1 adaptive control* is studied and evaluated as it is applied to a pitch-unstable fighter aircraft. The recently developed L1 adaptive control method originates from aerospace adaptive control problems and achieves fast adaptation while robust stability to bounded plant parameter changes is claimed. Even though large adaptation gains create large and rapidly varying internal signals, the L1 adaptive controller output is limited in amplitude and frequency, since a low-pass filter directly at the output, is used to make the controller act within the control channel bandwidth.

An L1 adaptive controller of piecewise constant type has been applied to a fighter aircraft by augmenting a baseline linear state feedback controller. Once some experience is gained, it is relatively straightforward to apply this design procedure because only a few controller parameters need tuning. To design an L1-controller for roll-pitch-yaw-motion of an aerial vehicle, a five-state reference system with desired dynamics was created and five bandwidths of low-pass filters were tuned. The L1-controller activates when the vehicle aided by the state feedback controller deviates from the reference dynamics resulting in better reference following. Load disturbance rejection was improved by the L1-controller augmentation. This comes at the cost of having high frequency control signals fed into the plant.

The L1 adaptive controller is in its original design sensitive to actuator limitations and to time delays when compared to the baseline controller. Introducing nonlinear design elements corresponding to actuator dynamics (e.g. rate limits) makes tuning easier if such dynamics interfere with the reference system dynamics. Sensitivity to known time delays can be reduced using prediction in a state observer. With these additions to the design, the L1-controller augmentation can be tuned to achieve improved

nominal performance and robust performance when compared to a typical aeronautical linear state feedback controller. This was verified by simulations using a high fidelity model of the aircraft.

Use of feedforward can alleviate feedback and adaptive actions. Feedforward signals can be generated from reference models and corresponding models can also be used as reference models in adaptive control. A method for aerial vehicle reference model design was developed, that makes it possible to find reference models that scale to the present flight condition and vehicle configuration.

In some situations the closed-loop system obtained by L1 adaptive control is equivalent to linear systems. The architectures of these systems were investigated. An effort was made to understand and describe what fundamental characteristic of L1 adaptive controllers make them suitable for aeronautical applications.

With the L1-controller, performance and robustness was increased when compared to the baseline controller. It is possible to add L1-controller characteristics gradually to a linear state feedback design, which is something that this thesis recommends to aerospace industry.

Acknowledgements

First of all I would like to thank my supervisors, Prof. Rolf Johansson, Prof. Anders Robertsson and Prof. em. Karl Johan Åström, for their substantial and objective knowledge in the field of automatic control. Support has been given to me at all times and especially when presenting results at international conferences.

Questions regarding my application of L1 adaptive control have always been answered by Prof. Naira Hovakimyan, Enric Xargay, Evgeny Kharisov at the University of Illinois at Urbana-Champaign. They also have been supporting and encouraging at publications.

At SAAB AB, Dr. Henrik Jonson, Dr. Ola Härkegård and Daniel Simon have contributed with relevant questions and guidelines that pushed this project forward in a path that is relevant for industry. Tekn. Lic. Torbjörn Crona has encouraged and allowed me to go ahead with academic studies.

The thesis is part of a project "2009-01333 Adaptive Control in Airborne Vehicles" financed by Vinnova, a Swedish governmental agency for innovation, together with SAAB AB, a Swedish aeronautical company. The project is part of a program "NFFP5" the fifth in a series of Swedish governmental, academia and industry flight research co-operations. This project incorporates participants from SAAB and University of Lund (LU). The project has been proposed by SAAB to Vinnova which has approved the planned work. Industry (SAAB) provides expertise in aerial vehicles and LU provides expertise in adaptive control and guides the SAAB-employed Ph.D. student that carries out most of the work.

The author is part of the LCCC Linnaeus Center supported by the Swedish Research Council, and the ELLIIT Excellence Center, supported by the Swedish Government.

I would also like to thank my wife Jenny for pep-talk and kind words in moments of doubt.

Contents

1 Introduction

Control of fighter aircraft and missiles that results in good maneuver performance and a system with high safety is a key to being competitive in the aerospace industry. An aerial vehicle (Figure 1.1) inherently has challenging control characteristics such as nonlinear dynamics, uncertain aerodynamics and actuator limitations. Maneuvering requirements are set to high levels while guarantees for graceful degradation and stability are crucial.

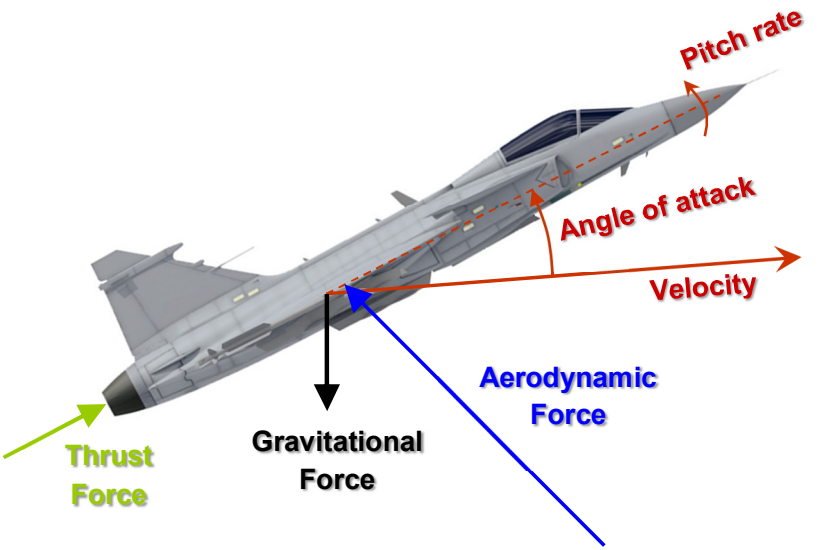

Figure 1.1 Fighter aircraft with forces that affect quantities of flight such as velocity, angle of attack and pitch angular rate.

To excel in the market, industry wants to get as much performance as possible out of a design, using a limited engineering work effort. Seeking control methods that exploit fundamental knowledge about limits in the

application and that pushes performance as far as possible to those limits are desired. Adaptive control could offer a way to exploit new levels of performance with reduced effort and it could also increase safety by performing adjustment to unexpected in-flight changes of the flight dynamics.

In this thesis, aerial vehicle control is addressed by an L1 adaptive control method. There are several types of L1 adaptive controllers [6], here the special version with piecewise constant parameter estimates is analyzed. Design of a controller for fighter aircraft with L1 adaptive technique is performed and the results are analyzed.
Three main topics are:

- Analysis of linear L1 adaptive control architectures for aerial vehicle applications.
- L1 adaptive augmentation of piecewise constant type to a baseline controller that uses linear state feedback.
- Design of linear reference systems and nonlinear feedforward for use together with an adaptive flight controller.

1.1 Background

There are two fundamentally different ways of controlling systems with dynamics that change over time: adaptive or robust control. The aerospace industrial baseline today is to use robust control, which caters to the effect of parametric uncertainties, although that baseline can come with an associated loss of performance. An adaptive controller it is often possible to boost the performance of the closed-loop system, but then the inherent robustness may be insufficient [8].

Adaptive control methods have been developed for more than 50 years but have not been widely used in aerospace industry. There are appealing features in adaptive control, such as adaptation to the present flight condition, on-line cancellation of uncertainties and possibly a reduction in controller verification effort, all of which certainly are desired in aerospace applications.

The start of adaptive control came in the 1950s [5], research and design was driven by control of high performance aircraft. A single fixed gain controller was not enough to control extreme aircraft throughout the full airspeed and altitude flight envelope. This period of time is called the brave era since there was a very short path from idea to flight test with very little analysis in between. The X-15-3 [23] extended the possible

flight envelope of an aircraft significantly and unfortunately it resulted in a tragic accident which damaged the reputation of adaptive control. To gain schedule a controller with airspeed and altitude was found to be an adequate and safe strategy for flight control.

In the 1960s research increased knowledge in state-space theory, stability theory, stochastic control, dynamic programming and system identification made it possible to develop adaptive control further.

Interest in adaptive control increased in the 1970s and early 1980s when proofs of stability of adaptive systems appeared, where efforts to merge robust control and system identification were important [5]. In the late 1980s and early 1990s research achieved increased robustness of adaptive controllers when used together with nonlinear systems.

At the beginning of this adaptive flight control project, it was agreed amongst the participants to evaluate L1 adaptive control, a relatively new (2006) and promising alternative to more traditional adaptive control methods. Established adaptive schemes such as MRAC [5] has go limitations, it can give large transients and slow convergence [8]. L1 adaptive control has been developed with aerospace control in mind and has been found suitable for aerial vehicles in several applications [7], [25] and [30]. In L1 adaptive control fast adaptation is achieved while robust stability to bounded plant parameter changes is claimed. Even though large adaptation gains create large and rapidly varying internal signals, the L1 adaptive controller output is limited in amplitude and frequency, since a low-pass filter direct at the controller output, is used to make the controller act within the available control channel bandwidth [31], a frequency up to which the control object can be modeled with sufficient fidelity.

This work used findings from [25] and applied much of the same ideas. However the aircraft in this application is unstable in the pitch channel so the nominal dynamics is far from the desired, which motivates an L1-controller augmentation to a linear state feedback. It was noted in [15] that L1-controllers that use output feedback are linear, here a similar discussion for full state feedback L1-controllers of piecewise constant type is made. Tuning of low-pass filter parameters was accomplished by evaluating roll-pitch-yaw channel Monte-Carlo-simulations as was done for a pitch channel implementation in [24]. Linear system analysis of L1-controllers was done in [28] for the pitch channel; this work extends this approach for a roll-pitch-yaw system. In this application the actuators are rate saturated for notable periods of time, so it was necessary to use a combination of ideas from [14] and [30] to be able to tune an L1-controller for this aircraft. In short; this work has used findings from previous L1-controller

applications/analysis and put together a design procedure. Results that are relevant for considering L1-control architectures for aeronautical SAAB products such as fighters and missiles are explored.

1.2 Problem formulation

It is important for aerospace industry to address the question if maneuver performance is lost throughout the aerial vehicle envelope by using robust control methods together with gain-scheduling (Figure 1.2). Much is gained if performance and safety could be increased with an adaptive controller. Also the work effort for clearance (formal approval) of the controller throughout the full flight envelope is significant and requires a careful strategy. Possibly the engineering and computing effort as well as the risk of late controller redesign could be reduced with adaptive techniques.

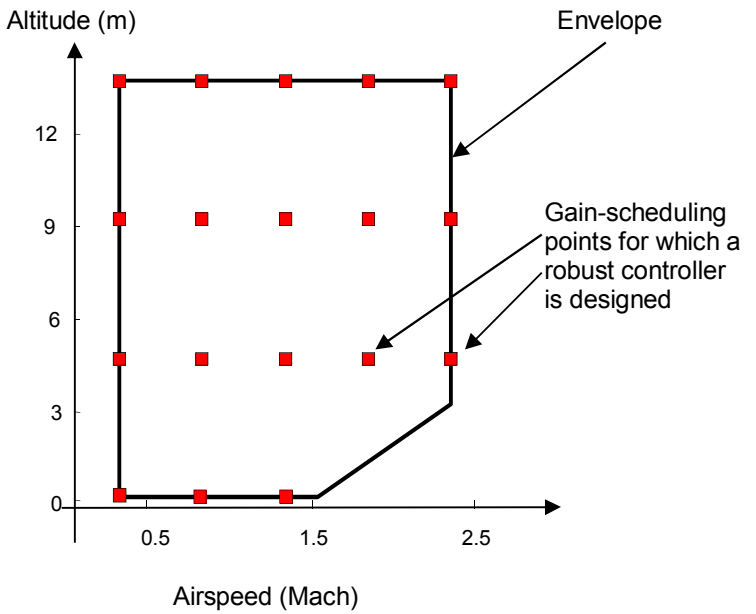

Figure 1.2 Schematic airspeed & altitude gain-scheduling chart for an aerial vehicle.

1.3 Goal

The ultimate goal is to address the question whether adaptive control can be used in aerial vehicles that SAAB develops today or in the future. This evaluation should include and assess various industrial aspects such as tuning and flight clearance.

More specifically the goal was to properly derive a representative model of flight dynamics and to relate this model to previous work and also to the parameter models that are used in adaptive control. Using this flight dynamics model, knowledge is desired of how to design, tune and test L1 adaptive controllers of piecewise constant type in aerospace applications. It was also desirable to indicate limitations and possibilities when using L1-controllers in aerial vehicles.

1.4 Outline

The thesis is organized in the following way: Initially generic dynamics of an aerial vehicle are derived. This model is then parameterized to represent a Gripen-like fighter.

Reference systems with desired flight dynamics, used for adaptive and feedforward compensation, are created. This is accomplished using the nominal flight dynamics and based on that information, a fast but still reasonable linear reference system is defined. A linear state feedback is then created that will place the poles of the closed loop at the desired positions, corresponding to the dynamics of the reference system. A feedforward compensator from the reference signal that makes the nominal nonlinear dynamics, act like the linear reference system is also derived.

An L1 adaptive controller of piecewise constant type is described and designed to control the aerial vehicle. This controller is analyzed and alternative views of the controller are given which admit comparisons to robust controllers. Simulations are made in a Matlab Simulink implementation of the model. A range of systematic realizations of flight conditions that deviates from the nominal assumptions are generated and simulated. The adaptive control laws are compared to linear state feedback controllers with integral action. Results are presented and analyzed from a performance and robustness point of view. Linear transfer function analysis of the system in the frequency domain is presented.

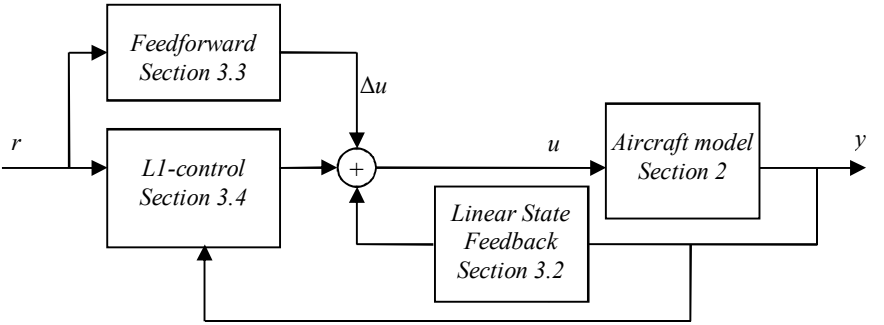

Figure 1.3 Schematic thesis outline indicated in a system block diagram.

1.5 Publications

The publications on which this thesis is based are the following:

A. Pettersson, K. J. Åström, A. Robertsson and R. Johansson, "Augmenting L1 adaptive control of piecewise constant type to a fighter aircraft. Performance and robustness evaluation for rapid maneuvering", in *Proc. AIAA GNC Conference*, Minneapolis, MN, Aug. 2012, AIAA-2012-4757.

A. Pettersson, K. J. Åström, A. Robertsson and R. Johansson, "Analysis of Linear L1 Adaptive Control Architectures for Aerospace Applications", in *Proc. IEEE Conference on Decision and Control* (CDC2012), Maui, HI, Dec 2012.

A. Pettersson, K. J. Åström, A. Robertsson and R. Johansson, "Nonlinear Feedforward and Reference Systems for Adaptive Flight Control", accepted for *AIAA GNC Conference*., Boston, MA, Aug. 2013.

The author has been responsible for analysis, design, implementation and evaluation of L1-control in these three publications.

1.6 Contribution

The main contributions of this thesis are:

- Performance and robustness analysis of an L1-controller and comparisons with a linear state feedback, using a disturbed and perturbed nonlinear aircraft model.
- Comparison of L1-control laws and robust control laws. Use of linear system theory to analyze an L1 adaptive controller of piecewise constant type controlling a linearized model of an aircraft.
- A procedure to generate linear reference systems and feedforward from reference signals for generic aerial vehicles.

A generic method is developed to generate linear reference systems. Three parameters corresponding to roll, pitch and yaw motion are tuned for one flight condition. The reference system design then scales to the flight condition using physical data such as airspeed, altitude, mass, mass inertia and aerodynamics properties. Linear state feedback gains that nominally make the linearized system follow the reference system are then derived. The thesis also contributes with a design of nonlinear feedforward signals that make the flight dynamics act like the linear reference system, by using the angular velocity vector as a virtual control signal. This feedforward design exploits the particular structure of flight dynamics.

Further contribution is the insight that the piecewise constant L1-controller leads to a linear time invariant control law. This makes it possible to analyze controller robustness in a well-known framework. Frequency responses from "gang-of-six" [19], transfer functions, singular value diagrams etc. are presented. This is carried out for an L1-controller and compared to a linear state feedback controller with integral action. Also the application of these types of controllers to e.g. a pitch-unstable fighter aircraft, including simulation results with various alterations such as parameter uncertainties and actuator failures, has a value for industries such as SAAB. It is also important to know that an L1-controller which estimates parameters and disturbances make it possible to include nonlinearities that will make the controller act on effects that can be compensated for and ignore others.

Another contribution is the insight that the L1 adaptive controller of piecewise constant type generates a control signal which can be seen as a modification to a multivariable controller using state feedback with integral action. Comparisons are also made to disturbance observers. It is seen that these types of controllers use the nominal dynamics inverse while

L1-controllers use the inverse of the desired dynamics. This analysis and finding a controller that is equivalent to an L1-controller is valuable for industries like SAAB when online implementation is designed. The vague "sample rate of the available CPU" mentioned in [6] would give problems when prioritizing update rates in real-time software. Knowledge that the resulting inverse is done with a fidelity that is proportional to the inverse of the sample rate will be helpful when choosing update rates and optional algorithm iterations within each control signal calculation. Industry is also served by the insight that since L1-controllers of this type are linear time invariant, there are a lot of methods that could end up with the same controller. However, the L1 approach leads naturally to a control architecture that is well suited to aerospace applications. A physical understanding of how the controller operates is possible due to the state predictor and this allows for design elements such as time delays and actuator dynamics.

Inspired by the results from this work, a feasibility study [39] was carried out at SAAB, addressing the possibility of using a piecewise constant L1-controller for the backup law in a Gripen-like SAAB fighter. The results are commented in the conclusions of this thesis.

2 Aerial Vehicle Modeling

A proper derivation of the flight dynamics of an aerial vehicle is needed both for choosing the desired performance and for design of a suitable controller. A thorough examination of the resulting equations in order to understand how the dynamics are built up and connected is crucial for making correct feedforward and feedback controller design decisions, including analysis of parameter choices for e.g. adaptive control.

States expressing the rigid-body-motion will be established, together with the time derivatives of these states. The equations of motion, aerodynamics and actuator dynamics will result in a model that uses 20 states. This model will then be used both for deriving linear systems for design of control algorithms in Section 3 as well as for simulating the full environment in Section 4. This modeling section will also serve as an introduction to dynamic systems that arise for generic (rotorless) aerial vehicles, including missiles.

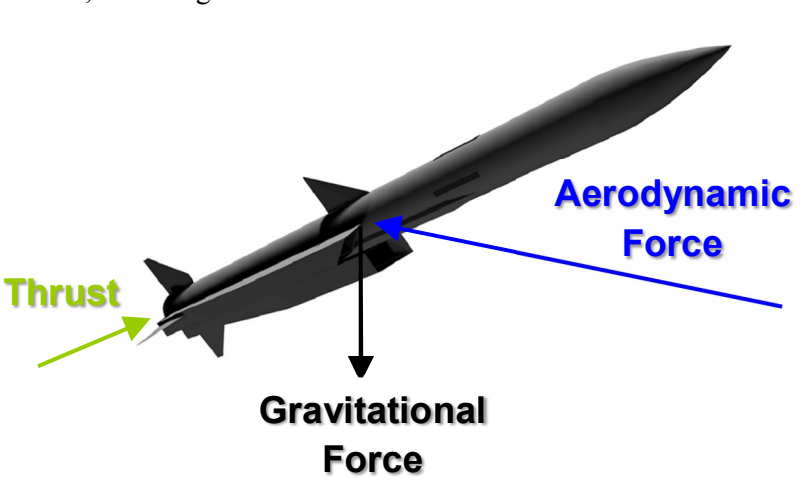

Figure 2.1 Example of a missile body on which forces and moments will create a flying dynamic system.

2.1 Definitions and motion equations

Motion equations will be created with six degrees of freedom; this is a well-known procedure within aerospace applications [1]. It is essential for this work to have suitable definitions and expressions of the motion equations in order to identify properties that can be compensated for, both by feedforward and feedback.

Assumptions

Modeling is done assuming a flat, non-rotating earth. This is no limitation for the short period, relatively short range and moderate speeds for which the equations are used later on. It is also assumed that the center of gravity is close to stationary in the airframe (but it can be arbitrarily placed during a simulation). Finally it is assumed that the mass and mass inertia are slowly varying so that time derivatives of these quantities can be neglected. These assumptions are commonly used in flight dynamics analysis and in aeronautical simulation models [4].

Coordinate and vector definitions

Two Cartesian, three-dimensional, right-hand coordinate systems will be defined, one that is inertial and one that is fixed relative the airframe. These coordinate systems are suitable for expressing quantities that will define the flight dynamics.

Figure 2.2 illustrates the inertial coordinate system. This is the non-moving, non-rotating system that is used as inertial reference. The inertial system in this application is fixed to the surface over which the aerial vehicle is flying, pointing north, east and down with its respective axis, X, Y and Z.

A body fixed coordinate system is defined as illustrated in Figure 2.3. The body system is fixed relative the airframe with its origin placed in the center of gravity. The body system xz-plane is parallel to the assumed airframe left-right symmetry-plane and its complete orientation is defined by the z-axis pointing downwards from the body.

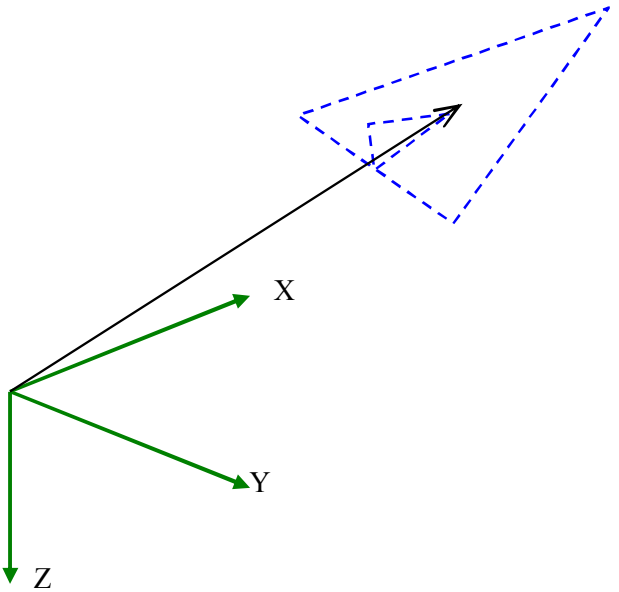

Figure 2.2 Inertial coordinate system (green) and a schematic aerial vehicle (blue).

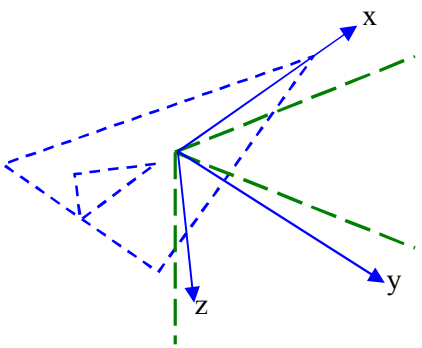

Figure 2.3 Body fixed coordinate system (blue). Orientation of the inertial system indicated by dashed lines (green).

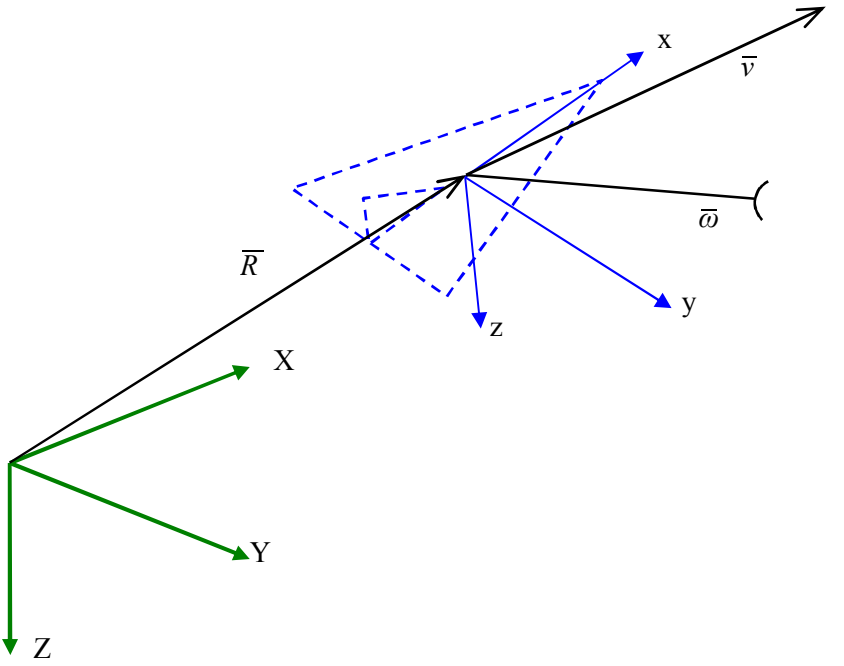

Figure 2.4 Vectors for body velocity v, body angular velocity ω and body position R.

Now vectors are defined in Figure 2.4 that will be used for expressing body system velocity, angular velocity and position:

Velocity vector of the body system origin, relative inertial system, is denoted $\overline{v}$. Velocity vector components expressed in body system are denoted u, v and w.

$$\overline{v} = \begin{pmatrix} u \\ v \\ w \end{pmatrix} \tag{2.1}$$

Angular velocity vector of the body system, relative inertial system, is denoted $\overline{\omega}$. Angular rate components expressed in body system are denoted p, q and r.

$$\overline{\omega} = \begin{pmatrix} p \\ q \\ r \end{pmatrix} \tag{2.2}$$

Velocity vector component u and angular velocity component r use the same symbol as the later defined control signal u and reference signal r. It is considered clear by the context which quantity that is referred to in this thesis.

Body attitude (angular orientation) in roll, pitch and yaw is expressed by three Euler angles as in Figure 2.5.

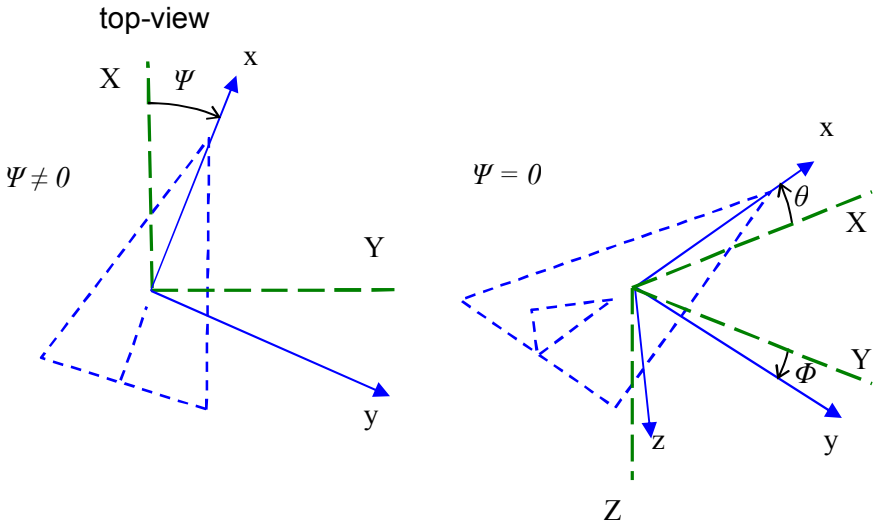

Figure 2.5 Attitude of body coordinate system, defined by Euler angles Ψ, θ, Φ.

Body system orientation is created from the inertial orientation by first rotating a yaw angle Ψ around the body z-axis (as in left part of Figure 2.5), then a pitch angle θ around the body y-axis and finally a roll angle Φ around the body x-axis. These Euler angles ([2] p.45) of the body system, relative to the inertial system can be written as a vector:

$$\begin{pmatrix} \Phi \\ \theta \\ \Psi \end{pmatrix} \tag{2.3}$$

Position of the body system origin, relative inertial system, is denoted $\overline{R}$. Position vector components expressed in inertial system are denoted R_X, R_Y and R_Z. The negative value of R_Z is equivalent to the flight altitude H.

$$\overline{R} = \begin{pmatrix} R_X \\ R_Y \\ R_Z \end{pmatrix} \tag{2.4}$$

Also needed is a rotation for expressing components of a vector in the inertial system which has its components expressed in the body system and vice versa. If the velocity vector is to be expressed in the inertial system, this vector $\overline{V}$ is related to the body velocity $\overline{v}$ as:

$$\overline{V} = T_{IB}\,\overline{v} \tag{2.5}$$

The rotation matrix T_{IB} (from body to inertial) is defined by the Euler angles ([1] p.105) according to:

$$T_{IB} = \begin{pmatrix} \cos\Psi\cos\theta & -\sin\Psi\cos\Phi + \cos\Psi\sin\theta\sin\Phi & \sin\Psi\sin\Phi + \cos\Psi\sin\theta\cos\Phi \\ \sin\Psi\cos\theta & \cos\Psi\cos\Phi + \sin\Psi\sin\theta\sin\Phi & -\cos\Psi\sin\Phi + \sin\Psi\sin\theta\cos\Phi \\ -\sin\theta & \cos\theta\sin\Phi & \cos\theta\cos\Phi \end{pmatrix} \tag{2.6}$$

To achieve rotation in the opposite way, from inertial system to body, the following rotation matrix properties and naming conventions are used:

$$\overline{v} = T_{IB}^{-1}\,\overline{V} = T_{IB}^{T}\,\overline{V} = T_{BI}\,\overline{V} \tag{2.7}$$

Alternative expression for the velocity vector

Figure 2.6 shows an alternative way of expressing the velocity vector in the body coordinate system, using the velocity vector magnitude V (called airspeed) and two azimuth and elevation angles α and β (called angle of attack and angle of sideslip) This representation is often used for examining results and for expressing aerodynamic properties, instead of using vector components u, v and w.

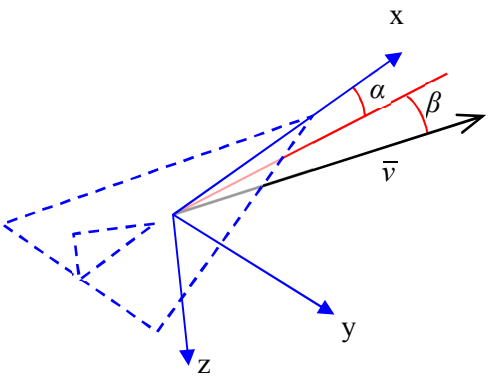

Figure 2.6 Velocity vector $\bar{v}$, positive angle of attack α and positive angle of sideslip β.

The angle of attack α is defined as the angle between the body x-axis and the velocity vector projected to the body xz-plane. The angle of sideslip β is defined as the angle between the body xz-plane and the velocity vector, measured in the plane defined by the body y-axis and the velocity vector itself.

Relations between velocity vector components u, v, w and the airspeed, angle of attack and angle of sideslip become:

$$\begin{aligned} V &= |\bar{v}| = \sqrt{u^2 + v^2 + w^2} \\ \alpha &= \arctan\left(\frac{w}{u}\right) \\ \beta &= \arctan\left(\frac{v}{\sqrt{u^2 + w^2}}\right) = \arcsin\left(\frac{v}{V}\right) \end{aligned} \tag{2.8}$$

V, α and β are used in Section 2.3 for expressing aerodynamic forces and moments. These forces and moments are considered for nose forward flight which assumes that the x-component of the body expressed velocity u is strictly positive. Wind and gust effects can be included by subtracting corresponding velocity components from u, v and w.

2.2 Forces and moments equations

Now Newton's second law and Euler's equation will be used. This will make it possible to find relations that express how forces and moments acting on the airframe change the velocity and angular velocity over time.

The sum of all forces $\bar{F}$ acting on the body equals the mass m times acceleration $\bar{a}$ according to Newton's second law:

$$\bar{F} = m\bar{a} = m\frac{d\bar{v}}{dt} = m(\dot{\bar{v}} + \bar{\omega} \times \bar{v}) \tag{2.9}$$

where the cross product comes from the velocity vector projection change onto the body system due to the angular velocity of the body system.

The sum of all moments $\bar{M}$ acting on the body equals the time derivative of angular momentum $I_i\bar{\omega}$ according to Euler's equation:

$$\bar{M} = \frac{d}{dt} I_i \bar{\omega} = I_i \dot{\bar{\omega}} + \bar{\omega} \times I_i \bar{\omega} \tag{2.10}$$

Forces $\bar{F}$ and moments $\bar{M}$ will be a sum of terms related to aerodynamics, gravitation and propulsion. These terms are presented in Section 2.3, 2.4 and 2.5 respectively.

Equations of motion

Now the time derivatives of velocity, angular velocity, position and attitude can be expressed, using definitions from Section 2.1 and 2.2. These derivatives will be integrated over time to model the motion in the simulation model. These expressions will also be simplified to get linear dynamic models of the dynamics.

Velocity vector time derivative:

$$\dot{\bar{v}} = \frac{1}{m}\bar{F} - \bar{\omega} \times \bar{v} \tag{2.11}$$

with elements:

$$\begin{pmatrix}\dot{u}\\ \dot{v}\\ \dot{w}\end{pmatrix}=\frac{1}{m}\begin{pmatrix}F_x\\ F_y\\ F_z\end{pmatrix}-\begin{pmatrix}p\\ q\\ r\end{pmatrix}\times\begin{pmatrix}u\\ v\\ w\end{pmatrix}=\frac{1}{m}\begin{pmatrix}F_x\\ F_y\\ F_z\end{pmatrix}-\begin{pmatrix}wq-vr\\ ur-wp\\ vp-uq\end{pmatrix} \tag{2.12}$$

Angular velocity vector time derivative:

$$\dot{\overline{\omega}}=I_i^{-1}(\overline{M}-\overline{\omega}\times I_i\overline{\omega}) \tag{2.13}$$

with elements:

$$\begin{pmatrix}\dot{p}\\ \dot{q}\\ \dot{r}\end{pmatrix}=\begin{pmatrix}I_x & -I_{xy} & -I_{xz}\\ -I_{xy} & I_y & -I_{yz}\\ -I_{xz} & -I_{yz} & I_z\end{pmatrix}^{-1}\left(\begin{pmatrix}M_x\\ M_y\\ M_z\end{pmatrix}-\begin{pmatrix}p\\ q\\ r\end{pmatrix}\times\begin{pmatrix}I_x & -I_{xy} & -I_{xz}\\ -I_{xy} & I_y & -I_{yz}\\ -I_{xz} & -I_{yz} & I_z\end{pmatrix}\begin{pmatrix}p\\ q\\ r\end{pmatrix}\right)=$$

$$\begin{pmatrix}I_x & -I_{xy} & -I_{xz}\\ -I_{xy} & I_y & -I_{yz}\\ -I_{xz} & -I_{yz} & I_z\end{pmatrix}^{-1}\left(\begin{pmatrix}M_x\\ M_y\\ M_z\end{pmatrix}-\begin{pmatrix}I_z qr-I_{xz}pq-I_{yz}q^2-I_y qr+I_{xy}pr+I_{yz}r^2\\ I_x pr-I_{xy}qr-I_{xz}r^2-I_z pr+I_{xz}p^2+I_{yz}pq\\ I_y pq-I_{xy}p^2-I_{yz}pr-I_x pq+I_{xy}q^2+I_{xz}qr\end{pmatrix}\right) \tag{2.14}$$

Inertial position derivative, expressed in inertial system, equals the body expressed velocity, rotated to the inertial coordinate-system:

$$\dot{\overline{R}}=T_{IB}\overline{v} \tag{2.15}$$

or:

$$\begin{pmatrix}\dot{R}_X\\ \dot{R}_Y\\ \dot{R}_Z\end{pmatrix}=T_{IB}\begin{pmatrix}u\\ v\\ w\end{pmatrix} \tag{2.16}$$

Euler angle time derivatives can be projected onto body coordinates and then relate to body angular velocities as ([1] p.105):

$$\begin{pmatrix}p\\ q\\ r\end{pmatrix}=\begin{pmatrix}1 & 0 & -\sin\theta\\ 0 & \cos\Phi & \cos\theta\\ 0 & -\sin\Phi & \cos\theta\cos\Phi\end{pmatrix}\begin{pmatrix}\dot{\Phi}\\ \dot{\theta}\\ \dot{\Psi}\end{pmatrix} \tag{2.17}$$

so Euler angle time derivatives expressed in body angular rates become:

$$\begin{pmatrix} \dot{\Phi} \\ \dot{\theta} \\ \dot{\Psi} \end{pmatrix} = \begin{pmatrix} p + \tan\theta(q\sin\Phi + r\cos\Phi) \\ q\cos\Phi - r\sin\Phi \\ (q\sin\Phi + r\cos\Phi)/\cos\theta \end{pmatrix} \tag{2.18}$$

Euler angles are intuitive for understanding attitude; however expressions for roll and yaw Euler angle derivatives Φ and Ψ become singular when the pitch angle θ is $\pm\pi/2$. Numerical problems will be at hand when flying close to straight up or down. To cope with this the simulation model uses quaternions to keep track of attitude instead of (2.18). Quaternions cover the full attitude envelope by the help of one additional state [4]. The quaternions are then used to achieve rotation matrices and also for generating Euler angles when presenting results from simulations.

Alternative time derivative expression for the velocity vector

Time derivatives of velocity components u, v and w have been expressed in (2.12). However, it is often more natural to use velocity V, angle of attack α and angle of sideslip β as states.

The following change of variables and resulting expressions will be used:

$$\begin{aligned} V^2 = u^2 + v^2 + w^2 \quad &\Rightarrow \quad \dot{V} = \frac{1}{2V}\frac{dV^2}{dt} = \frac{u\dot{u} + v\dot{v} + w\dot{w}}{\sqrt{u^2 + v^2 + w^2}} \\ \tan\alpha = \frac{w}{u} \quad &\Rightarrow \quad \dot{\alpha} = \frac{1}{1+\tan^2\alpha}\frac{d\tan\alpha}{dt} = \frac{\dot{w}u - w\dot{u}}{u^2 + w^2} \\ \tan\beta = \frac{v}{\sqrt{u^2 + w^2}} \quad &\Rightarrow \quad \dot{\beta} = \frac{1}{1+\tan^2\beta}\frac{d\tan\beta}{dt} = \frac{\dot{v}(u^2 + w^2) - v(u\dot{u} + w\dot{w})}{\sqrt{u^2 + w^2}(u^2 + v^2 + w^2)} \end{aligned} \tag{2.19}$$

It will be assumed at linearization and for some feedforward compensations that the velocity component u is significantly larger than velocity components v and w. This is valid as long as α and β are limited in magnitude (below some 30º). These assumptions make u and V similar in magnitude and all but a few terms negligible in (2.19) so significant simplifications can be obtained:

$$\dot{V} \approx \dot{u},\ \dot{\alpha} \approx \frac{\dot{w}}{V},\ \dot{\beta} \approx \frac{\dot{v}}{V} \tag{2.20}$$

2.3 Aerodynamic forces and moments

Aerodynamic forces and moments acting on the airframe are expressed in non-dimensional coefficients, Figure 2.7.

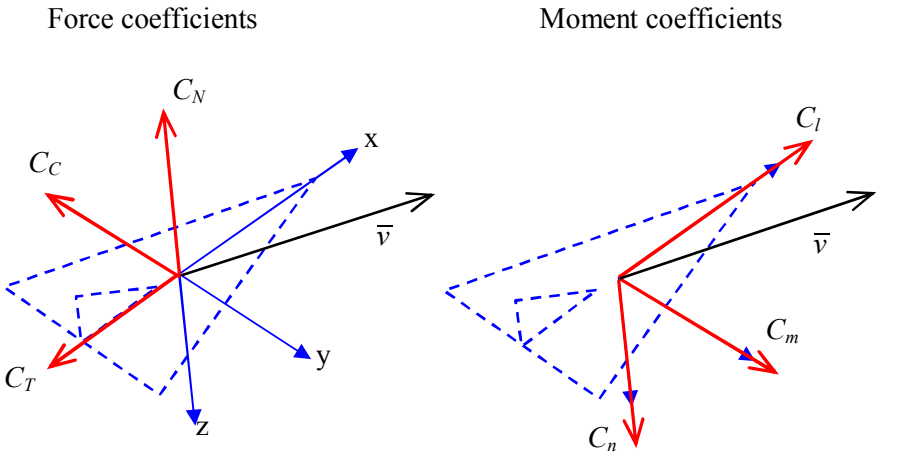

Figure 2.7 Definition of aerodynamic force and moment coefficients.

These coefficients are normalized versions of forces and moments [3]. This will make the coefficients independent of the airspeed and air density (within a certain range). This normalizing factor is, for aerodynamic forces, the dynamic pressure q_d times a reference area S. For aerodynamic moments the factor is dynamic pressure times a reference area S and a reference length denoted b, c or d.

So the aerodynamic forces and moments expressed in the body-system become:

$$\overline{F}_a = -q_d S \begin{pmatrix} C_T \\ C_C \\ C_N \end{pmatrix} \qquad \overline{M}_a = q_d S \begin{pmatrix} bC_l \\ cC_m \\ bC_n \end{pmatrix} \tag{2.21}$$

The reference area S is related to some kind of area of the airframe. For fixed-wing aircraft it is usually the wing area, for missiles it is usually the area of the circular body. The reference lengths b and c are related to a relevant length of the airframe. For an aircraft, b is usually the wing span

and c is the mean wing cord. For missiles b and c are equally chosen as the missile diameter and this reference length is denoted d.

The dynamic pressure q_d is related to airspeed V and air density ρ according to:

$$q_d = \frac{\rho V^2}{2} \tag{2.22}$$

(Section 2.7 defines ρ and its variation with altitude)

Instead of a force and a moment, aerodynamic quantities can be seen as a force and a distance to the center of gravity at which this force act. $\bar{r}_{cp}$ in Figure 2.8, which defines this lever arm, goes from the center of gravity to the center of pressure and give the relation $\bar{M}_a = \bar{r}_{cp} \times \bar{F}_a$.

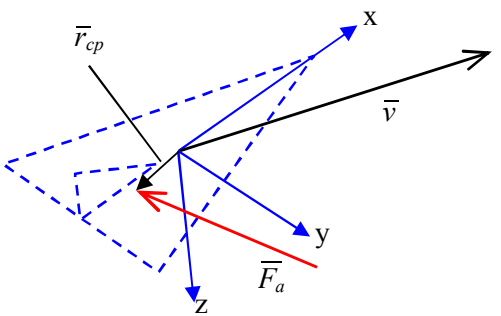

Figure 2.8 Aerodynamic force and lever arm from body origin to the center of pressure at which the force act.

If this center of pressure is located behind the center of gravity the aerodynamic configuration is defined as statically stable. The other way around is defined as statically unstable. Stability length is measured along the body x-axis and will be slightly different for pitch and yaw. Pitch is statically stable if the aerodynamic force cut the body xy-plane behind the center of gravity. Yaw is statically stable if the aerodynamic force cut the body xz-plane behind the center of gravity.

Aerodynamic moments are usually given relative a body position different than the center of gravity so a relation for moving moments from one position to another is needed. Using the aerodynamic force and moment expressed for one body position, a point where the aerodynamic

force act on the body can be calculated and then moment acting at an arbitrary body position can be achieved.

Aerodynamic control surfaces

The fundamental property that is accomplished by aileron, elevator and rudder deflections in aerial vehicles is moments in roll, pitch and yaw. These three moments will create angular velocity to achieve and maintain a desired roll angle, angle of attack and angle of sideslip. These three angles are then used to accelerate the airframe perpendicular to its velocity vector. (Acceleration along the velocity vector is done mainly by the help of propulsion forces, Section 2.5).

Figure 2.9 shows an example of aerodynamic control surface configuration and deflections that create moments in roll, pitch and yaw.

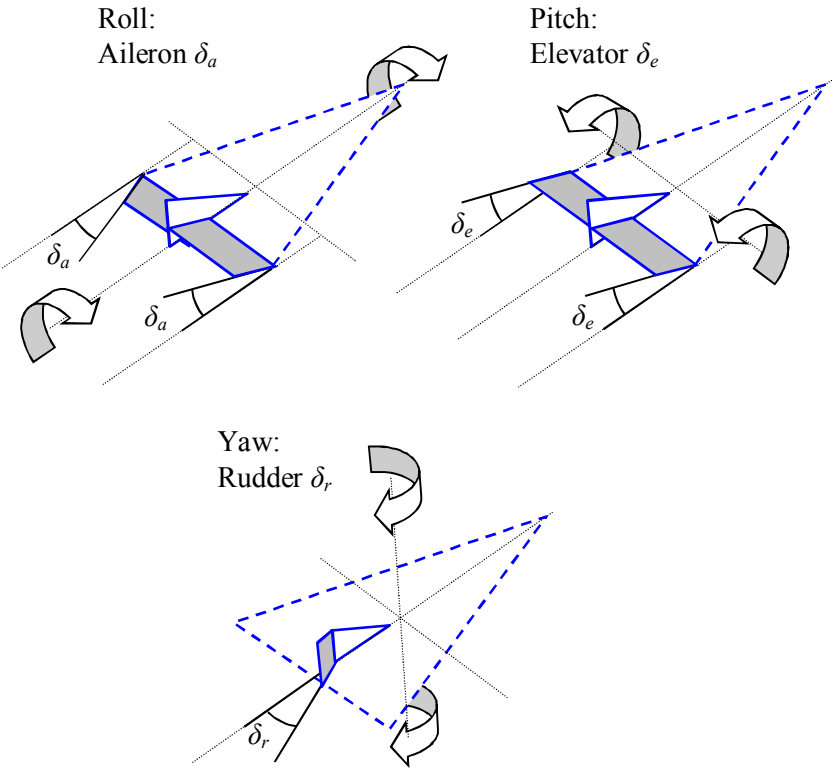

Figure 2.9 Aileron, elevator and rudder deflections create moments in three axes.

The position and number of control surfaces can of course be different from the example in Figure 2.9. Missiles usually use four control surfaces in a cross configuration in the rear part of the airframe. Deflections shown in Figure 2.9 create positive moments around body x, y and z-axis. These deflections can be defined as negative, which is the case for δ_e and δ_r in this application, (that is, a Gripen-like fighter model).

Control surface deflections generate moments also in other axis than the main intended one. These undesired moments are usually designed to be small, except for that a rudder deflection located on a dorsal fin generates considerable roll moments. Dorsal fin moment is mainly a linear effect and can be counteracted by a linear static gain to aileron in controller design.

To maintain an α and/or a β using control surface deflection is called to trim the aerodynamic configuration. If the center of pressure, where the force generated by α and β act, is close to the center of gravity, small moments are generated and it will be possible to trim a maneuver using small control surfaces or small deflections.

Forces generated by control surface deflection are usually small compared to forces generated by α and β. Depending on control surface position and moments created by α and β, a trim gain or a trim loss is generated by these deflection forces. A trim gain will be achieved if the deflection needed to counteract the moments generated by e.g. α creates a force in the same direction as the force from the angle of attack itself. If the deflection force instead acts in the opposite direction of the intended total force, a trim loss is at hand. If the configuration is statically stable, a control surface behind the center of gravity will create a trim loss and a surface in front of it will create a trim gain. For unstable configurations the opposite is true, aft surfaces gives a trim gain and front ones gives a trim loss.

Linearized aerodynamics

Five of the six aerodynamic coefficients (all but C_T) are usually linearized close to zero values of α, $\dot{\alpha}$, β, $\dot{\beta}$, p, q, r, δ_a, δ_e and δ_r:

$$
\begin{aligned}
C_C &= C_{C_\beta}\beta + C_{C\delta_r}\delta_r + C_{C\delta_a}\delta_a + \frac{b}{2V}\left(C_{C_p}p + C_{C_r}r + C_{C_{\dot{\beta}}}\dot{\beta}\right) \\
C_N &= C_{N_0} + C_{N_\alpha}\alpha + C_{N\delta_e}\delta_e + \frac{c}{2V}\left(C_{N_q}q + C_{N_{\dot{\alpha}}}\dot{\alpha}\right) \\
C_l &= C_{l_\beta}\beta + C_{l\delta_a}\delta_a + C_{l\delta_r}\delta_r + \frac{b}{2V}\left(C_{l_p}p + C_{l_r}r\right) \\
C_m &= C_{m_0} + C_{m_\alpha}\alpha + C_{m\delta_e}\delta_e + \frac{c}{2V}\left(C_{m_q}q + C_{m_{\dot{\alpha}}}\dot{\alpha}\right) \\
C_n &= C_{n_\beta}\beta + C_{n\delta_r}\delta_r + C_{n\delta_a}\delta_a + \frac{b}{2V}\left(C_{n_p}p + C_{n_r}r + C_{n_{\dot{\beta}}}\dot{\beta}\right)
\end{aligned}
\tag{2.23}
$$

([1] p.150 & p.199)

To make the coefficients related to angular rates $\dot{\alpha}$, $\dot{\beta}$, p, q and r dimensionless and less dependent of the airspeed V, these factors are normalized by $b/2V$ and $c/2V$ respectively. The relatively small C_{N_0} and C_{m_0} come from the airframe asymmetry above and underneath the xz-plane of the body axis, which generate a force and (most common) a moment at zero angle of attack.

The force coefficient along body x-axis C_T, is not suitable for linearization around zero values since it is an even function of the states and inputs.

Linearized aerodynamics is of course only valid in a limited area around the point of linearization. Aerodynamic force coefficient linearizations are usually a good approximation; aerodynamic moments can have more nonlinear dependencies.

2.4 Gravitational forces and moments

Gravitational force for the relatively low altitudes that are relevant here is proportional to mass m and earth gravitational constant g.

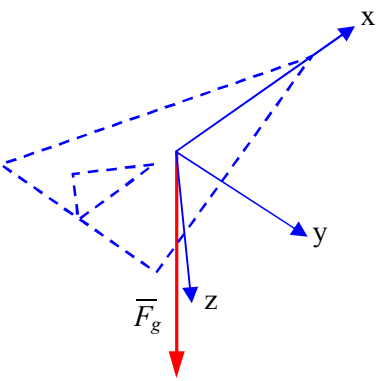

Figure 2.10 Force generated by gravity acting on airframe mass.

The gravitational vector, which is naturally expressed along the inertial system z-axis, is rotated to be expressed in the body system as follows:

$$\overline{F}_g = T_{IB}^T \begin{pmatrix} 0 \\ 0 \\ mg \end{pmatrix} = mg \begin{pmatrix} -\sin\theta \\ \sin\Phi\cos\theta \\ \cos\Phi\cos\theta \end{pmatrix} = m \begin{pmatrix} g_x \\ g_y \\ g_z \end{pmatrix} \tag{2.24}$$

No body system moments will be created by the gravitational force since the body coordinate system origin is positioned in the center of gravity.

2.5 Propulsion forces and moments

In Figure 2.11 the force generated by the propulsion is shown together with its lever arm to the center of gravity.

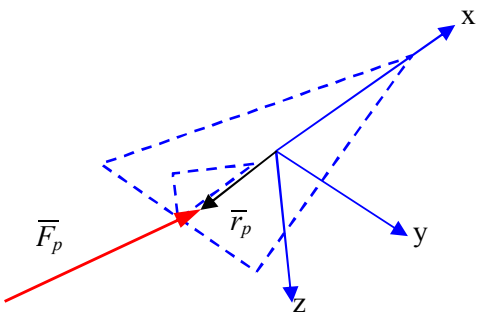

Figure 2.11 Force generated by propulsion and lever arm to the center of gravity.

The moment generated by the propulsion becomes:

$$\overline{M}_p = \overline{r}_p \times \overline{F}_p \tag{2.25}$$

where $\overline{r}_p$ is the vector from center of gravity to the point at which the propulsion force acts.

The propulsion force is often aligned with the body x-axis for fighter aircraft and missiles, so moments generated around the center of gravity are small. This is assumed to be the case so that the propulsion reduces to a scalar denoted T holding the magnitude of the thrust vector.

2.6 State equation details

Now state equations on element form (as opposed to vector expressions) can be calculated. These equations will be used to create feedforward as well as feedback and will display how the state dynamics are built up and

connected. Some simplifications will be made in this section to be able to get shorter expressions and to accomplish approximated linear dynamics. Different levels of expression fidelity will be created that can be used for design decisions later on. However, when using the motion expressions in the simulation model, full state equations according to Section 2.2 will be used.

Expressing velocity derivative $\dot{\overline{v}} = m^{-1}\overline{F} - \overline{\omega} \times \overline{v}$ and angular velocity derivative $\dot{\overline{\omega}} = I_i^{-1}(\overline{M} + \overline{\omega} \times I_i\overline{\omega})$ together with change of variables according to (2.19) gives the following time derivatives expressions for the system state *x*:

$$\begin{pmatrix} \dot{V} \\ \dot{\alpha} \\ \dot{\beta} \\ \dot{p} \\ \dot{q} \\ \dot{r} \end{pmatrix} = \begin{pmatrix} \begin{pmatrix} \frac{1}{m}\left(F_x\cos\alpha\cos\beta + F_y\sin\beta + F_z\sin\alpha\cos\beta\right) \\ \frac{1}{mV\cos\beta}\left(-F_x\sin\alpha + F_z\cos\alpha\right) + q - \left(p\cos\alpha + r\sin\alpha\right)\tan\beta \\ \frac{1}{mV}\left(-F_x\cos\alpha\sin\beta + F_y\cos\beta - F_z\sin\alpha\sin\beta\right) - r\cos\alpha + p\sin\alpha \end{pmatrix} \\ \begin{pmatrix} I_x & -I_{xy} & -I_{xz} \\ -I_{xy} & I_y & -I_{yz} \\ -I_{xz} & -I_{yz} & I_z \end{pmatrix}^{-1} \begin{pmatrix} M_x + \left(I_y - I_z\right)qr + I_{xz}pq + I_{yz}\left(q^2 - r^2\right) - I_{xy}pr \\ M_y + \left(I_z - I_x\right)pr + I_{xy}qr + I_{xz}\left(r^2 - p^2\right) - I_{yz}pq \\ M_z + \left(I_x - I_y\right)pq + I_{yz}pr + I_{xy}\left(p^2 - q^2\right) - I_{xz}qr \end{pmatrix} \end{pmatrix} \quad (2.26)$$

([1] p.105)

In (2.26) force elements $F_{x,y,z}$ and moment elements $M_{x,y,z}$ are the sum of terms from aerodynamics, gravity and propulsion in Section 2.3, 2.4 and 2.5 respectively.

State relations of (2.26) for α and q are called the short period longitudinal mode of the system. Relations for β, p and r are called the lateral mode.

To take one step towards linearization around zero of angle of attack/sideslip, trigonometric expressions are approximated by "cos $\alpha = 1$" and products "sin α sin $\beta = 0$" etc., so that (2.26) becomes:

$$\begin{pmatrix} \dot{V} \\ \dot{\alpha} \\ \dot{\beta} \\ \dot{p} \\ \dot{q} \\ \dot{r} \end{pmatrix} \approx \begin{pmatrix} \frac{T - q_d S C_T}{m} + g_x + \left(\frac{-q_d S C_C}{m} + g_y \right) \sin\beta + \left(\frac{-q_d S C_N}{m} + g_z \right) \sin\alpha \\ q - \frac{q_d S}{mV} C_N - p \tan\beta + \frac{1}{V} \left(g_z - \left(\frac{T - q_d S C_T}{m} + g_x \right) \sin\alpha \right) \\ -r - \frac{q_d S}{mV} C_C + p \sin\alpha + \frac{1}{V} \left(g_y - \left(\frac{T - q_d S C_T}{m} + g_x \right) \sin\beta \right) \\ \frac{1}{I_x - I_{xz}/I_z} \left(q_d S b \left(C_l + \frac{I_{xz}}{I_z} C_n \right) + \left(I_y - I_z - \frac{I_{xz}^2}{I_z} \right) qr + I_{xz} \left(1 + \frac{I_x - I_y}{I_z} \right) pq \right) \\ \frac{q_d S c}{I_y} C_m + \frac{I_z - I_x}{I_y} pr + \frac{I_{xz}}{I_y} (r^2 - p^2) \\ \frac{1}{I_z - I_{xz}/I_x} \left(q_d S b \left(C_n + \frac{I_{xz}}{I_x} C_l \right) + \left(I_x - I_y + \frac{I_{xz}^2}{I_x} \right) pq - I_{xz} \left(1 + \frac{I_z - I_y}{I_x} \right) qr \right) \end{pmatrix} \quad (2.27)$$

where aerodynamic coefficients $C_{N,C,l,m,n}$ follow (2.23) and gravity components in body system $g_{x,y,z}$ are defined in (2.24).

In order to simplify the inverse of the moment of inertia tensor I_i somewhat in (2.27), elements I_{xy} and I_{yz} have been assumed negligible. This is possible since symmetric mass distribution in body xy and yz-planes often are at hand for aerial vehicles [1].

2.7 Atmospheric model

A standard atmospheric model according to ISA, (ISO 2533:1975) is used. In this model a static air-pressure p_{s0} and a temperature T_0 at sea-level as a starting point. It is then assumed that the temperature drop at a rate L_H as altitude above sea-level increase. This temperature drop continues up to 11 km altitude and from there on the temperature is constant. This will give an atmospheric model that is a relevant approximation for this application up to at least 20 km altitude.

So temperature T depends on altitude H according to:

$$\begin{aligned} T &= T_0 - L_H H \quad H \le 11000\text{m} \\ T &= T_0 - L_H H_{11} \quad H > 11000\text{m} \end{aligned} \quad (2.28)$$

where $L_H = 0.0065$ºK/m and $H_{11} = 11000$ m.

It is further assumed that the pressure drop with altitude follows:

$$\begin{aligned} \frac{dp_s}{dH} &= -\rho g \\ p_s &= \rho R T \end{aligned} \tag{2.29}$$

where g = 9.82 m/s^2 is the earth gravitational constant, R is the specific gas constant for dry air, holding a value of R = 286.9 m^2/s^2/K and ρ is the air density at altitude H.

No difference is made between geopotential altitude and geometric altitude. Up to 20 km altitude, gravity is assumed to be constant.

This assumption of temperature decrease and pressure decrease with altitude, together with a setting of static pressure p_{s0} and temperature T_0 at sea-level gives the following explicit static pressure p_s at altitude H:

$$\begin{aligned} p_s &= p_{s0}\left(\frac{T_0 - L_H H}{T_0}\right)^{\frac{g}{L_H R}} && H \le 11000\text{m} \\ p_s &= p_{s11} e^{(H_{11}-H)\frac{g}{T_{11}R}} && H > 11000\,\text{m} \end{aligned} \tag{2.30}$$

where parameters p_{s11} and T_{11} are static pressure and temperature at 11 km altitude (found from the low altitude expressions evaluated at an altitude of 11 km).

With static pressure p_s and temperature T expressed for different altitudes, the air density ρ and the speed of sound a, can be obtained by:

$$\begin{aligned} \rho &= \frac{p_s}{RT} \\ a &= \sqrt{\kappa R T} \end{aligned} \tag{2.31}$$

where κ = 7/5 is the adiabatic index for a diatomic gas such as air.

The quotient between the airspeed V and the speed of sound a defines the Mach number M so that:

$$M = \frac{V}{a} \tag{2.32}$$

2.8 Control surfaces and actuator models

Actuators used to manipulate the aerodynamic control surfaces have dynamics which are modeled by a second order system with states for angular position and angular rate. Saturations in angular acceleration, rate and position are incorporated into the model. A real physical actuator is a complex control system in itself, the model created here will capture relevant dynamics for this application.

The second order actuator system is defined by bandwidth ω_a and damping ς_a so that:

$$\ddot{\delta} = -2\zeta_a \omega_{0a} \dot{\delta} + \omega_{0a}^2 \left(\delta_d - \delta\right) \tag{2.33}$$

where δ is effectuated angular deflection and δ_d is the demanded actuator deflection.

There are four actuators modeled. Two for left and right trailing edge wing elevons that are combined to achieve aileron and elevator deflections δ_a and δ_e. One actuator manipulates the rudder δ_r and one manipulates the left and right connected canards δ_c. Elevons, rudder and canards are displayed in blue color in Figure 2.12. There are often additional actuators and corresponding control surfaces present in a real configuration (such as the ones in red color in Figure 2.12) but this model is adequately modeling the short term behavior in most scenarios [1] and [39].

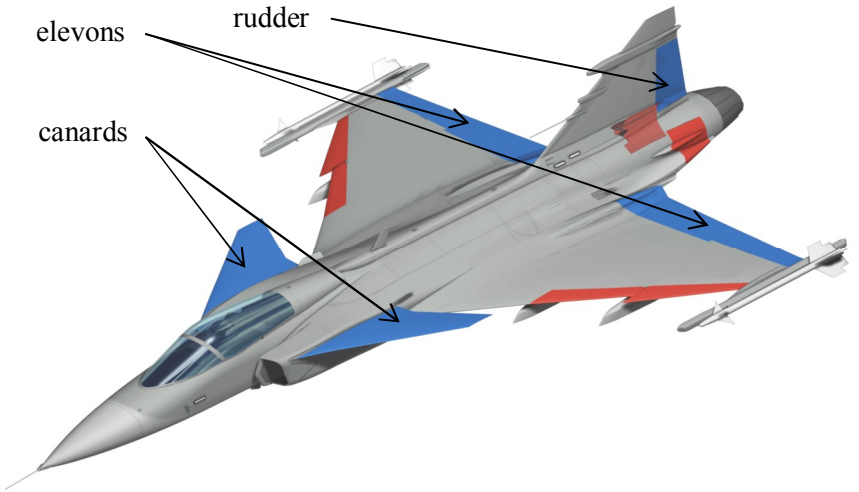

Figure 2.12 Control surfaces in blue, actuated to control the short period pitch and lateral roll-yaw dynamics of the aircraft.

Each actuator has a hard stop saturation in positive and negative angular position as implemented by the rightmost integrator in Figure 2.13 below. The demand is limited at the input, so that the hard stop is not reached, this limit will also make the model act better after position integrator limitation. There are also angular rate saturations that limit the maximum rate that can be achieved (in the leftmost integrator of Figure 2.13). Angular acceleration is also limited, corresponding to an amplitude limit in the torque of the motor.

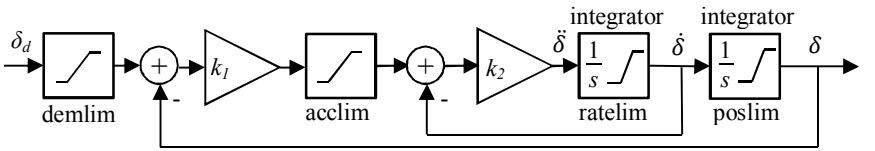

Figure 2.13 Block diagram of actuator model used in simulations.

3 Aircraft Control

Using the derived dynamic model of the aircraft, a controller can be designed that will make the aircraft follow pilot demands by giving control demands to the actuators which move the control surfaces of the aircraft.

The control objective is to follow demands in roll rate, angle of attack and angle of sideslip. In an aircraft positive/negative roll rate demand is proportional to right/left pilot stick deflection and positive angle of attack demand corresponds to the pilot pulling the stick backwards [1]. Angle of sideslip is demanded by pushing foot-pedals to the right and to the left.

Control will be designed according to Figure 3.1 using a linear state feedback L as a baseline controller. Feedforward from reference signals FF will be added to reduce known effects in order to make the nominal system together with the linear state feedback act similar to the desired reference dynamics. An adaptive controller will be augmented to the baseline controller and different characteristics of these two designs (with and without the adaptive controller) will be examined.

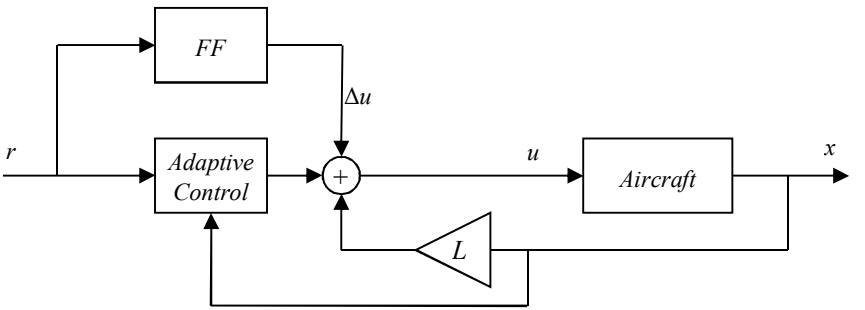

Figure 3.1 Controller design built up by Feedforward from reference (*FF*), Adaptive controller and linear state feedback (*L*).

3.1 Linear dynamics

A linearization of the flight dynamics is made in order to create adequate reference systems for adaptive controllers. Reference systems will also be

used to design a corresponding linear state feedback and to design feedforward signals from pilot demands.

Expressions from Section 2.1 will be linearized around zero angle of attack/sideslip. One state space equation for the pitch dynamics and one for the roll-yaw dynamics will be created assuming that the airspeed is maintained by the propulsion and also assuming linear aerodynamics as in (2.23).

There are no linear dependencies between the states of these two models (pitch vs. roll-yaw) and therefore no (linear) information will be lost even though the dynamics are split into two separate parts. Couplings from the roll-yaw motion to the pitch motion are nonlinear around zero values, due to the symmetry of the airframe. That is, couplings from sideslip to pitch motion is the same from both a right and left flat-turn and therefore nonlinear.

Coefficients related to angle of attack/sideslip time derivatives:

$$C_{N_{\dot{\alpha}}}, C_{m_{\dot{\alpha}}}, C_{C_{\dot{\beta}}}, C_{n_{\dot{\beta}}} \tag{3.1}$$

have been left out in this section. They could be incorporated but would result in more complicated algebraic expressions. When the linearization is done numerically, to generate controllers for simulations in Section 4, coefficients related to angle of attack/sideslip time derivatives are included in the design and therefore (nominally) compensated for. Full expressions, including all aerodynamic coefficients, are presented in Appendix.

Linear Pitch dynamics

In pitch motion there is one input from elevator deflection δ_e that affects two states: angle of attack α and nose-up angular rate q.

The linearized pitch dynamics will use the following state space form:

$$\dot{x}_p = A_p x_p + B_p \delta_e \tag{3.2}$$

Linearized pitch dynamics from (2.27), matrix elements expressed:

$$\begin{pmatrix} \dot{\alpha} \\ \dot{q} \end{pmatrix} = \begin{pmatrix} -\frac{q_d S}{mV} C_{N_\alpha} & 1 - \frac{q_d Sc}{2mV^2} C_{N_q} \\ \frac{q_d Sc}{I_y} C_{m_\alpha} & \frac{q_d Sc^2}{2I_y V} C_{m_q} \end{pmatrix} \begin{pmatrix} \alpha \\ q \end{pmatrix} + \begin{pmatrix} -\frac{q_d S}{mV} C_{N\delta_e} \\ \frac{q_d Sc}{I_y} C_{m\delta_e} \end{pmatrix} \delta_e \tag{3.3}$$

Linear Roll-Yaw dynamics

In roll-yaw motion there are two inputs, aileron δ_a and rudder δ_r, that affect three states p, β and r.

The linearized roll-yaw dynamics will use the following state space form:

$$\dot{x}_y = A_y x_y + B_y \begin{pmatrix} \delta_a \\ \delta_r \end{pmatrix} \tag{3.4}$$

Matrix elements expressed for linearized roll-yaw dynamics from (2.27), where some simplifications are made since I_{xz} is small compared to diagonal elements in I_i, as in [1], p.194:

$$\begin{pmatrix} \dot{p} \\ \dot{\beta} \\ \dot{r} \end{pmatrix} = \begin{pmatrix} \frac{q_d Sb^2}{2I_x V}\left(C_{l_p} + \frac{I_{xz}}{I_z}C_{n_p}\right) & \frac{q_d Sb}{I_x}\left(C_{l_\beta} + \frac{I_{xz}}{I_z}C_{n_\beta}\right) & \frac{q_d Sb^2}{2I_x V}\left(C_{l_r} + \frac{I_{xz}}{I_z}C_{n_r}\right) \\ -\frac{q_d Sb}{2mV^2}C_{C_p} & -\frac{q_d S}{mV}C_{C_\beta} & -1-\frac{q_d Sb}{2mV^2}C_{C_r} \\ \frac{q_d Sb^2}{2I_z V}\left(C_{n_p} + \frac{I_{xz}}{I_x}C_{l_p}\right) & \frac{q_d Sb}{I_z}\left(C_{n_\beta} + \frac{I_{xz}}{I_x}C_{l_\beta}\right) & \frac{q_d Sb^2}{2I_z V}\left(C_{n_r} + \frac{I_{xz}}{I_x}C_{l_r}\right) \end{pmatrix} \begin{pmatrix} p \\ \beta \\ r \end{pmatrix} + \begin{pmatrix} \frac{q_d Sb}{I_x}\left(C_{l\delta_a} + \frac{I_{xz}}{I_z}C_{n\delta_a}\right) & \frac{q_d Sb}{I_x}\left(C_{l\delta_r} + \frac{I_{xz}}{I_z}C_{n\delta_r}\right) \\ -\frac{q_d S}{mV}C_{C\delta_a} & -\frac{q_d S}{mV}C_{C\delta_r} \\ \frac{q_d Sb}{I_z}\left(C_{n\delta_a} + \frac{I_{xz}}{I_x}C_{l\delta_a}\right) & \frac{q_d Sb}{I_z}\left(C_{n\delta_r} + \frac{I_{xz}}{I_x}C_{l\delta_r}\right) \end{pmatrix} \begin{pmatrix} \delta_a \\ \delta_r \end{pmatrix} \tag{3.5}$$

3.2 Reference system design

The linear system derived for pitch and roll-yaw motion will be used to create reference systems with desired dynamics. Reference systems are needed for most adaptive control designs such as in [5] and [23]. Open-loop system dynamics achieved for aerial vehicles of today are often poorly damped and sometimes deliberately unstable so they cannot be used as a reference for desired dynamics straight away. (This in contrast to the old direct-stick-to-surface days, where an open-loop system was designed which had manageable properties, because a man in the loop was the only controller, the Wright Flyer being a notable exception, man-in-the-loop control with unstable pitch dynamics)

Reference system creation is done by designing a linear state feedback which places the poles of the system so that desired, yet achievable, dynamics are realized. This way an arbitrary aerial vehicle, with properties that can be linearized, can be applied by this method.

This linear state feedback will also form an inner loop together with the augmented adaptive controller. This, together with feedforward from reference, will create a system that nominally does not activate the adaptive controller. This is the case since the reference model in the adaptive controller and the system, as it appears to the adaptive controller, nominally has equal dynamics (if actuator dynamics is negligible, otherwise see Section 3.5). The adaptive controller will then only act on (unavoidable) imperfections in the system consisting of the flight dynamics, controlled by the state feedback, aided by the feedforward.

Pitch dynamics

The goal is to find a parameter, related to the nominal flight dynamics, which will make it possible to scale reference systems suitable to the present flight conditions. First a fundamental characteristic of the pitch motion is found. Then this characteristic is used to decide a linear state feedback that creates a reference system that is fast and yet reachable.

Pitch dynamics, open-loop

To find fundamental dynamics of the pitch motion, the moment coefficient related to angle of attack is set to zero. Setting $C_{m_\alpha} = 0$ in the linearized pitch dynamics (3.3) results in the lower left element in the state matrix being zero as in:

$$\begin{pmatrix} \dot{\alpha} \\ \dot{q} \end{pmatrix} = \begin{pmatrix} -\frac{q_d S}{mV} C_{N_\alpha} & 1 - \frac{q_d Sc}{2mV^2} C_{N_q} \\ 0 & \frac{q_d Sc^2}{2I_y V} C_{m_q} \end{pmatrix} \begin{pmatrix} \alpha \\ q \end{pmatrix} + \begin{pmatrix} -\frac{q_d S}{mV} C_{N\delta_e} \\ \frac{q_d Sc}{I_y} C_{m\delta_e} \end{pmatrix} \delta_e \qquad (3.6)$$

This corresponds to that aerodynamic force due to angle of attack acts through the center of gravity and will display fundamental characteristics of the pitch motion.

With $C_{m_\alpha} = 0$ the inverse of the two diagonal elements in A_p become the eigenvalues of the matrix and equivalently the poles of the system. Now two time constants are defined in relation to these poles as follows:

$$T_{sp} = \frac{1}{\frac{q_d S}{mV} C_{N_\alpha}} \qquad \tau_{\omega p} = -\frac{1}{\frac{q_d S c^2}{2 I_y V} C_{m_q}} \tag{3.7}$$

These time constants define the position of the systems two poles when $C_{m_\alpha} = 0$ as seen in the Figure 3.2 root locus.

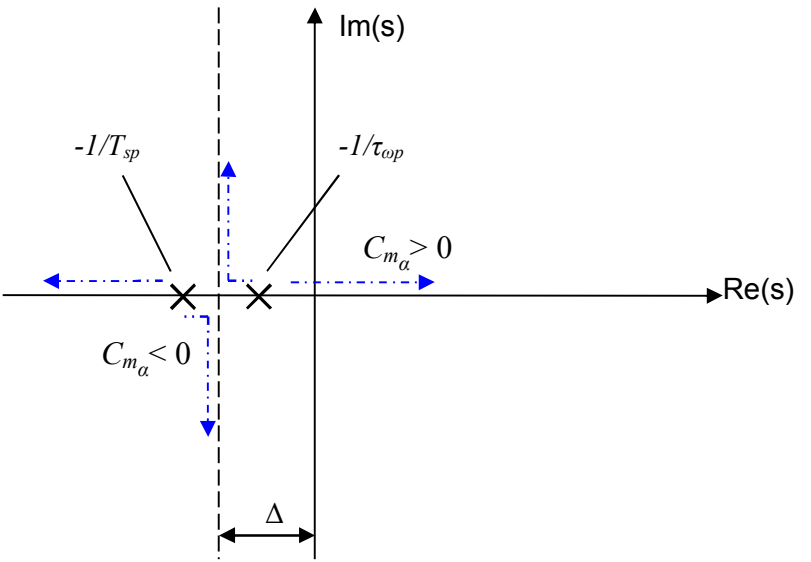

Figure 3.2 Root locus of pitch dynamics as C_{m_α} goes from 0 to negative and from 0 to positive values.

As C_{m_α} goes to large negative values the poles will meet and form a complex-conjugated pair that follows the dashed line with negative and positive imaginary values. As C_{m_α} goes to positive values, one pole goes in to the right half-plane (destabilizing the configuration) and the other goes further into the left half-plane. Using linear state feedback from α to δ_e can be seen as manipulating the value of C_{m_α} to move pole positions and when

adding feedback from angular rate q the poles can be placed even more arbitrary.

This fundamental line, in-between the poles, is defined by its distance to the imaginary axis and gives information about the rise-time that can be expected from the system. The distance to the imaginary axis is:

$$\Delta = \frac{1}{2}\left(\frac{1}{T_{sp}} + \frac{1}{\tau_{\omega p}}\right) \tag{3.8}$$

and this distance will be used to place poles for the reference system later on.

Possible rise-time of the system is of course also defined by the available control signal amplitude, in this case aerodynamic control surface deflection. It is most often the case and it is assumed here, that in these aeronautical applications, the control surface deflection amplitude and efficiency is designed from the start to be sufficient for normal maneuver amplitudes, so that the poles in Figure 3.2 characterize the possible system performance.

Also actuator dynamics play a role in possible speedup of system dynamics. It is assumed that actuator dynamics are faster than the flight dynamics poles that are placed by state feedback in these applications, so they can be neglected in a large part of the airspeed and altitude envelope. In regions of the envelope with high dynamic pressure, actuator dynamics could limit the possible reference bandwidth.

Pitch reference dynamics and linear state feedback

A relevant reference system will be created by using the nominal dynamics with an applied state feedback. This feedback should give fast dynamics while respecting the natural dynamics set by the physical design. A feedback gain will be created by speeding up the system using the distance Δ in Figure 3.2 and scale this "angular frequency" by a parameter denoted p_{factor}.

Linear state feedback will be applied:

$$\delta_e = -L_p \begin{pmatrix} \alpha \\ q \end{pmatrix} = -\begin{pmatrix} l_1 & l_2 \end{pmatrix} \begin{pmatrix} \alpha \\ q \end{pmatrix} \tag{3.9}$$

The closed-loop system will have the following state space matrix A_{mp} which will be given desired eigenvalues:

$$A_{mp} = A_p - B_p L_p = \begin{pmatrix} a_{11} - b_1 l_1 & a_{12} - b_1 l_2 \\ a_{21} - b_2 l_1 & a_{22} - b_2 l_2 \end{pmatrix} \tag{3.10}$$

The poles given by $-1/T_{sp}$ and $-1/\tau_{\omega p}$ are moved from their original positions (black), to positions further into the left half plane (blue), as illustrated in Figure 3.3.

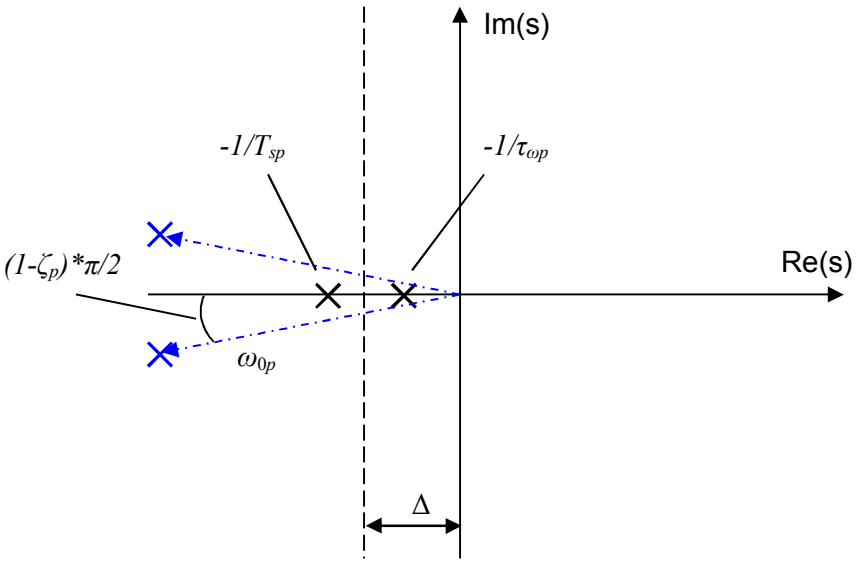

Figure 3.3 Poles of the reference system, moved by the feedback into desired position.

This task is started by expressing dynamics, in the parameters ω_{0p} and ς_p for pole assignment (in Figure 3.3). This new parameterized system is expressed in state-space form and it will be possible to decide how to choose an L_p that gives the desired dynamics by identifying elements in A_{mp}. Parameters will also be added to express zeros and steady-state gains of the system, denoted ω_{1p} and τ_{sp}.

The transfer function from control signal δ_e to angle of attack α, using parameters related to poles and zeros is:

$$\alpha(s) = K_{gp}^{-1} \frac{\frac{s}{\omega_{1p}} + 1}{\frac{s^2}{\omega_{0p}^2} + 2\zeta_p \frac{s}{\omega_{0p}} + 1} \delta_e(s) \tag{3.11}$$

where K_{gp} parameterizes the inverse of the steady-state gain from δ_e to α.

This will later on lead to dynamics from demanded angle of attack α_d to controlled angle α according to:

$$\alpha(s) = \frac{\frac{s}{\omega_{1p}} + 1}{\frac{s^2}{\omega_{0p}^2} + 2\zeta_p \frac{s}{\omega_{0p}} + 1} \alpha_d(s) \tag{3.12}$$

The transfer function from control signal δ_e to pitch angular rate q becomes:

$$q(s) = K_{gp}^{-1} \frac{s + \frac{1}{\tau_{sp}}}{\frac{s^2}{\omega_{0p}^2} + 2\zeta_p \frac{s}{\omega_{0p}} + 1} \delta_e(s) \tag{3.13}$$

These transfer functions also give the following relation between α and q, independent of δ_e:

$$\alpha(s) = \frac{\frac{s}{\omega_{1p}} + 1}{s + \frac{1}{\tau_{sp}}} q(s) \tag{3.14}$$

which shows that the steady-state gain between α and q is governed by the parameter τ_{sp}. This parameter, the so called turning rate time constant ([9] p.489), will be unaffected by feedback and is closely related to T_{sp} in (3.7):

$$\tau_{sp} = T_{sp}\left(1 - \frac{C_{m_\alpha} C_{N\delta_e}}{C_{N_\alpha} C_{m\delta_e}}\right)^{-1} \tag{3.15}$$

where the factor which scales T_{sp} compensate for the trim gain or trim loss depending on the magnitude and positions at which the force due to angle of attack and control surfaces act on the body as mentioned in Section 2.3.

Also the parameter ω_{1p} will be unaffected by feedback and it is related to elements in A_p and B_p according to:

$$\omega_{1p} = \frac{a_{12} b_2}{b_1} - a_{22} \tag{3.16}$$

Expressed in these parameters, state-space for the pitch motion becomes:

$$\begin{pmatrix} \dot{\alpha} \\ \dot{q} \end{pmatrix} = k_p \begin{pmatrix} -\frac{1}{\tau_{sp}} + \frac{1}{\omega_{1p}}\left(\frac{2\zeta_p \omega_{0p}}{\tau_{sp}} - \omega_{0p}^2\right) & 1 - \frac{1}{\omega_{1p}}\left(2\zeta_p \omega_{0p} - \frac{\omega_{0p}^2}{\omega_{1p}}\right) \\ \frac{2\zeta_p \omega_{0p}}{\tau_{sp}} - \omega_{0p}^2 - \frac{1}{\tau_{sp}^2} & \frac{1}{\tau_{sp}} - 2\zeta_p \omega_{0p} + \frac{\omega_{0p}^2}{\omega_{1p}} \end{pmatrix} \begin{pmatrix} \alpha \\ q \end{pmatrix} + \omega_{0p}^2 K_{gp}^{-1} \begin{pmatrix} \frac{1}{\omega_{1p}} \\ 1 \end{pmatrix} \delta_e, \quad k_p = \frac{1}{1 - \frac{1}{\omega_{1p}\tau_{sp}}} \tag{3.17}$$

To get desired dynamics the following expression that scales response is defined:

$$\omega_{0p} = p_{factor}\Delta = p_{factor}\frac{1}{2}\left(\frac{1}{T_{sp}} + \frac{1}{\tau_{\omega p}}\right) \tag{3.18}$$

Finally, feedback gains $L_p = (l_1 \;\; l_2)$ can be determined that will give the desired dynamics:

$$B_p L_p = \begin{pmatrix} b_1 l_1 & b_1 l_2 \\ b_2 l_1 & b_2 l_2 \end{pmatrix} = A_p - A_{mp} \tag{3.19}$$

The expression in (3.19) is over-determined for l_1 and l_2 but thanks to the tailored parameterization in (3.17), an L_p that solves the equation exactly will be found. The difference between the system's nominal and desired A-matrix is in the span of the B-matrix.

This p_{factor} becomes a reference system tuning parameter that will work on fundamentals of the flight dynamics, it will be tuned once and then the current flight condition and airframe configuration will place the poles in suitable positions.

Roll-Yaw dynamics

The roll-yaw feedback is chosen in a similar way to the pitch feedback. That is, fundamental characteristics of the flight dynamics are found and this is used to speed up the dynamics to a desired degree. In roll-yaw there are three poles to be placed. Two poles from yaw motion are similar to the ones in pitch. One additional pole comes from the roll motion, a first-order system with a stable pole.

Linear state feedback will be applied:

$$\begin{pmatrix} \delta_a \\ \delta_r \end{pmatrix} = -L_y \begin{pmatrix} p \\ \beta \\ r \end{pmatrix} \tag{3.20}$$

and a feedback gain L_y will be created so that:

$$A_{my} = A_y - B_y L_y \tag{3.21}$$

gets desired dynamics.

This is done by setting elements of the state space matrix A_{my} to desired values:

$$A_{my} = \begin{pmatrix} a_{11} - b_{11}l_{11} - b_{12}l_{21} & a_{12} - b_{11}l_{12} - b_{12}l_{22} & a_{13} - b_{11}l_{13} - b_{12}l_{23} \\ a_{21} - b_{21}l_{11} - b_{22}l_{21} & a_{22} - b_{21}l_{12} - b_{22}l_{22} & a_{13} - b_{21}l_{13} - b_{22}l_{23} \\ a_{31} - b_{31}l_{11} - b_{23}l_{21} & a_{32} - b_{31}l_{12} - b_{32}l_{22} & a_{33} - b_{31}l_{13} - b_{32}l_{23} \end{pmatrix} \tag{3.22}$$

The pitch procedure can be used for the four lower right elements of A_{my}, due to similar dynamics in α and q compared to β and r. The upper left element will set desired roll dynamics and finally for the four remaining elements of A_{my}, an L_y is chosen so that these elements get zero values. This will isolate the roll motion p from the yaw motion β and r (in this linear approximation).

Roll dynamics, open-loop and reference

Roll rate p obeys the following simple equation when focusing purely on its relation to roll control input δ_a (for the moment neglecting its couplings to other states β and r):

$$\dot{p} = a_{11}p + b_{11}\delta_a = \frac{q_d S b^2}{2I_x V} C_{l_p} p + \frac{q_d S b}{I_x} C_{l\delta_a} \delta_a = -\frac{1}{\tau_{r0}} p + \frac{1}{k_{g0}} \delta_a \qquad (3.23)$$

The desired dynamics is set by the parameter τ_r:

$$\dot{p} = -\frac{1}{\tau_r} p + \frac{1}{k_{gr}} p_d \qquad (3.24)$$

The open-loop dynamics will be made faster by feedback to a degree expressed by r_{factor}:

$$\tau_r = r_{factor}\, \tau_{r0} \qquad (3.25)$$

This τ_r will be used create the reference system dynamics.

Yaw dynamics, open-loop and reference

A method analogue to what was used in pitch dynamics will be applied to the yaw dynamics, the lower right four elements of A_{my}.

The relations for pitch dynamics can be used after replacing all entries in equations with the corresponding yaw aerodynamics and mass properties. Similarly in this case, parameters for desired dynamics are defined and denoted ω_{0y} and ς_y for poles, ω_{1y} and τ_{sy} for zeros.

With $C_{n_\beta} = 0$ in this case, time constants are defined for the yaw motion as follows:

$$T_{sy} = \frac{1}{\frac{q_d S}{mV} C_{C_\beta}} \qquad \tau_{\omega y} = -\frac{1}{\frac{q_d S b^2}{2I_y V} C_{n_r}} \qquad (3.26)$$

Parameters corresponding to transfer function zeros will as for the pitch channel be unaffected by feedback so τ_{sy} becomes:

$$\tau_{sy} = T_{sy}\left(1 - \frac{C_{n_\beta} C_{C\delta_r}}{C_{C_\beta} C_{n\delta_r}}\right)^{-1} \tag{3.27}$$

and ω_{1y} will be related to elements in A_y and B_y according to

$$\omega_{1y} = \frac{a_{23} b_{32}}{b_{22}} - a_{33} \tag{3.28}$$

To get adequate dynamics the following factor that speeds up dynamics is defined:

$$\omega_{0y} = y_{factor}\,\Delta = y_{factor}\,\frac{1}{2}\left(\frac{1}{T_{sy}} + \frac{1}{\tau_{\omega y}}\right) \tag{3.29}$$

Roll-Yaw reference dynamics and linear state feedback

A matrix A_{my} with the following values for the roll-yaw reference system will be created:

$$A_{my} = \begin{pmatrix} -\frac{1}{\tau_r} & 0 & 0 \\ 0 & \frac{1}{1-\frac{1}{\omega_{1y}\tau_{sy}}}\left(-\frac{1}{\tau_{sy}} + \frac{1}{\omega_{1y}}\left(\frac{2\zeta_y\omega_{0y}}{\tau_{sy}} - \omega_{0y}^2\right)\right) & \frac{1}{1-\frac{1}{\omega_{1y}\tau_{sy}}}\left(1 - \frac{1}{\omega_{1y}}\left(2\zeta_y\omega_{0y} - \frac{\omega_{0y}^2}{\omega_{1y}}\right)\right) \\ 0 & \frac{1}{1-\frac{1}{\omega_{1y}\tau_{sy}}}\left(\frac{2\zeta_y\omega_{0y}}{\tau_{sy}} - \omega_{0y}^2 - \frac{1}{\tau_{sy}^2}\right) & \frac{1}{1-\frac{1}{\omega_{1y}\tau_{sy}}}\left(\frac{1}{\tau_{sy}} - 2\zeta_y\omega_{0y} + \frac{\omega_{0y}^2}{\omega_{1y}}\right) \end{pmatrix} \tag{3.30}$$

Then the roll and yaw motion in (3.30) are separated by zero gains at four relevant positions. This will not always be fully achieved by a state feedback but a good approximation will be found below.

Feedback gains L_y that will give the desired dynamics are determined by the following relation:

$$B_y L_y = A_y - A_{my} \tag{3.31}$$

This relation is, as for pitch, over-determined but this time a least-squares solution will give good results, as long as the first element of the second row of A_y is close to zero:

$$A_y = \begin{pmatrix} \frac{q_d Sb^2}{2I_x V}\left(C_{l_p} + \frac{I_{xz}}{I_z}C_{n_p}\right) & \frac{q_d Sb}{I_x}\left(C_{l_\beta} + \frac{I_{xz}}{I_z}C_{n_\beta}\right) & \frac{q_d Sb^2}{2I_x V}\left(C_{l_r} + \frac{I_{xz}}{I_z}C_{n_r}\right) \\ -\frac{q_d Sb}{2mV^2}C_{C_p} & -\frac{q_d S}{mV}C_{C_\beta} & -1-\frac{q_d Sb}{2mV^2}C_{C_r} \\ \frac{q_d Sb^2}{2I_z V}\left(C_{n_p} + \frac{I_{xz}}{I_x}C_{l_p}\right) & \frac{q_d Sb}{I_z}\left(C_{n_\beta} + \frac{I_{xz}}{I_x}C_{l_\beta}\right) & \frac{q_d Sb^2}{2I_z V}\left(C_{n_r} + \frac{I_{xz}}{I_x}C_{l_r}\right) \end{pmatrix} \quad (3.32)$$

The element that has to be small in (3.32) is usually negligible in the linear approximation that was made in Section 3.1. This corresponds to that the sideway force due to roll angular rate p is relatively small (the coefficient C_{C_p} is small). This is the case for most aerial vehicles since forces due to angular rates are small when compared to other forces.

In the nonlinear real world this p to β coupling is small as long as the angle of attack α is close to zero as can be seen in (2.27). However α cannot be assumed to be small and some effort to reduce the coupling needs to be done. In the design made here, couplings of this type are reduced by feedforward (Section 3.3) instead of feedback.

So the feedback gains L_y found by a least-squares solution will be correct from a linear point of view and other couplings will be taken care of by feedforward signals. As for pitch there will be a roll-yaw steady state gain K_{gy} that parameterizes the inverse of the static gain from δ_a and δ_r to roll rate p and angle of sideslip β.

Comment on choosing the linear state feedback gain

When choosing a state feedback gain L that will give desired linear dynamics an approximation to the following over-determined relation is done:

$$BL = A - A_m \quad (3.33)$$

In (3.33), A_m now corresponds to the desired reference dynamics and A is the state-space matrix for the roll, pitch and yaw dynamics with five states in total. B is the gain from three control surface deflections to these five state derivatives.

When the reference system is used for adaptive control, the elements in A_m that could not be cancelled out by L could be set to zero. Then the

adaptive part of the controller will reduce the undesired coupling that the linear feedback cannot cancel. This has not been necessary in the application here since non-zero elements are negligible.

If a linear combination of states and inputs are measured, so that:

$$y_m = C_m x + D_m u \tag{3.34}$$

as opposed to the states being measured directly, the expression in (3.33) is changed. This would be the case if linear acceleration is measured by sensors in the airframe, a common aerospace configuration.

Then the measurement could be fed back as:

$$u = -Ly_m = -LC_m x - LD_m u \tag{3.35}$$

which implies that:

$$u = -\left(I + LD_m\right)^{-1} LC_m x \tag{3.36}$$

Instead of (3.33) this would mean that the following equation:

$$C_m B\left(I + LD_m\right)^{-1} L = A - A_m \tag{3.37}$$

should be solved or approximated for L to find the linear feedback gain that gives desired dynamics.

Comparison to an LQ-feedback law

The pole-placement procedure that is carried out could be questioned with respect to its resulting controller qualities. Therefore the result of the pole placement could be compared to a linear-quadratic (LQ) feedback law which is known to give suitable controllers, especially for aeronautical applications [34].

Such comparisons have been done for the flight dynamics in this work. For a system with five poles, pole placement is equivalent to an LQ-feedback. That is, there is an equivalent feedback gain L created with LQ methodology for both pitch and roll-yaw as the one created by the ω_0 and ς parameters of Figure 3.3.

For example in pitch motion of this application, a quick LQ check gives that a state weight matrix with diagonal elements 2 and 0 combined with a control signal weight of 1, creates an L_p which results in poles placed with a relative norm error of less than 10 % compared to the pole positions generated by the reference system in this application.

So using the proposed method, instead of designing a feedback gain L with LQ-weighting matrices, an L can be found by choosing the more intuitive parameters ω_{0p}, ς_p, ω_{0y}, ς_y and τ_r. This will result in similar robustness features as would be the case with LQ-design using feedback from the states α, β, p, q and r.

Comparison to acceleration feedback control

Linear state feedback controllers discussed so far achieve demanded angle of attack α and angle of sideslip β. An alternative is to control linear acceleration in body y-axis a_y and z-axis a_z. Demand and control of such lateral and vertical acceleration is often used in missile applications.

Acceleration perpendicular to the body x-axis is in a linear view proportional to α and β, with the addition of smaller terms proportional to control surface deflection and angular velocity. So control of α is in many respects equal to body z-acceleration control and the same is valid for β and body y-acceleration. Below it will be shown that under linear assumptions the two are equivalent.

Looking at pitch control, acceleration in z-axis a_z becomes:

$$a_z = -\frac{q_d S}{m}\left(C_{N_\alpha}\alpha + C_{N\delta_e}\delta_e + \frac{c}{2V} C_{N_q} q \right) \tag{3.38}$$

and this gives a relation between acceleration and angle of attack:

$$\alpha = \frac{1}{C_{N_a}}\left(\frac{m}{q_d S} a_z - C_{N\delta_e}\delta_e - \frac{c}{2V} C_{N_q} q \right) \tag{3.39}$$

So the control law which feeds back α:

$$\delta_e = -l_\alpha \alpha - l_q q + k_\alpha \alpha_d \tag{3.40}$$

is equivalent to the z-acceleration feedback law:

$$\begin{aligned} \delta_e &= \frac{1}{1 - l_\alpha \dfrac{C_{N\delta_e}}{C_{N_\alpha}}}\left(l_\alpha \frac{q_d S}{m C_{N_\alpha}} a_z + \left(-l_q + l_\alpha \frac{c}{2V}\frac{C_{N_q}}{C_{N_\alpha}} \right) q \right) + k_{az} a_{zd} \\ &= -l_{az} a_z - l_{qa} q + k_{az} a_{zd} \end{aligned} \tag{3.41}$$

So for every state feedback using α there is an equivalent feedback law that uses a_z instead. By choosing l_{az} and l_{qa} according to (3.41) and feeding

back a_z and q, a closed-loop will be created with same dynamics as the one created by instead feeding back α and q with gains l_α and l_q.

This comparison between feeding back α and a_z indicates that results and conclusions achieved by the work done here can be used for pitch and yaw acceleration control as well. Linear dynamics will be the same for both principles. Sensitivity to noise and other imperfections will be similar but not equivalent.

The non-minimum phase of acceleration control for an aerial vehicle with tail control surfaces can be problematic; on the other hand canard control gives non-minimum phase response to angle of attack. When creating reference systems for L1 adaptive controllers a non-minimum phase zero give problems since an inversion of the reference system is taking place. Both angle of attack and acceleration control principles can have the issue of non-minimum phase depending on front and aft control surface placement. Instead of controlling acceleration in the center of gravity, controlling acceleration of a position that is in front of the center of percussion [26] provides a way to overcome non-minimum phase problems.

An advantage with acceleration control is that when maneuvering to reach a position it is natural to demand acceleration, since double integration over time connects the two. Also limits in structural and human load factor are given in acceleration, so to handle these limits, acceleration control is more convenient. On the other hand, validated aerodynamics intervals and engine air intake limits are set by angle of attack/sideslip, so this fact favors control of angle quantities. Both acceleration and angle of attack/sideslip can be measured and or estimated. So, on the whole it is necessary to keep track of both acceleration and angle of attack/sideslip [34]. One of the quantities can be chosen as the control objective and attention to the other will be necessary in any case.

3.3 Nonlinear feedforward design

Feedforward terms will be added to the control signals to compensate for five different effects.

- The feedforward will take into account *deviation moments* due to mass asymmetries.
- Feedforward has been chosen as the method for making it possible to perform a *velocity vector roll*.
- It will also reduce *gravitational forces* influence to angle of attack and sideslip.
- *Aerodynamic drag* will be compensated by adding thrust through feedforward signals.
- Compensations to counteract pitch *force and moments at zero angle of attack* will be designed.

These effects are mainly nonlinear and with this feedforward compensation the feedback controller will work with a system that is closer to linear as proposed in [21]. Dynamic inversion [10], [32]and backstepping [12], [33] designs use the angular velocity vector as a virtual control signal to manipulate angle of attack/sideslip, as is done in the design created here. This feedforward design exploits the particular structure of flight dynamics. An alternative method to generate feedforward signals for nonlinear systems based on the notion of flatness is given in [20].

Design of feedforward from reference signals

There are six states to consider: V, α, β, p, q and r. Four control signals are available: control surface deflections δ_a, δ_e, δ_r and engine thrust T. By using that α and β over short periods of time are approximate time integrals of q and r, good compensations will be accomplished. There will be uncompensated phenomena and the feedforward itself will create disturbances in angle of attack and angle of sideslip but a design will be made for which these effects are limited.

State deviations from the nominal system that are created by the feedforward will be subtracted from measured states before these quantities go to the feedback controllers. The feedforward control signal Δu and the state deviations Δx are incorporated in the design as in Figure 3.4.

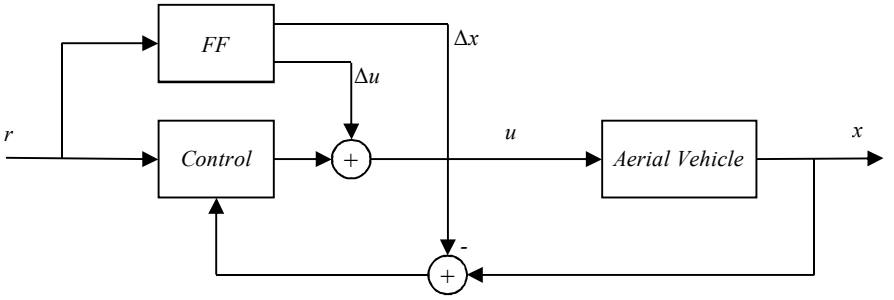

Figure 3.4 Feedforward *FF* generates deltas to control signal Δu and states Δx.

To be able to compensate using feedforward, nominal system state values over time are needed. To get state values over time ($\bar{\omega}$ and $\bar{v}$), copies of reference systems for the adaptive controller are used as in (3.86). They mimic the desired behavior of the system and obtaining state values from them will make this design feedforward. Using measured states would create an additional feedback which would jeopardize the overall stability or at least make it harder to analyze and guarantee (especially since nonlinearities will be created here). However, Euler angles will be used to compensate gravity, so this will create some feedback. Euler angles are one integration level above angular velocities $\bar{\omega}$ so this feedback is slow compared to other effects created by this feedforward.

An alternative would be to design feedback controllers that would compensate for one or several of the effects dealt with in this section. Here, the feedforward approach was chosen instead of feedback, it will compensate for known effects close to the intended trajectories and the adaptive controller will take care of other effects. The dynamics together with this feedforward will nominally be linear and similar to the reference systems. So the controllers will only need to deal with imperfections from this assumption. This is suitable for adaptive controllers since they use a

reference system and are designed to reduce deviation from this reference system. By adding feedforward the parameter interval that the adaptive controllers will be left with for dealing with deviation from reference system behavior will be larger using this design. A structure will be created in which the adaptive controller output will be close to zero if no model errors are at hand, since nonlinearities are compensated for, leaving the adaptive controller with signals that are exponential time functions, corresponding to what the reference systems of the adaptive controller were designed for.

In order to generate appropriate feedforward, nominal values for how the inputs affect the system are needed. This input gain and other aerodynamic dependencies of this feedforward design will assume that a linearization can be done as in (2.23). The linear part of generating moments by control surface deflection $\overline{M}_\delta \overline{\delta}$ obeys the equation:

$$\overline{M} = \overline{M}_0 + M_\delta \overline{\delta} = \overline{M}_0 + q_d S \begin{pmatrix} bC_{l\delta_a} & bC_{l\delta_e} & bC_{l\delta_r} \\ cC_{m\delta_a} & cC_{m\delta_e} & cC_{m\delta_r} \\ bC_{n\delta_a} & bC_{n\delta_e} & bC_{n\delta_r} \end{pmatrix} \begin{pmatrix} \delta_a \\ \delta_e \\ \delta_r \end{pmatrix} \tag{3.42}$$

where $\overline{M}_0$ is a collection of moments generated by other parts than control surfaces (and nonlinear effects of control surface deflection). The matrix M_δ is invertible since creating large diagonal elements in this matrix is essential to aerodynamic control surface design. Some non-diagonal elements in M_δ are usually zero, since there are usually no linear couplings between for example pitch elevator and roll moment.

Deviation moments

Deviation moments can be directly compensated for by feedforward since change in angular velocity follow Euler's equation:

$$\dot{\overline{\omega}} = I_i^{-1}(\overline{M} - \overline{\omega} \times I_i \overline{\omega}) \tag{3.43}$$

where the deviation moment (the last term) is added to the moments $\overline{M}$ which can be manipulated by feedforward according to (3.42).

This means that deviation moments can be compensated by adding the following term to the actuator demand:

$$\Delta u_1 = M_\delta^{-1}\left(\overline{\omega} \times I_i \overline{\omega}\right) \tag{3.44}$$

Here $\bar{\omega}$ elements are outputs p, q and r from reference systems with the same demands as the controller and with the added effects of compensations created from velocity vector roll rate (3.52) and gravitation (3.55).

This deviation moment feedforward term (3.44) will not create any delta effects in states Δx so the first term is zero:

$$\Delta x_1 = \bar{0} \tag{3.45}$$

Velocity vector roll rate

Compensations will be created so that the motion will be a velocity vector roll or a "bank to turn" as it also is called (in contrast to e.g. skid to turn). A demanded roll rate will be performed *around the velocity vector as opposed to the body x-axis* so that angle of attack/sideslip will follow the linear dynamics that are desired. Roll rotation around an axis close to the body x-axis in Figure 3.5 would otherwise be the case since the moment that roll control surfaces naturally create is around body x-axis. This rotation solely around body x-axis would create severe nonlinear cross-couplings between α and β which are undesired in many applications.

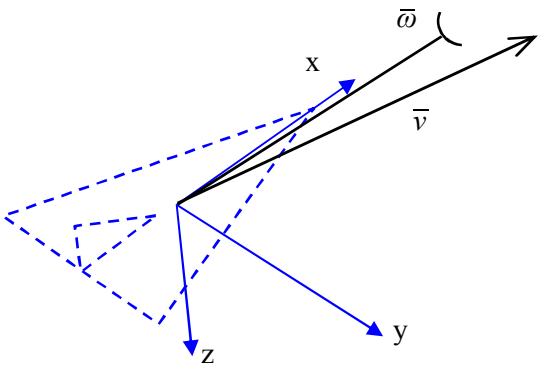

Figure 3.5 Body velocity vector $\bar{v}$ and body angular velocity vector $\bar{\omega}$.

This change of angular velocity vector, from body x-axis to velocity vector, will be accomplished by adding control surface deflections that make the angular velocity vector, corresponding to a roll rate demand, parallel to the velocity vector. The magnitude of this additional angular

velocity vector will be such that the projection onto the body x-axis will be the demanded roll rate.

When the roll angular velocity vector and velocity vector are parallel, small change in velocity vector components due to roll rate will be at hand, since the cross product will ideally be zero in Newton's second law:

$$\dot{\bar{v}} = \frac{1}{m}\bar{F} - \Delta\bar{\omega} \times \bar{v} \tag{3.46}$$

So the first element p in $\Delta\bar{\omega}$ will be created by the roll controller and the other two elements corresponding to additional pitch rate Δq_2 and yaw rate and Δr_2 will be created by feedforward so that this vector becomes parallel to $\bar{v}$. By expressing the velocity vector $\bar{v}$ in u, α and β using (2.8), the resulting angular velocity will be expressed in p, α and β, which is desired, since these are the states that are used for feedforward.

To achieve a pure bank to turn, the following cross product should be zero:

$$\Delta\bar{\omega} \times \bar{v} = \begin{pmatrix} p \\ \Delta q_2 \\ \Delta r_2 \end{pmatrix} \times \begin{pmatrix} u \\ v \\ w \end{pmatrix} = \begin{pmatrix} p \\ \Delta q_2 \\ \Delta r_2 \end{pmatrix} \times \begin{pmatrix} u \\ u\tan\beta/\cos\alpha \\ u\tan\alpha \end{pmatrix} = \bar{0} \tag{3.47}$$

so Δq_2 and Δr_2 are set to create an angular velocity vector parallel to the velocity vector:

$$\begin{pmatrix} p \\ \Delta q_2 \\ \Delta r_2 \end{pmatrix} = \begin{pmatrix} p \\ p\tan\beta/\cos\alpha \\ p\tan\alpha \end{pmatrix} \tag{3.48}$$

This change in Δq_2 and Δr_2 will be done by altering $\dot{\bar{\omega}}$ using (3.42) through changing the control surface generated moment in:

$$\dot{\bar{\omega}} = I_i^{-1}(\bar{M}_0 + M_\delta\bar{\delta} - \bar{\omega} \times I_i\bar{\omega}) \tag{3.49}$$

So using time derivatives of Δq_2 and Δr_2 the following addition to the control signal:

$$\Delta u_2 = M_\delta^{-1} I_i \frac{d}{dt} \begin{pmatrix} 0 \\ p \tan\beta / \cos\alpha \\ p \tan\alpha \end{pmatrix} \tag{3.50}$$

will accomplish the proper compensation. This addition to the control signal will create a desired addition to $\dot{\bar{\omega}}$, which will be integrated by flight dynamics over time to achieve the desired Δq and Δr.

Time derivation of Δq_2 and Δr_2 in (3.51) could be approximated by a transfer function:

$$\frac{s}{\frac{s}{\omega_a} + 1} \tag{3.51}$$

where ω_a is the bandwidth of the actuator system. This transfer function will create time derivatives of signals up to an angular frequency close to ω_a, any effort to feed signals forward beyond that bandwidth will be attenuated by the actuator anyway.

The added angular velocity due to this feedforward is:

$$\Delta x_2 = \begin{pmatrix} 0 \\ \Delta q_2 \\ \Delta r_2 \end{pmatrix} = \begin{pmatrix} 0 \\ p \tan\beta / \cos\alpha \\ p \tan\alpha \end{pmatrix} \tag{3.52}$$

so this quantity are subtracted from system states before being used in the controller. If not, the feedback part of the controller would reduce these elements Δq_2 and Δr_2 that are created by feedforward.

This compensation will create forces $\bar{F}$ that will disturb the angle of attack/sideslip but these deviations will be relatively small, since forces generated by control surface deflection and angular rates are small compared to the ones generated by e.g. angle of attack/sideslip.

Gravitation effects on angle of attack and sideslip

Compensation will be made so that the *change* in projection of the gravity vector onto the body system will not affect the control objective. In other words, even though the attitude changes over time and the force due to

gravity is inertial, workload will be taken off controllers in keeping the angle of attack/sideslip constant. No effort will be made here to counteract the constant effect of gravity, (for example to maintain altitude).

Angle of attack/sideslip derivative expressions in (2.27) will give input to what needs to be added to body rates q and r to compensate for gravity in (3.53).

$$\begin{pmatrix} \dot{\alpha} \\ \dot{\beta} \end{pmatrix} = \begin{pmatrix} q - \dfrac{q_d S}{mV} C_N - p \tan\beta + \dfrac{g}{V} \cos\Phi \cos\theta \\ -r - \dfrac{q_d S}{mV} C_C + p \sin\alpha + \dfrac{g}{V} \sin\Phi \cos\theta \end{pmatrix} \tag{3.53}$$

To compensate for that gravity will affect α and β, the same method as for a velocity vector roll is used. Additional rates Δq_3 and Δr_3 are used as virtual control signals to keep angle of attack/sideslip rates follow the linear dynamics that is desired.

Change in Δq_3 and Δr_3 will as for a velocity vector roll be done by altering $\dot{\bar{\omega}}$ using (3.42). So setting Δq_3 and Δr_3 to the corresponding last term in (3.53) and generating time derivatives of these quantities, the following addition to the control signal:

$$\Delta u_3 = M_\delta^{-1} I_i \frac{d}{dt} \begin{pmatrix} 0 \\ -\dfrac{g}{V} \cos\Phi \cos\theta \\ \dfrac{g}{V} \sin\Phi \cos\theta \end{pmatrix} \tag{3.54}$$

will compensate for gravity effects coming from that the attitude changes over time.

The time derivation in (3.54) could again be approximated using the transfer function in (3.51).

The added pitch and yaw rates due to this gravity compensation will be:

$$\Delta x_3 = \begin{pmatrix} 0 \\ \Delta q_3 \\ \Delta r_3 \end{pmatrix} = \frac{g}{V} \begin{pmatrix} 0 \\ -\cos\Phi \cos\theta \\ \sin\Phi \cos\theta \end{pmatrix} \tag{3.55}$$

so this quantity will be subtracted from the states before being used in feedback controllers.

The natural equilibrium point (constant states) that will be maintained by this design is zero angle of attack. In this case gravity will accelerate the body downwards by an amount corresponding to the gravity constant g and rotate the velocity vector downwards with an angular rate g/V accordingly. At this equilibrium, the body will rotate with a nose down rate corresponding to the rate at which the velocity vector is rotated by gravity. As the attitude changes, these angular rates will be projected to the y and z-axis of the body coordinate system according to the last terms of (3.53).

Another natural equilibrium point for an aerial vehicle is straight and level flight. During straight and level flight an angle of attack is maintained to counteract gravity and angle of sideslip and angular rates are zero. To maintain straight and level flight will be considered a guidance problem in this design. That is, the pilot or an altitude autopilot will be used to demand an appropriate nose up quantity to the controller that is designed.

Drag and gravity effects on airspeed

Aerodynamic drag effects will be compensated by adding propulsion thrust so that airspeed is maintained even though the motion effectuates angle of attack/sideslip demands. When angle of attack/sideslip is generated airspeed is reduced due to induced drag. Induced drag comes from that a large part of aerodynamic body forces ($q_d SC_C$ and $q_d SC_N$) are generated in a plane perpendicular to the body x-axis, not perpendicular to the velocity vector. Because of this property a significant part of the aerodynamic forces project onto the negative direction of the velocity vector and create induced drag. Also the gravity vector project onto the direction of the velocity vector and will be compensated for by feedforward thrust alteration.

According to (2.26) the change in airspeed V over time follows:

$$\dot{V} = \frac{1}{m}\left(F_x \cos\alpha \cos\beta + F_y \sin\beta + F_z \sin\alpha \cos\beta\right) \tag{3.56}$$

where force elements are:

$$\begin{aligned} F_x &= T - q_d S C_T - mg\sin\theta \\ F_y &= -q_d S C_C + mg\sin\Phi\cos\theta \\ F_z &= -q_d S C_N + mg\cos\Phi\cos\theta \end{aligned} \tag{3.57}$$

By adding a feedforward term to the thrust T denoted ΔT, aerodynamic and gravity effects can be reduced. It is assumed that the nominal thrust is set to counteract the zero incidence drag, $q_d S C_T$. So ΔT will compensate for the other terms that affect airspeed in (3.56).

The following addition ΔT to the thrust demand will nominally keep airspeed constant:

$$\Delta T = q_d S\left(C_C \frac{\tan\beta}{\cos\alpha} + C_N \tan\alpha \right) + mg \frac{\sin\gamma}{\cos\alpha\cos\beta} \tag{3.58}$$

where γ is the climb angle, the elevation angle of the velocity vector above the horizontal plane (the xy-plane of the inertial system). This angle γ is related to angle of attack/sideslip and Euler angles according to:

$$\sin\gamma = \sin\theta\cos\alpha\cos\beta - \cos\theta\left(\sin\Phi\sin\beta + \cos\Phi\sin\alpha\cos\beta\right) \tag{3.59}$$

Compensating force and moment at zero angle of attack

At zero angle of attack there are usually small aerodynamic forces and moments acting in the pitch channel. This is due to asymmetry of the airframe above compared to underneath the xz-plane of the body axis. The zero force coefficient C_{N_0} and the moment coefficient C_{m_0} in (2.23) will be compensated so that zero angle of attack is maintained. Small compensations in pitch rate and elevator deflections will be made assuming linear aerodynamics.

If zero α is desired as steady state in:

$$\begin{pmatrix} \dot{\alpha} \\ \dot{q} \end{pmatrix} = \begin{pmatrix} q - \dfrac{q_d S}{mV}\left(C_{N_0} + C_{N_\alpha}\alpha + C_{N\delta_e}\delta_e + \dfrac{c}{2V}\left(C_{N_q} q + C_{N_{\dot{\alpha}}}\dot{\alpha} \right) \right) \\ \dfrac{q_d S b}{I_y}\left(C_{m_0} + C_{m_\alpha}\alpha + C_{m\delta_e}\delta_e + \dfrac{c}{2V}\left(C_{m_q} q + C_{m_{\dot{\alpha}}}\dot{\alpha} \right) \right) \end{pmatrix} \tag{3.60}$$

the solution in pitch rate q and elevator δ_e becomes:

$$\begin{pmatrix} q_0 \\ \delta_{e_0} \end{pmatrix} = \begin{pmatrix} 1 - \frac{q_d Sc}{2mV^2} C_{N_q} & -\frac{q_d S}{mV} C_{N\delta_e} \\ \frac{q_d Sc}{2I_y V} C_{m_q} & \frac{q_d Sc}{I_y} C_{m\delta_e} \end{pmatrix}^{-1} \begin{pmatrix} \frac{q_d S}{mV} C_{N_0} \\ -\frac{q_d Sc}{I_y} C_{m_0} \end{pmatrix} \tag{3.61}$$

so the constant feedforward control signal to maintain zero α is:

$$\Delta u_5 = \begin{pmatrix} 0 \\ \delta_{e_0} \\ 0 \end{pmatrix} \tag{3.62}$$

and the constant deviation in pitch rate to maintain zero α becomes:

$$\Delta x_5 = \begin{pmatrix} 0 \\ q_0 \\ 0 \end{pmatrix} \tag{3.63}$$

Feedforward summary

Now the sought addition to the control signal Δu and state deviation Δx can be added up of terms Δu_i and Δx_i. Also, an addition to the thrust demand, ΔT has been obtained.

The linearized aerodynamic moment expression has a component that is dependent on the angular velocity as expressed by the last term in:

$$\overline{M} = \overline{M}_0 + M_\delta \overline{\delta} + M_\omega \overline{\omega} \tag{3.64}$$

This is a small effect but the adding the term $M_\omega \overline{\omega}$ to the feedforward signal compensates for this resistance to angular rates. This is done in the implemented and simulated design of the feedforward compensation.

It could be mentioned that if there is a spin vector and a corresponding mass inertia from a rotor in the propulsion (e.g. jet engine) that is significant, this effect could be compensated the same way as was made for mass inertia effects. The spin corresponds to the last term in the expression:

$$\dot{\overline{\omega}} = I_i^{-1}(\overline{M} - \overline{\omega} \times I_i \overline{\omega} - I_{sx} \overline{\omega} \times \overline{s}) \tag{3.65}$$

that could be compensated by feedforward. I_{sx} is a scalar corresponding to the rotor mass inertia and $\overline{s}$ is an angular velocity vector expressing the rotor spin relative body system coordinates. So an addition:

$$M_\delta^{-1}\left(I_{sx} \overline{\omega} \times \overline{s}\right) \tag{3.66}$$

to the feedforward signal would compensate for propulsion rotor spin.

To get a steady state roll angle that corresponds to the time integral of the roll rate demand, an addition to the state deviation Δx has been implemented. This addition to the roll rate p will be activated if the achieved roll angle Φ does not correspond to the time integral of the roll rate demand. This is done in order to get comparable diagrams and visualizations of the flight. The compensation is not activated over short periods, it will e.g. make the motion slowly roll to wings level in cases where the roll rate demand is not followed perfectly. It has also been incorporated in order to be at correct attitude for an upcoming roll demand with the intended start conditions.

3.4 L1 adaptive controller

An L1 adaptive controller will be augmented (added) to the design. The L1-controller will be used in an outer loop, where the inner loop has the flight dynamics as it is controlled by a linear state feedback with the additions of the feedforward from reference as in Figure 3.7. This inner loop dynamics will nominally have equal dynamics to the reference system dynamics that is used in the L1-controller.

In this application an L1 adaptive controller of piecewise constant type is applied to a pitch-unstable fighter aircraft. Piecewise constant refers to that the controller is sampled; it internally operates in discrete time and produces parameter estimates that are piecewise constant. These controllers use the system state as controller input and can compensate for matched and unmatched disturbances. Analysis and evaluation of L1-

controllers are performed together with comparisons to a typical linear state feedback control. Piecewise constant L1-controllers are fully defined in [6] Section 3.3.

Piecewise constant L1-controller design

The piecewise constant L1-controller uses a **state predictor**, an **adaptation law** and a **control law** according to:

State predictor:

$$\dot{\hat{x}}(t) = A_m \hat{x}(t) + B_m(u(t) + \hat{\sigma}_1(t)) + B_{um}\hat{\sigma}_2(t) \tag{3.67}$$

Adaptation law:

$$\begin{bmatrix} \hat{\sigma}_1(t) \\ \hat{\sigma}_2(t) \end{bmatrix} = M(\hat{x}(kT_s) - x(kT_s)) = -B^{-1}\Phi^{-1}(T_s)e^{A_m T_s}(\hat{x}(kT_s) - x(kT_s)) \tag{3.68}$$

where

$$B = \begin{bmatrix} B_m & B_{um} \end{bmatrix}, \quad \Phi = A_m^{-1}(e^{A_m T_s} - I)$$

Control law:

$$u(s) = C(s)\left(K_g r(s) - \hat{\sigma}_1(s) - H_m^{-1}(s)H_{um}(s)\hat{\sigma}_2(s)\right) \tag{3.69}$$

where

$$H_m(s) = CH_{xm}(s) = C(sI - A_m)^{-1}B_m$$

$$H_{um}(s) = CH_{xum}(s) = C(sI - A_m)^{-1}B_{um}$$

System state x and state predictor $\hat{x}$ are vectors of equal size. The state matrix A_m sets the desired reference dynamics. A natural choice for augmentation to a linear state feedback is $A_m = A\text{-}B_mL$, where A is the nominal linearized plant dynamics and L corresponds to the linear state feedback gain. The matrix C defines plant outputs, $y = Cx$ that will be controlled to follow the equally sized, demand vector r.

The matrix B_m, given by the plant input model, is called the matched input matrix, acting on the control signal u which has the same size as y and r. The matrix B_{um} is created as the null-space of B_m^T (solving the equation $B_m^T B_{um} = 0$) while keeping the square matrix $\begin{bmatrix} B_m & B_{um} \end{bmatrix}$ of full rank. This way an unmatched input matrix B_{um} is created orthogonal to the direction of the matched input B_m. The unmatched B_{um} is not unique even

if orthogonality is specified, a B_{um} with the same norm as B_m was chosen to be able to compare matched and unmatched parameter estimates in the controller.

Time argument kT_s in the adaptation law effectuates zero order sample and hold using index k at sampling intervals T_s, hence the name "L1 piecewise constant".

$H_m(s)$ is the reference transfer function from the matched input acting through B_m. $H_{um}(s)$ is the reference transfer function from unmatched inputs, which is how the outputs are affected in input directions that are orthogonal to the directions defined by B_m. This design (3.69) of creating one term in the control signal u by taking the estimated unmatched error and feed it through the inverse of the matched transfer function $H_m(s)$ and the unmatched transfer function $H_{um}(s)$, creates a way to compensate for unmatched disturbances. For each element in the control input u there is a matched element in $\hat{\sigma}$, unmatched elements are added so that the size of $\hat{\sigma}$ matches the total number of states. This is not unique for L1-control; the matched together with unmatched compensation could be used in other types of control designs.

The low-pass filter is realized as:

$$C(s) = \left(I + KD(s)\right)^{-1} KD(s) \tag{3.70}$$

Bandwidth is set by $KD(s)$ which in its simplest form is a diagonal matrix K and an integrator $1/s$. In the control law K_g is can be set to the steady state gain:

$$K_g = -(CA_m^{-1}B_m)^{-1} \tag{3.71}$$

This will, in steady state, couple one reference signal to one output signal by a unity gain. For the pitch L1-controller in this application, K_{gp} (a scalar) will be calculated to get correct nominal steady state gain from demanded to effectuated angle of attack. A matrix K_{gy} (2 by 2 elements) will be calculated for the roll-yaw L1-controller to handle gains from demanded roll rate and demanded angle of sideslip. Roll rate and angle of sideslip motion will nominally be separated from each other as mentioned in Section 3.3.

In Figure 3.6 a block diagram of a closed-loop system with an L1-controller is presented.

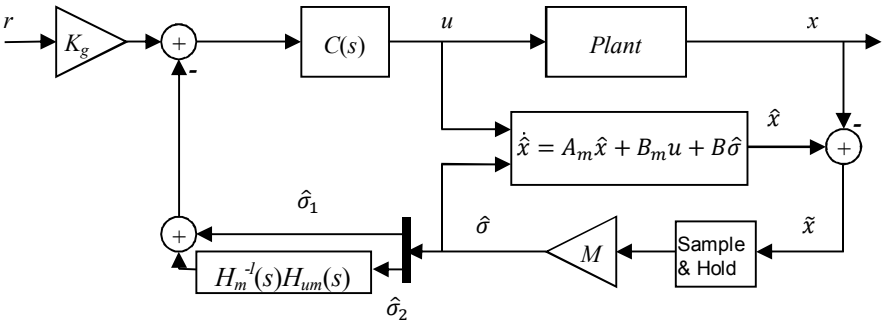

Figure 3.6 Block diagram of system with L1-controller of piecewise constant type [6].

For the pitch channel the L1-controller has two components in its estimate $\hat{\sigma}$, one matched and one unmatched. The roll-yaw L1-controller is similar, the main difference being that it has three components in $\hat{\sigma}$, two matched corresponding to the two input directions and one unmatched. Since control surface deflections in aeronautical applications most often produce moments which result in angular velocity, body rates p, q and r correspond to the matched directions. Unmatched directions mainly correspond to angle of attack and angle of sideslip respectively.

An anti-aliasing filter where the state x enters the controller in Figure 3.6 should be considered. However, since state measurements of x are sampled at the same or a lower frequency than the sampling rate in the L1-controller, it is assumed that the sensor has anti-aliasing filters that are tuned to the output rate. Also, it is common that the state x is estimated by an observer so that the state-estimate high-frequency contents will be limited. Results presented here correspond to an implementation with estimates from a state observer.

Piecewise constant L1-controller characteristics

Consider the following system with nonlinear state dependent input disturbances represented by matched and unmatched functions f_1 and f_2:

$$\begin{aligned} \dot{x}(t) &= A_m x(t) + B_m\left(u(t) + f_1\left(t, x(t)\right)\right) + B_{um} f_2\left(t, x(t)\right) \\ y(t) &= Cx(t) \end{aligned} \tag{3.72}$$

The reference system used in piecewise constant type of L1-control is [29]:

$$\begin{aligned} \dot{x}_{ref}(t) &= A_m x_{ref}(t) + B_m\left(u_{ref}(t) + f_1\left(t, x_{ref}(t)\right)\right) + B_{um} f_2\left(t, x_{ref}(t)\right) \\ u_{ref}(s) &= KD(s)\left(K_g r(s) - H_m^{-1}(s) C x_{ref}(s)\right) \\ y_{ref}(t) &= C x_{ref}(t) \end{aligned} \tag{3.73}$$

The reference system will be stable if certain limits related to the norms of f_1 and f_2 and to the norm of $KD(s)$ are fulfilled. It is proven in [6] that if the control signal is chosen as in (3.67), (3.68) and (3.69), the controlled system will follow the reference system within the following limits:

$$\begin{aligned} \left\| x_{ref} - x \right\|_{L_\infty} &< \gamma_1(T_s) \\ \left\| u_{ref} - u \right\|_{L_\infty} &< \gamma_2(T_s) \end{aligned} \quad \text{where} \quad \begin{aligned} \gamma_1(0) &= 0 \\ \gamma_2(0) &= 0 \end{aligned} \tag{3.74}$$

The reference system follows an ideal, desired system behavior:

$$y_{id}(s) = H_m(s) K_g r(s) \tag{3.75}$$

closer as the following sum of transfer function L1-norms decreases:

$$\left\| G_m(s) \right\|_{L_1} + \left\| G_{um}(s) \right\|_{L_1} l_0 \tag{3.76}$$

where the parameter l_0 is a ratio expressing a relative maximum rate of change in f_2 compared to f_1 and where:

$$
\begin{aligned}
G_m(s) &= H_{xm}(s)\big(I - C(s)\big) \\
G_{um}(s) &= \big(I - H_{xm}(s)C(s)H_m^{-1}(s)C\big)H_{xum}(s) \\
C(s) &= \big(I + KD(s)\big)^{-1}KD(s) \\
H_{xm}(s) &= \big(sI - A_m\big)^{-1}B_m \\
H_{xum}(s) &= \big(sI - A_m\big)^{-1}B_{um}
\end{aligned}
\tag{3.77}
$$

As the sampling period T_s goes to zero, the system in (3.72) will follow the reference system (3.73) arbitrarily closely. The reference system is unknown due to input disturbance functions f_1 and f_2, but it has a known response from these two unknown functions [14] and [15]. The functions γ_1 and γ_2 are of class K, that is strictly increasing from zero. The functions γ_1 and γ_2 become dependent on bounds on f_1 and f_2 and also on the L1-controller design elements, A_m, K and $D(s)$.

Comments on piecewise constant L1-control

A reference system (3.73) can be obtained that has stable but unknown responses from the reference signal r and from deviations entering via f_1 and f_2 to the output y. This reference system will be followed by the closed-loop system (3.72) arbitrarily closely as gains that speed up the response to the parameter estimates are increased in the L1-controller. The reference system will follow ideal, desired system dynamics closer as L1-norms (hence the name "L1") of transfer functions $G_m(s)$ and $G_{um}(s)$ are decreased (3.76), by choosing desired dynamics set by the matrix A_m and controller design parameters K and $D(s)$.

It is an important observation that stability and performance guarantees are easy to obtain as long as the norms of f_1 and f_2 are small. If large functions f_1 and f_2 are at hand, the bandwidth of $C(s)$ can be increased to guarantee stability and reference following, which will result in a controller with high gain and that will amplify noise. As an alternative the bandwidth of $H_m(s)$ can be decreased to fulfill stability. There is no known systematic way to find a controller that handles realizations of f_1 and f_2, so manual tuning of low-pass filter parameters K and $D(s)$ is needed.

3.5 Design choices made for the fighter application

A number of design choices have been made to be able to tune an L1-controller to the aircraft. Full state feedback control, time delays and flight/actuator dynamics nonlinearities have to be handled.

Augmentation of an L1-controller to a linear state feedback

The L1-controller has been used in an augmentation setup according to Figure 3.7.

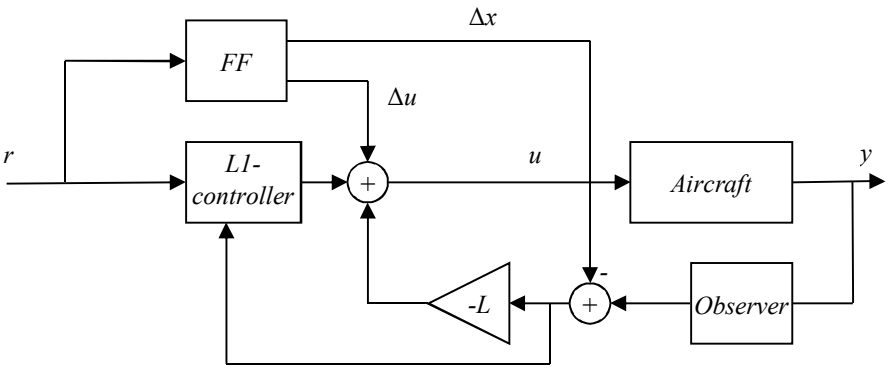

Figure 3.7 Block diagram with reference feedforward *FF*, linear state feedback *L*, *L1*-controller and *Observer*.

The feedforward block *FF* in Figure 3.7 creates feedforward signals Δu and Δx using the reference r that reduces known aircraft nonlinearities so that the inner loop act more linear to the controller than otherwise would be the case. In this application the feedforward will accomplish roll motion around the velocity vector and compensate for mass inertia asymmetries. It will also compensate for gravity and trim the aerodynamic configuration to the linearization point. This will take workload off the controllers since the feedforward nominally will compensate for nonlinear effects and bias.

A state observer is used to produce estimates of aircraft states from measurements y. The observer also predicts state estimates forward in time to compensate for known time delays (T_d = 0.02s) in sensors models and corresponding to delays in an on-board computer.

The following relation between the four actuator demands to δ_{al} δ_{ar} δ_c δ_r and the three control signals corresponding to δ_a δ_c δ_r were chosen by design:

$$\begin{pmatrix} \delta_{al} \\ \delta_{ar} \\ \delta_c \\ \delta_r \end{pmatrix} = \begin{pmatrix} 1 & 1 & 0 \\ -1 & 1 & 0 \\ 0 & 1 & 0 \\ 0 & 0 & 1 \end{pmatrix} \begin{pmatrix} \delta_a \\ \delta_e \\ \delta_r \end{pmatrix} \tag{3.78}$$

Left and right elevon deflections δ_{al} and δ_{ar} are linearly combined from aileron δ_a and elevator δ_e control signals. The elevator demand δ_e is distributed equally on the canards δ_c and elevons, a frequently used design decision for such a configuration [13].

To make relevant comparisons the reference signal for the L1-controller is fed directly to the aircraft actuator. It is not passed through the low-pass filter as proposed in the original L1-controller design in [6]. This way the control signal for L1-control and state feedback both uses a constant gain K_g acting on the reference signal r.

If no baseline state feedback controller would be used and the open-loop aircraft deviates significantly from the reference system, pre-filtering of the reference r based on nominal and desired dynamics should be considered and the L1-controller would get a larger workload.

Neither a gain-scheduled gain L in the state feedback nor variable dynamics A_m, B_m in the controllers were used in this implementation. No scheduling in bandwidth of low-pass filters in the L1-controller is done; the controllers are expected to deal with deviations without any type of scheduling even though the design would allow for it.

Creating the reference system dynamics

Reference systems are created by choosing design factors in roll, pitch and yaw in (3.18), (3.25) and (3.29). Corresponding feedback gains will be achieved by using (3.19) for pitch dynamics and (3.31) for roll-yaw dynamics.

In the procedure of choosing reference systems, limited actuator response comes into play. It has been found suitable using simulations in Section 4 that a possible roll bandwidth is given by about one fifth of the actuator bandwidth ω_a as illustrated in Figure 3.8. This corresponds to an r_{factor} with a value of 1.5 for the aircraft that is considered here resulting in $1/\tau_r$ = 5.7 rad/s. It is then suitable to place the pitch and yaw poles a little

closer to the imaginary axis as shown in Figure 3.8. To accomplish this, p_{factor} is set to 3 and y_{factor} is set to 7, resulting in ω_{0p} = 4.9 rad/s and ω_{0y} = 4.7 rad/s. This will create reference systems with a desired pole map and dynamics that will be possible to achieve and that corresponds to other control designs for this aircraft [13].

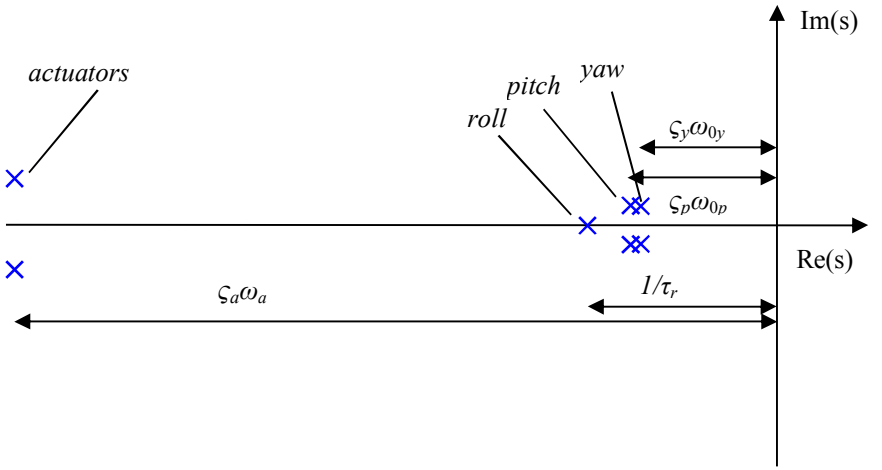

Figure 3.8 Pole map for actuator and reference system dynamics.

The damping for pitch and yaw complex conjugated pole pairs ς_p and ς_y are both set to 0.9 in this application, a relatively high damping, to avoid introduction of oscillations already in the reference system.

Low-pass filter bandwidth and sample rate design

The low-pass filters that are placed at the output of the L1-controller are first-order, discrete-time filters with sampling period T_s in this design. Guidelines in [6] for setting bandwidths of these filters are not to let frequencies beyond the control channel bandwidth [31] pass to the control signal.

A design is chosen which makes the unmatched low-pass parameter path having separately tuned filters from the matched and using two first-order cascaded filters. This setup was inspired by L1-controller design in [24] for aerial vehicle applications. Filtering the unmatched path twice will reduce high-frequency noise fed through to the controller output since the unmatched parameter path otherwise amplify high frequencies. The first filter in the cascaded two-filter design uses a bandwidth that is lower than the second (by a factor 1/1.2), also an idea from [24].

So in total, five low-pass filter parameters need tuning, one per state as in:

$$\begin{aligned} u(s) &= K_g r(s) - C_m(s)\hat{\sigma}_1(s) \\ &- C_{um}(s)H_m^{-1}(s)H_{um}(s)C_{um0}(s)\hat{\sigma}_2(s) \end{aligned} \tag{3.79}$$

where

$$\begin{aligned} C_m(s) &= \left(sI + K_m\right)^{-1} K_m \\ C_{um}(s) &= \left(sI + K_{um}\right)^{-1} K_{um} \\ C_{um0}(s) &= \left(sI + K_{um0}\right)^{-1} K_{um0} \end{aligned} \tag{3.80}$$

and

$$\begin{aligned} K_m &= \begin{pmatrix} k_1\omega_{0p} & 0 & 0 \\ 0 & k_2/\tau_r & 0 \\ 0 & 0 & k_3\omega_{0y} \end{pmatrix} \\ K_{um} &= \begin{pmatrix} k_4\omega_{0p} & 0 & 0 \\ 0 & k_5\omega_{0y} & 0 \\ 0 & 0 & k_5\omega_{0y} \end{pmatrix}, K_{um0} = \frac{1}{1.2}\begin{pmatrix} k_4\omega_{0p} & 0 \\ 0 & k_5\omega_{0y} \end{pmatrix} \end{aligned} \tag{3.81}$$

Low-pass filter bandwidths for matched pitch and yaw parameters have been related to the corresponding reference system bandwidth through ω_{0p}, τ_r and ω_{0y} of Section 3.2. So five parameter values in K matrices were tuned to k_1=2 for the matched pitch channel and k_3=1.2 for matched yaw compensations. For roll the bandwidth k_2=1 was tuned for matched parameter estimates. Unmatched parameter estimates, have low-pass filter bandwidths with a value of k_4=1.2 and k_5=1.8 for pitch and yaw respectively. Filters are realized in discrete time using zero-order hold and sampling period T_s, the same sampling rate as in the piecewise constant L1-controller.

L1-controller low-pass filter bandwidths and sampling rate were tuned the following way: simulations with a set of random variations of parameters and characteristics were run and evaluated for different values of low-pass filter parameters and controller parameter update rates. Evaluation was done by creating a cost function from mean and peak deviations from desired responses in angle of attack/sideslip and roll rate together with the number of output sign shifts. The three terms from mean

deviation, max deviation and sign shifts were normalized to a nominal run and the sum of squares were calculated and minimized for filter bandwidths k_1 to k_5 and sampling period T_s.

Due to the fact that actuators become rate saturated for noticeable periods in this application, generally lower values were suitable than in other L1-control applications [25]. If the actuator rate limit was increased, higher low-pass filter bandwidths could be applied resulting in better performance and robustness.

The L1-controller sampling rate was designed to be 100 Hz. A higher sampling rate did not add notable performance or robustness in the simulation evaluation.

Handling actuator dynamics

Special care is required if the actuator has dynamics that cannot be neglected as will be shown by simulations. Estimating the parameter $\hat{\sigma}$ including the actuator limits would result in the controller trying to compensate for the actuator dynamics which is not possible because of actuator rate and position saturations. A better approach is presented in Figure 3.9 where an actuator model is placed before the state predictor. This way it is parameters corresponding to the aerodynamic forces and moments that will be estimated.

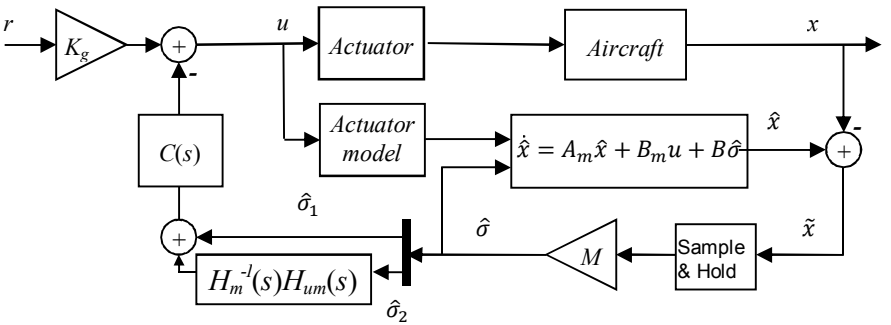

Figure 3.9 Block diagram of system with actuator model and reference signal not filtered by $C(s)$.

To be able to estimate a more adequate $\hat{\sigma}$ the L1-controller internal signals are interpreted physically and the state predictor is modified (the possibility is suggested in [14]) according to Figure 3.9, having an actuator

model including limits in rate and position at the input of the state predictor. This actuator model corresponds to the one that is used in the 6-DOF model as in Figure 2.13. In the scenario used here, rate limits are reached frequently, position limits are seldom reached. Missiles generally have higher actuator rate limits than aircraft, due to lower control surface hinge moments, even when related to the higher expected closed-loop bandwidth [9], so actuator rate saturation is not as notable.

Linear state feedback controller with and without integral action

The state feedback is used in two different ways. When the feedback controller is used on its own, integral action is activated and when an L1-controller is augmented to the state feedback, no integral action is used.

When using the state feedback controller without augmentation of an adaptive controller, terms for integral action are incorporated so that:

$$u = K_g r - Lx - L_i K_g x_i \tag{3.82}$$

where r includes reference signals for angle of attack, roll angular rate and angle of sideslip:

$$r = \begin{pmatrix} \alpha_d \\ p_d \\ \beta_d \end{pmatrix} \tag{3.83}$$

where integral states are created according to:

$$\frac{d}{dt} x_i = \begin{pmatrix} \alpha_r - \alpha \\ p_r - p \\ \beta_r - \beta \end{pmatrix} \tag{3.84}$$

and where the gain from reference r is:

$$K_g = \begin{pmatrix} K_{gp} & 0 \\ 0 & K_{gy} \end{pmatrix} = \begin{pmatrix} -(CA_{mp}^{-1}B_p)^{-1} & 0 \\ 0 & -(CA_{my}^{-1}B_y)^{-1} \end{pmatrix} \tag{3.85}$$

Reference signals α_r, p_r, and β_r in the integrators are generated by feeding demands to reference systems $H_m(s)$ from Section 3.2 so that:

$$\begin{pmatrix} \alpha_r(s) \\ p_r(s) \\ \beta_r(s) \end{pmatrix} = \begin{pmatrix} C_p\left(sI - A_{mp}\right)^{-1} B_p K_{gp} \alpha_d(s) \\ C_y\left(sI - A_{my}\right)^{-1} B_y K_{gy} \begin{pmatrix} p_d(s) \\ \beta_d(s) \end{pmatrix} \end{pmatrix} \tag{3.86}$$

The integral gain L_i is set to the unit matrix in this design so integrated signals will be weighted in as much as the reference r, by the factor K_g which, in the multivariable case, can be seen as transforming the integrated output error to the input side.

4 Results from 6DOF Simulations

Simulations have been carried out in a 6DOF model to display results of L1-control when compared to state feedback control. This is done in order to test the controllers and system responses when different kinds of disturbance and parameter perturbations are applied.

4.1 Control laws to be compared

The L1-controller augmented to a state feedback utilizes the reference r together with feedback from system states x and parameter estimates $\hat{\sigma}$ according to:

$$\begin{aligned} u(s) &= K_g r(s) - Lx(s) \\ &- C_m(s)\hat{\sigma}_1(s) - C_{um}(s)H_m^{-1}(s)H_{um}(s)C_{um0}(s)\hat{\sigma}_2(s) \end{aligned} \tag{4.1}$$

The linear state feedback with integral action utilizes the reference r together with feedback from system states x and output y:

$$u(s) = K_g r(s) - Lx(s) - K_g \frac{1}{s}\left(H_m(s)K_g r(s) - y(s)\right) \tag{4.2}$$

4.2 Scenario used in simulations

Demands will create changes in angle of attack and at the same time roll rotate the aircraft to different roll angles as viewed in Figure 4.1. Angle of sideslip is demanded to zero throughout maneuvers. To keep α and p at the demanded values while keeping β small is the major task that the controller work hard to accomplish in scenarios like these.

An altitude (nominally 1000 m) and an airspeed (nominally corresponding to M 0.6) will be kept roughly constant throughout the maneuver sequence. This way *changes* during the simulation to dynamic pressure q_d does not affect results to any large extent, however controller assumptions of altitude and airspeed are erroneous in runs with perturbations due to a constant deviation from the nominal. Observed phenomena will be due to effects created by rapid maneuvering, deviation from nominal assumptions and sensor noise.

1. Simulations started by pulling 10º of angle of attack (from 0º), as indicated in Figure 4.1
2. A roll rate p of 180º/s was demanded for a time period of 0.5 s so that a roll angle of 90º was obtained.
3. The α demand was decreased to 0º at the same time as a roll rate of -180º/s was demanded for 0.5 s to get a roll angle of 0º.
4. Then α was increased to 10º at a simultaneous roll rate demand of -180º/s for 0.5 s to a roll angle of -90º.
5. Now α was decreased to 5º at a simultaneous roll rate demand of 180º/s is for 0.5 s to a roll angle of 0º.
6. Finally α was maintained at 5º at a roll rate of 360º/s for 1 s so that a full roll revolution was accomplished.

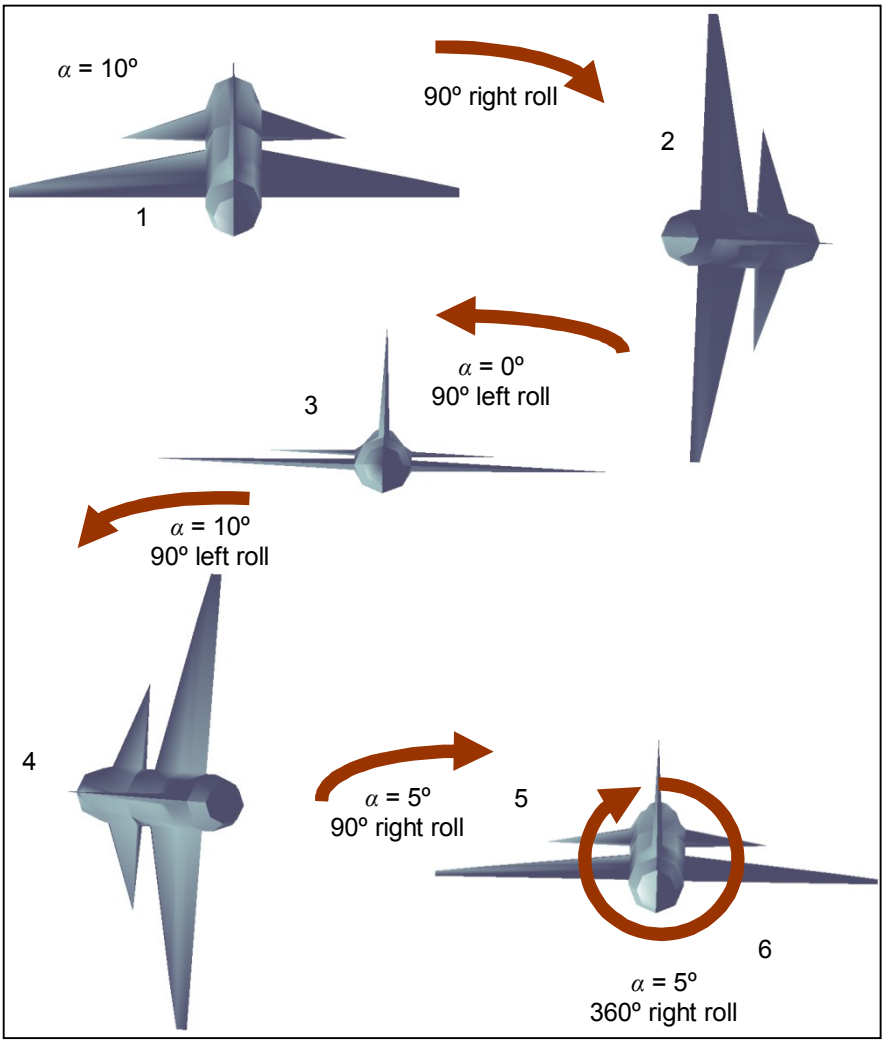

Figure 4.1 Schematic aircraft, rear view showing sequence of maneuvers performed in simulations.

Since roll rate demands are made open-loop with respect to achieved roll angle, they are just step functions of suitable time periods; a small roll addition is made to get roll angles that are even quarters of a turn.

4.3 Simulation setup and results

Seven sets of parameter and noise settings in the model were simulated:

Nominal settings:
All parameters were nominal, which correspond to values assumed when controller design was made.

Measurement noise:
Sensor noise was added to simulate a measurement procedure with sensors that produce a high level of noise. To angle of attack and angle of sideslip, normally distributed white noise with a 1σ-value of 0.5° was added at a 50 Hz frequency. To rates p, q and r normally distributed white noise with a 1σ-value of 2°/s was added (corresponding to a rotation sensor with a random walk of 5°/√h sampled at 400 Hz).

Parameter perturbations:
Error in parameter assumptions were created by using normally distributed values. Pre-sampled parameter realizations were saved and used for simulations so that comparisons can be made between runs. These values were then used to perturb parameter settings relative nominal values. Start position and velocity were varied so that the 1σ relative error became 10%. Atmospheric parameters were varied by 5%. Mass and mass inertia properties were varied by 5% and aerodynamic parameters by 20%. Center of gravity position related to the wing cord was varied by 2% and actuator bandwidth, rate limit and damping by 10%. The parameter realization for which simulations are presented was a challenging one; it made the needed control effort large. *Controller feedforward compensations were made with nominal parameter values*, making this a valid check also for feedforward robustness to perturbations.

Control surface actuation failure:
The right wing control surface deflection responded to an extent corresponding to half of the demand. This means that aerodynamic forces and moments created for demanded roll and pitch control surface deflection were reduced and also created a severe coupling between pitch and roll demands that the controller needed to compensate for, since an unforeseen right-left wing asymmetry was at hand. A challenging kind of load disturbance was created with this setup.

No feedforward applied:
Feedforward signals were not added to the control signal. Controllers needed to compensate for nonlinear couplings without aid from feedforward based on reference signal inputs. One effect was that a demanded roll rate creates large couplings between angle of attack and sideslip. Also effects of that the airframe naturally rotates around its principal mass inertia axis, as well as gravity effects, were left to controllers without aid from feedforward.

Flight at high altitude:
The simulation was performed at an altitude of 7000 m instead of the 1000 m that controllers were designed for. Dynamic pressure is about half of what was assumed due to lower air density. A low dynamic pressure makes the flight dynamics slower and the effects of control surface deflections are reduced.

No actuator model in the L1-controller:
In this setup, no actuator model was included in the state predictor of the L1-controller. There was no knowledge in the L1-controller of e.g. actuator rate limitations.

For each of the seven different settings above, two simulations were made and presented one figure on top of the other. One run is plotted for L1-control augmented to a state feedback. One run is plotted for state feedback acting on its own, including integral action.

Four subplots are presented for each simulation in Figure 4.2 to Figure 4.13. Demands in angle of attack/sideslip and roll rate (α_d, β_d and p_d) are dashed lines, effectuated signals are solid lines in the following subplot layout:

Subplot 1: angle of attack α (blue) and angle of sideslip β (green).	Subplot 2: body rates p, q and r (blue green red)
Subplot 3: demanded and effectuated pitch control signals δ_e.	Subplot 4: demanded and effectuated roll and yaw control signals δ_a and δ_r (blue green).

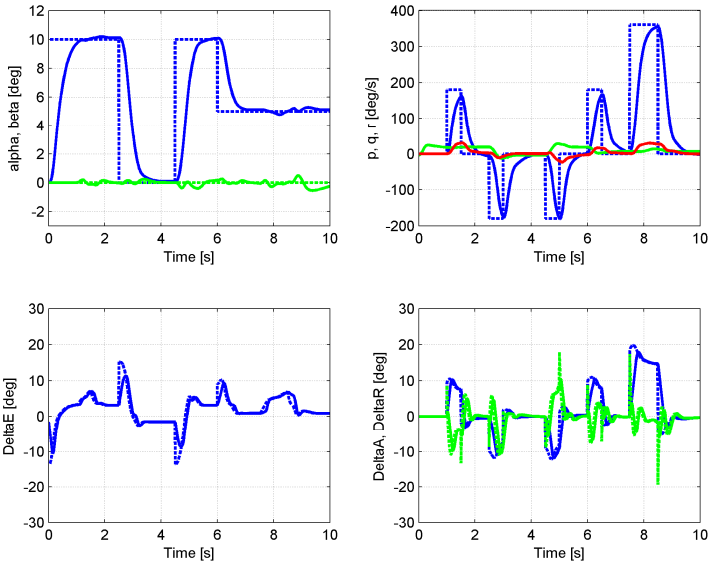

Figure 4.2 Simulation of the system with the L1-controller, nominal aircraft.

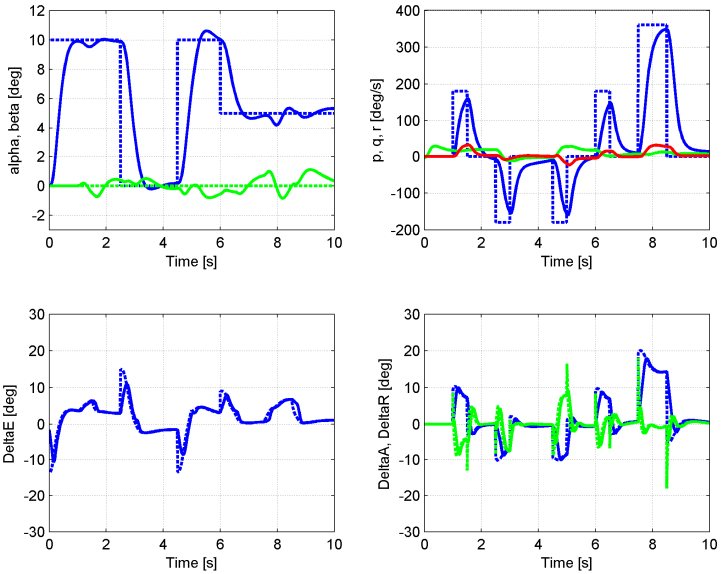

Figure 4.3 Simulation of the system with the state feedback controller, nominal aircraft.

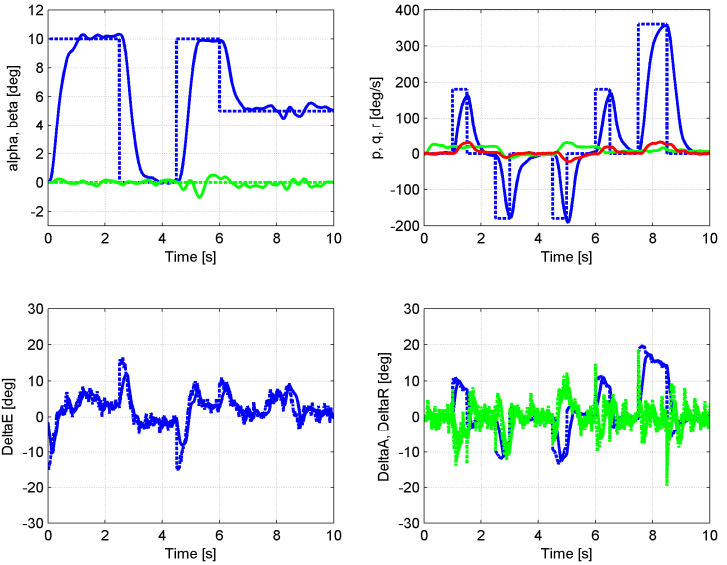

Figure 4.4 Simulation of the system with the L1-controller, measurement noise added.

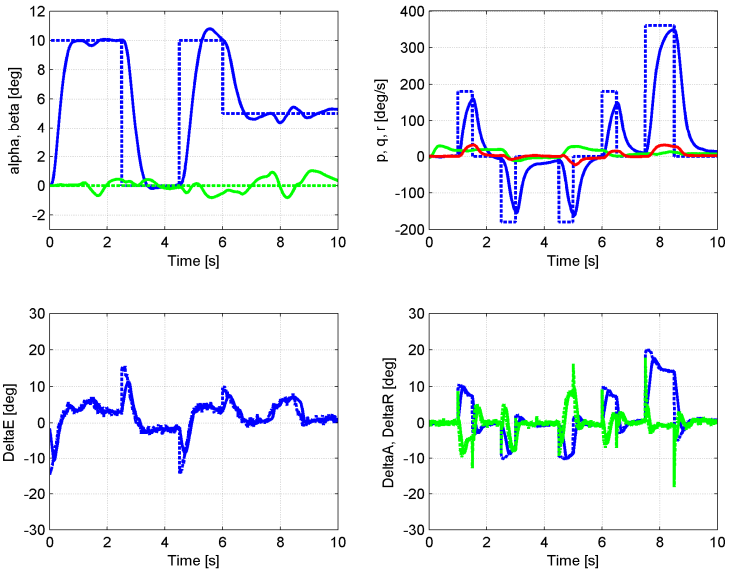

Figure 4.5 Simulation of the system with the state feedback controller, measurement noise added.

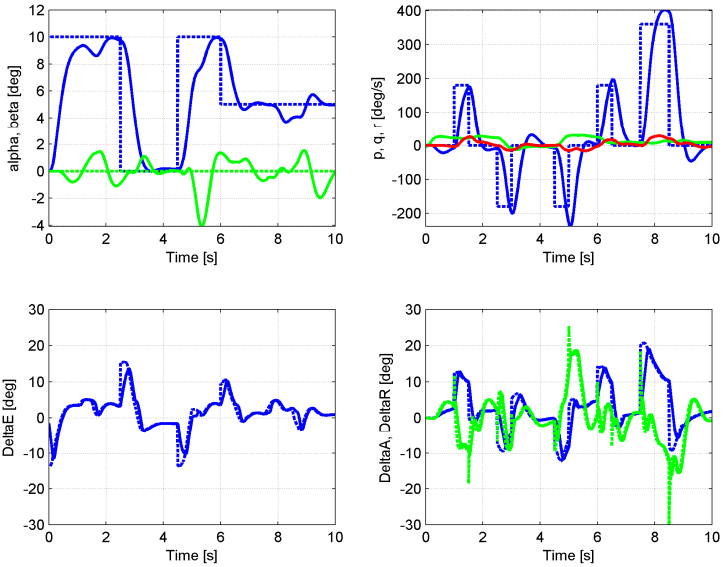

Figure 4.6 Simulation of the system with the L1-controller, perturbed parameters.

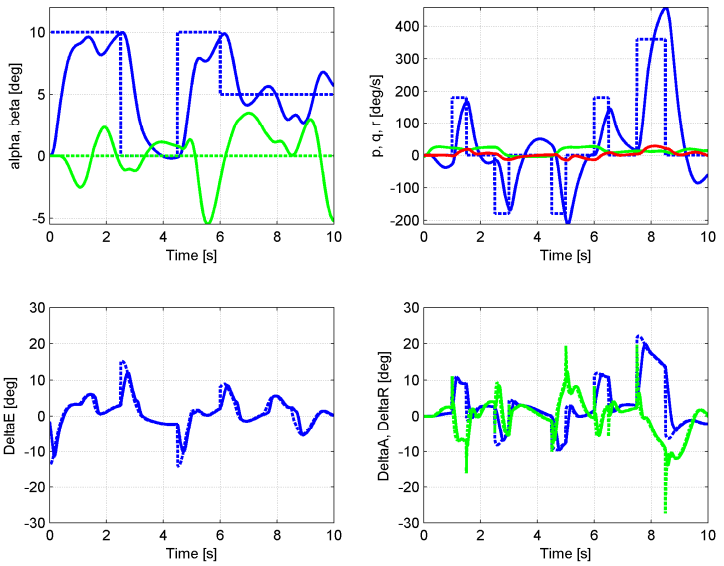

Figure 4.7 Simulation of the system with the state feedback controller, perturbed parameters.

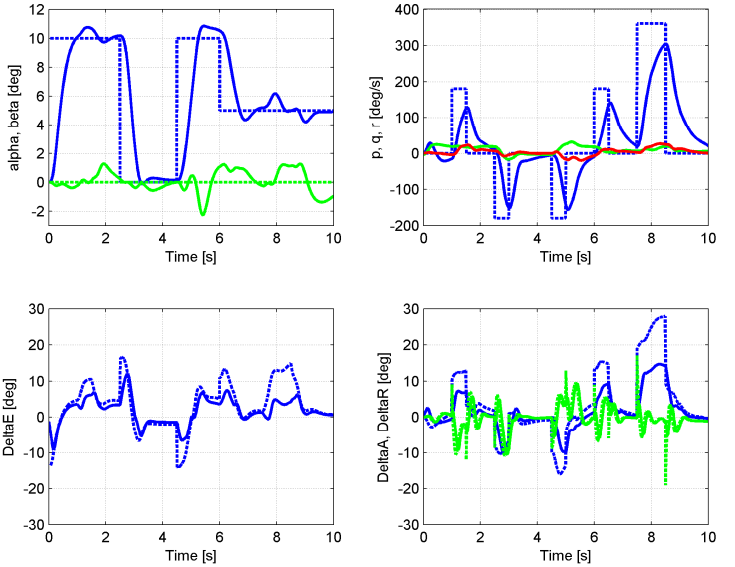

Figure 4.8 Simulation of the system with the L1-controller, control surface actuation failure.

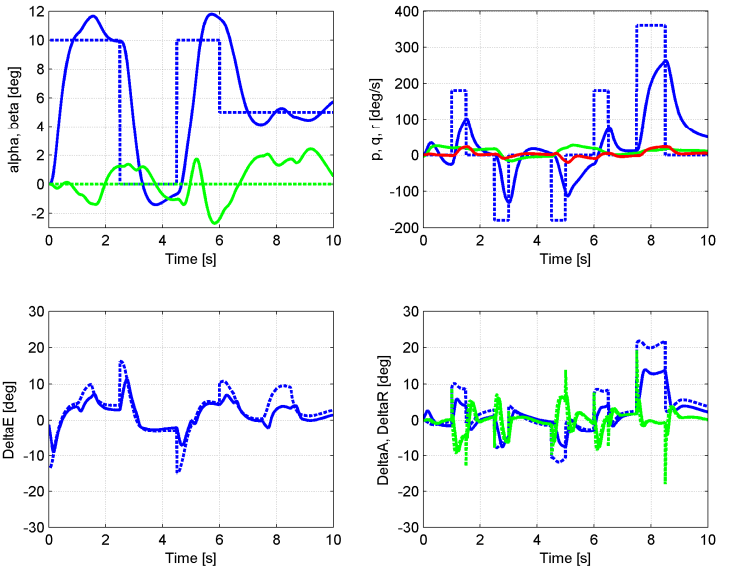

Figure 4.9 Simulation of the system with the state feedback controller, control surface actuation failure.

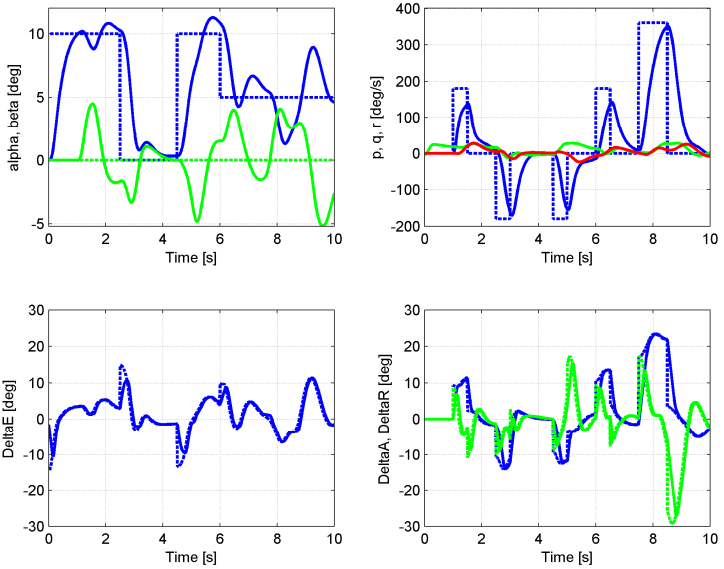

Figure 4.10 Simulation of the system with the L1-controller, without feedforward from reference.

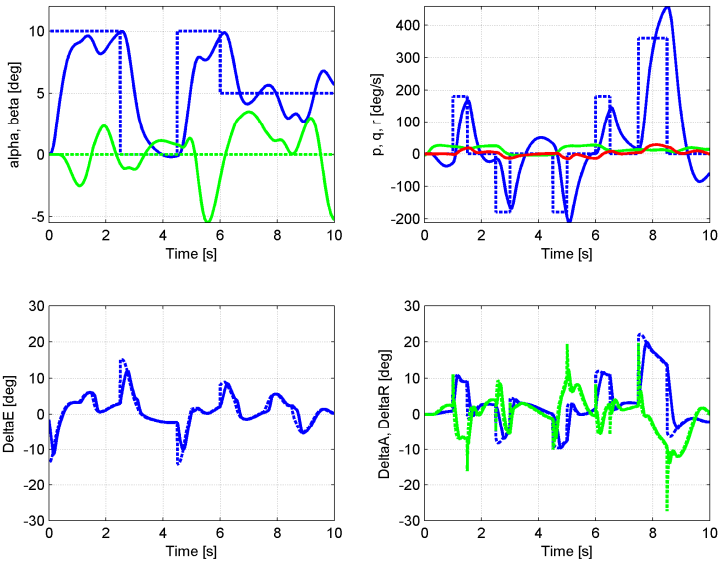

Figure 4.11 Simulation of the system with the state feedback controller, without feedforward from reference.

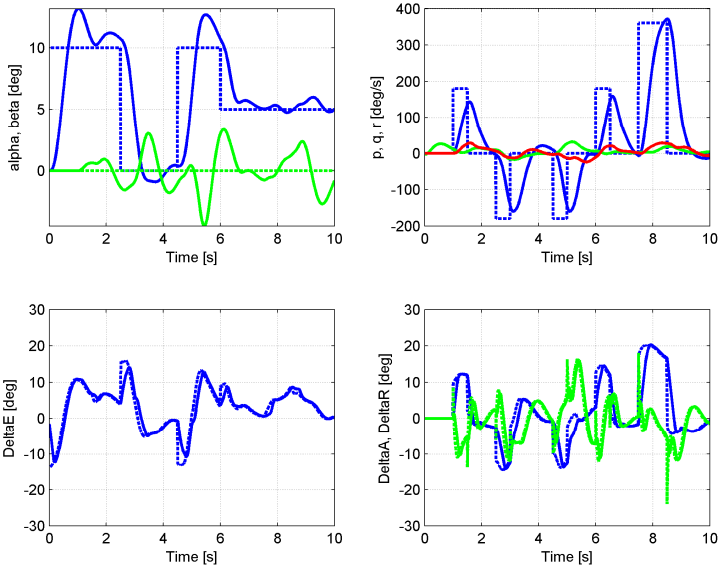

Figure 4.12 Simulation of the system with the L1-controller, at a flight altitude of 7000 m.

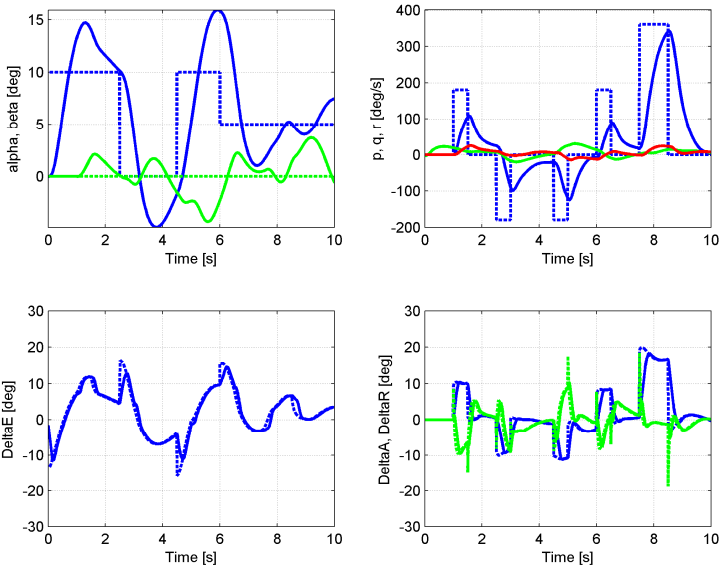

Figure 4.13 Simulation of the system with the state feedback controller, at a flight altitude of 7000 m.

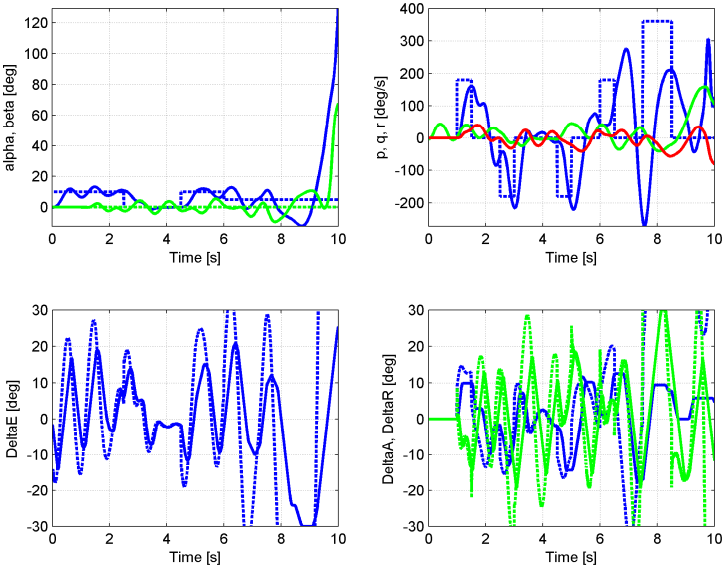

Figure 4.14 Simulation of the system with the L1-controller, no compensation of actuator rate limits in the L1-controller.

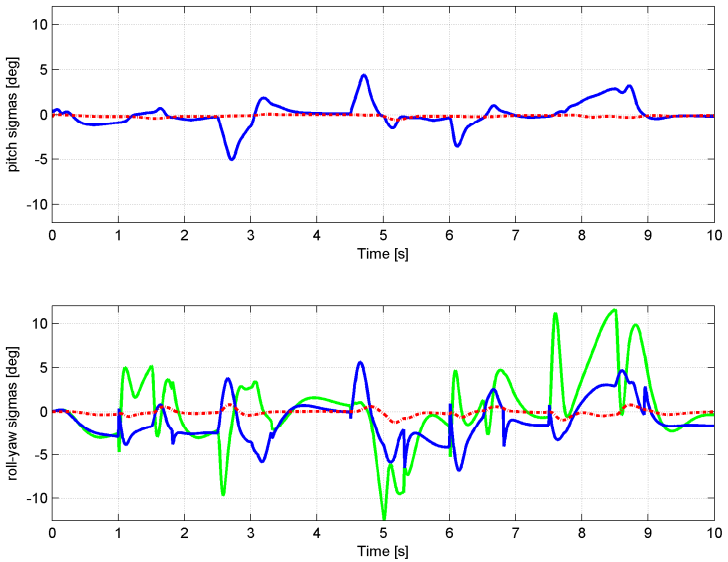

Figure 4.15 Matched parameter estimates $\hat{\sigma}_1$ (solid) and unmatched $\hat{\sigma}_2$ (dashed) of (3.68), for case with perturbed parameters.

Comments on simulation results

Overall the L1-controller augmented to a state feedback is more robust to changes than the state feedback with integral action. This comes at the cost of higher noise throughput and need for special attention regarding time delay and effects of saturation.

Nominal settings Figure 4.2 & Figure 4.3**:**
Results are similar for L1-control and state feedback control with integral action. L1-control does a little better job at keeping α and β close to demanded values throughout the maneuver sequence. Peak-to-peak values for β error are less than 1º throughout the simulation, a good result for both controller designs. Both controllers follow roll-rate demands properly and use similar control signal amplitudes (actuator demands).

Measurement noise Figure 4.4 & Figure 4.5**:**
Both controllers manage to keep α and β close to demanded values even though high noise levels were added (and the state observer was not optimized to reduce noise to the controller). The L1-control is feeding more of the noise through to the control signal so that the controlled states become more excited. Peak-to-peak values for the pitch L1-control signal demand to elevator δ_e was about 4º. For the state feedback the corresponding value was about 2º. For noise to the control signal aileron δ_a, the gain was low for both controllers. For the L1-controller this is due to that good robust performance is obtained, even though the corresponding low-pass filter had a relatively low bandwidth. For δ_r the opposite is true, a relatively high low-pass bandwidth is required to obtain robust performance, especially in the unmatched channel. This made the noise gain to δ_r higher (peak to peak of about 6º). Overall noise levels to actuator demands are not very problematic in this application. However, the fact that the controlled state (e.g. angle of attack) is excited by sensor noise is undesired. An effort to reduce the noise by use of e.g. a tuned state observer would be necessary to increase ride quality in an aircraft application. Missiles would not need the same noise consideration in most cases.

Perturbed parameters Figure 4.6 & Figure 4.7**:**
Both controllers stabilize the aircraft. The L1-controller manages to reduce effects of parameter changes to controlled states better. Other realizations of parameter values show similar results, the L1-controller was more robust to changes than the state feedback acting on its own.

This increase in robustness was not accomplished with significantly higher control demands.
Control surface actuation failure Figure 4.8 & Figure 4.9**:**
The L1-controller was less affected by this major change in matched input gains. It keeps α, β and p closer to demanded values. Control demands were higher for the L1-controller as it compensates for the reduced efficiency.
No feedforward applied Figure 4.10 & Figure 4.11**:**
Both controllers struggle to follow reference-values, large deviations occur. The L1-controller was however a bit less sensitive to this kind of severe deviation from linear behavior in the dynamics.
Flight at high altitude Figure 4.12 & Figure 4.13**:**
Demands were followed to lower degree for both controllers, the L1-controller made a little better. The performance was however not acceptable, the controllers that were designed for an altitude of 1000 m cannot be used for full performance missions at 7000 m. This fact could be changed by airspeed and altitude scheduling of the reference system, the linear state feedback and possibly the low-pass filter in the L1-controller but then the design could be considered as gain-scheduled.
No actuator model in the L1-controller Figure 4.14**:**
This L1-controller design cannot handle actuator rate saturation. Without an internal model of the actuator, the controller tried to compensate for the rate saturated actuator, which resulted in bad response and instability.

In the L1-controller an estimation of parameters corresponding to the input-load disturbance $\hat{\sigma}$ is done continuously. These matched and unmatched parameter estimates shown in Figure 4.15 for the simulation in which parameters were randomly varied (corresponding to Figure 4.6). For pitch there are two signals, one solid for the matched load disturbance estimate and one dashed for the unmatched estimate. In roll-yaw there are two matched estimates in solid lines and one dashed unmatched estimate. The parameters are high frequent, there is not much of learning and identification of physical changes as in other types of adaptive control. All deviation from the reference dynamics is lumped into relatively few parameters which are momentarily estimated and compensated for up to the control channel bandwidth.

5 Linear analysis of the system

The previous sections has indicated that flight control systems with good performance can indeed be obtained by L1 adaptive control, but also that some L1 adaptive controllers are linear systems with a special architecture. Comparisons with internal model control, input observer control and state feedback will give useful insights. One criticism against L1 adaptive control is that it uses high adaptive gains. Further analysis will give insight into the choice and implication of gains.

5.1 L1-controller comparison to a disturbance observer

In [14] and [15] it is shown that as the L1 adaptive gain Γ goes to infinity for continuous time controllers and as the sampling period T_s go to zero for piecewise constant controllers, there is an equivalent linear time-invariant controller. If the adaptive law only uses linear parameter estimates, one example being:

$$\dot{\hat{\sigma}}(t) = -\Gamma B^T P\left(\hat{x}(t) - x(t)\right) \tag{5.1}$$

of [6], and no projector operators are active, this equivalent controller exists. Since the state predictor and adaptive law in this limit becomes the inverse of a dynamic system, another interpretation of how the controller works can be made. That is to estimate a disturbance at the plant input by inverting the reference dynamics and then compensate for this disturbance by subtracting this quantity at the plant input. Alternative equivalent structures will also make it possible to compare the L1-controller to other linear control design methods.

An L1 equivalent controller in Figure 5.1 could be compared to a disturbance observer in Figure 5.2 ([16], [17] and [18]). The two have many common features. An input disturbance $\hat{\sigma}$ is estimated and a filter $C(s)$ attenuates the high-frequency content to the control signal u. There

are modifications to these types of controllers; for example the reference r does not have to pass through $C(s)$.

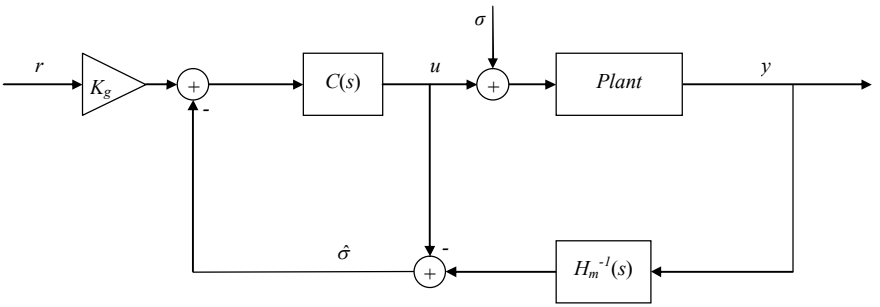

Figure 5.1 L1-controller with state predictor replaced by inverse, indicating how the input error estimate $\hat{\sigma}$ is generated.

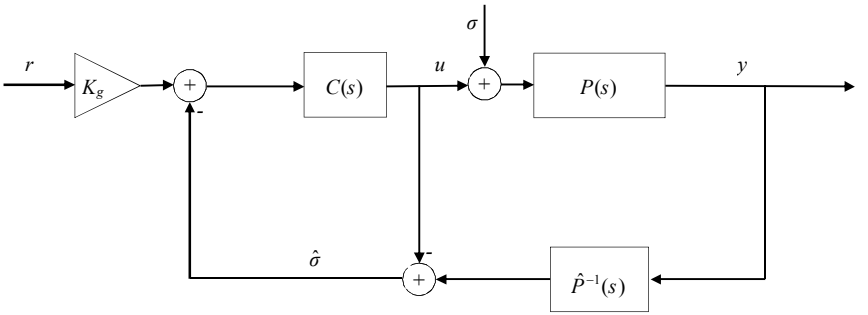

Figure 5.2 Disturbance observer design acting on plant $P(s)$, estimating input error $\hat{\sigma}$.

Even if Figure 5.1 shows similarities between the L1-controller and the input observer there are several issues that do not appear in Figure 5.1 compared to the more detailed block diagram in Figure 3.6 which also shows the state error $\tilde{x} = \hat{x} - x$. An important result for L1 adaptive control is that $\tilde{x}$ is reduced with increasing adaptation gains. The block diagram in Figure 3.6 is also useful because the reference model can be augmented with actuator saturation and other nonlinearities. These features are lost by reducing the block diagram to Figure 5.1 based on the assumption of linearity.

It is important to note that in the L1 equivalent controller the plant inversion is made based on the *reference system*. In a disturbance observer the *nominal plant dynamics* is inverted.

The Youla parameter $Q(s)$ of a disturbance observer is [22]:

$$Q(s) = C(s)\hat{P}^{-1}(s) \tag{5.2}$$

For L1 adaptive control of piecewise constant type, the Youla parameter $Q(s)$ is:

$$Q(s) = \left(I + \hat{P}(s)\left(I - C(s)\right)C(s)H_m^{-1}(s)\right)^{-1}\left(I - C(s)\right)C(s)H_m^{-1}(s) \tag{5.3}$$

or expressed in $KD(s)$:

$$Q(s) = \left(I + \hat{P}(s)KD(s)H_m^{-1}(s)\right)^{-1} KD(s)H_m^{-1}(s) \tag{5.4}$$

where $\hat{P}(s)$ is the plant nominal dynamics and $H_m^{-1}(s)$ is the reference system inverse.

The two methods become equal if the reference system inverse of the L1 equivalent controller is set to the nominal plant inverse.

5.2 Comparison of feedback laws

Feedback laws for three different system architectures will be discussed and expressed below in (5.5), (5.6) and (5.7).

The control law for state feedback with output integral action is:

$$u = K_g r - Lx - L_i K_g \frac{1}{s}(r - y) \tag{5.5}$$

which is essentially PID control in aeronautical applications. The state x contains a proportional P-part and a derivative D-part. Proportional parts are angle of attack and sideslip as being the control objective and approximate derivatives are pitch and yaw rates. The integral I-part is created as the control error ([19] p.221) and can be transformed to corresponding input directions by the closed-loop steady state gain K_g.

As an alternative to (5.5) the reference signal can be filtered by the reference system dynamics $H_m(s)$ to reduce overshoot due to integral windup:

$$u = K_g r - Lx - L_i K_g \frac{1}{s}\left(H_m(s)K_g r - y\right) \tag{5.6}$$

where the integrated output error nominally is zero.

An L1-controller of piecewise constant type augmented to a state feedback corresponds to the control law:

$$u = K_g r - Lx + KD_0(s)\frac{1}{s}\left(K_g r - H_m^{-1}(s)y\right) \tag{5.7}$$

Instead of integrating smoothed reference signals, the L1-controller takes the raw reference signal and feeds the output of the plant through an inverse approximation of the reference system. The fidelity of the approximation to the $H_m(s)$ inverse increases with increasing adaptive gains Γ and decreasing sampling periods T_s [6]. It should be noted that the reference signal is used both outside and inside the integral expression. The standard L1-controller procedure is to add it inside only, although the (5.7) alternative has been used as well in aircraft applications [7]. The transfer function $D_0(s)=sD(s)$ in (5.7) is in its simplest form unity. It can be noted that (5.6) and (5.7) are identical if $D_0(s)$ is set to $H_m(s)$. This could guide tuning of the low-pass filter $C(s)$ which is an important controller design variable. Using $D_0(s)$ it is possible to go gradually from a traditional integral action acting on the output to an L1-controller integral action. The low-pass filter uses the following structure:

$$C(s) = \left(I + KD(s)\right)^{-1} KD(s) = \left(sI + KD_0(s)\right)^{-1} KD_0(s) \tag{5.8}$$

The gain K in (5.8), which sets bandwidth of the low-pass filter $C(s)$, is usually a diagonal matrix. There will be three design parameters for a three channel aerospace roll-pitch-yaw controller (if $D_0(s)$ is unity). Nominal settings for the diagonal elements in K are available bandwidth values in the control channels (roll-pitch-yaw respectively).

The L1-controller structure aids the design of a control law by pointing out gain directions statically and dynamically using K_g and $H_m(s)$. It focuses on the error at the input instead of the commonly used output error. The input error is integrated over time to generate the control signal. It would be possible to use the direct input error (no integration, $D_0(s)=s$ or

even $D_0(s)=s^2$) as a term in the control law but then the available bandwidth recommendation would be violated.

5.3 Frequency domain analysis of the system

In the following sub-sections the L1-controller and the feedback controller, according to (5.6) and (5.7), will be presented and commented regarding frequency characteristics, assuming that the controller and actuator/aircraft dynamics are linear systems. Three actuators according to (2.33), a pitch dynamics as in (3.3) and roll-yaw dynamics as in (3.5) are assumed. This is carried out for the pitch channel in detail; the roll-yaw channel has similar frequency characteristics and will be included in subsequent singular value analysis. The L1-controller can be approximated by a continuous linear time invariant system as long as the sampling period T_s is low, parameter projection bounds [6] are inactive and actuator model rate and position are not saturated [28]. The linearized actuator dynamics and an actuator model according to Figure 3.9 are included in the analysis. No state observer dynamics was included, the observer that was tuned to this application only affect response at high frequencies, above the actuator bandwidth.

Gang-of-Six transfer functions

To investigate the relevant transfer functions, inputs and outputs as in Figure 5.3 were used. Inputs are from reference r, load disturbance σ and measurement noise n. Outputs are measurements y and control signal u.

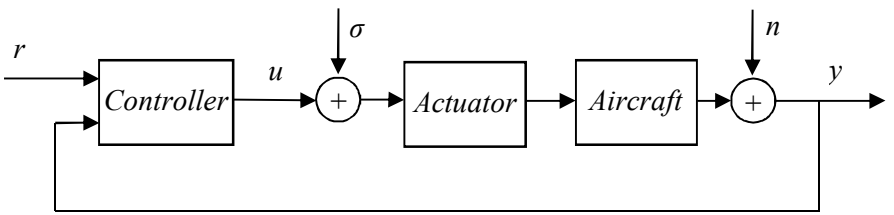

Figure 5.3 Block diagram defining inputs and outputs in ”Gang of Six” analysis

Bode responses are presented in Figure 5.4 and Figure 5.5. Commonly referred to as the "Gang of Six" [27], these responses display weakness and strength of controllers.

Regarding inputs, subplot columns start with the demanded angle of attack r=alphad, continues with load disturbance at the input σ=ddeltae and the last input is measurement error on angle of attack n=nalpha. The first row contains Bode outputs to measured angle of attack y=alpham and the second row are outputs to demanded control surfaces u=deltae.

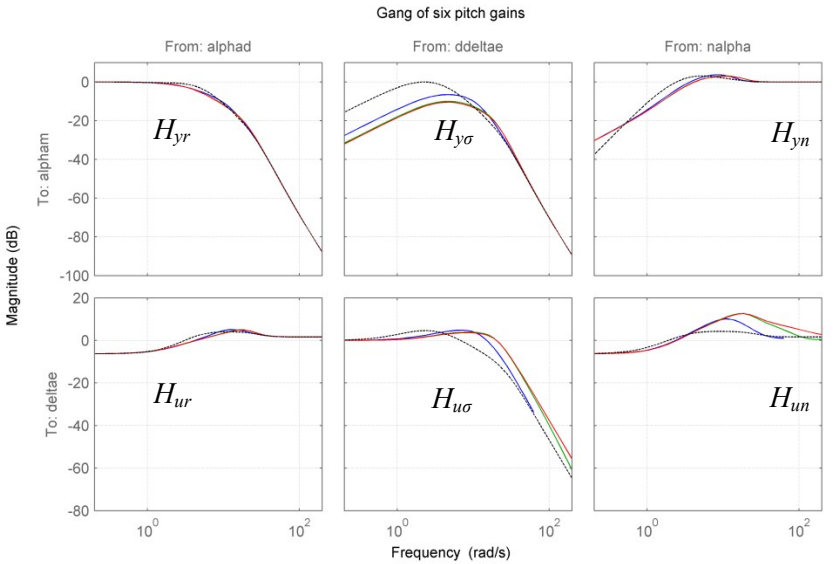

Figure 5.4 Bode gains "Gang of Six". Solid lines are L1-controllers for various T_s = [1/10, 1/100, 1/1000] s. Dashed are the corresponding gains for state feedback control.

For the L1-controller, three different settings are presented. They correspond to using three different sampling periods T_s (Figure 5.4) and three low-pass filter bandwidth parameters K in the controller design (Figure 5.5). The green curves of Figure 5.4 present a nominal setting of 1/100 s and blue present a value of T_s that is 10 times larger than the nominal (1/10 s). Red are shorter sampling periods, 10 times smaller (1/1000 s). The green curves of Figure 5.5 correspond to a nominal value of K, while blue are for a K value that is 10 times smaller and red are for a very high low-pass filter bandwidth value, 10 times that of the nominal K.

The pure state feedback responses, without an L1-controller, are presented with dashed lines in Figure 5.4 and Figure 5.5.

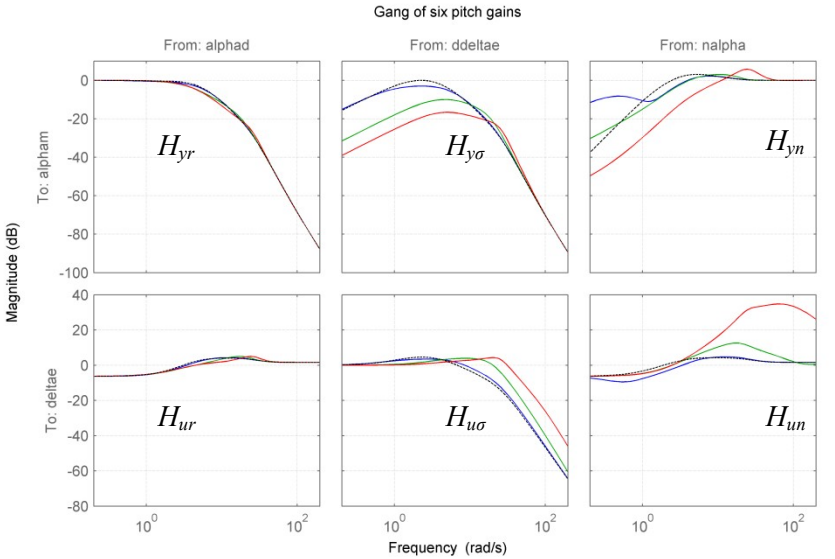

Figure 5.5 Bode gains ”Gang of Six”. Solid lines are L1-controllers for various low-pass bandwidth parameters K. Dashed are the corresponding gains for state feedback control.

Comments on closed-loop pitch responses

The bandwidth from demand to controlled state (angle of attack) were equal for L1-control and state feedback control (H_{yr} in Figure 5.4: From: alphad To: alpham). This response is presented with direct addition of reference signals to the control signal, without passing the low-pass filter $C(s)$. If the reference signal would be run through $C(s)$, responses for L1-control would fall slightly faster, so that a lower closed-loop bandwidth from the reference signal would be obtained.

The L1-controller attenuates input load disturbances to a larger extent and propagates output error up to a higher frequency ($H_{y\sigma}$ and H_{yn} in Figure 5.4 From: ddeltae & nalpha To: alpham).

The L1-control disturbance rejection comes at the cost of having higher gain from measurement error to the output (H_{un} Figure 5.4 From: nalpha To: deltae). This measurement error gain by the controller is increased for high frequencies as sampling period T_s is reduced. This high noise gain is reduced if bandwidths of low-pass filters are reduced but then the good load disturbance rejection of the L1-controller is undermined.

If the reference would pass through the low-pass filter $C(s)$, this would make a difference in how the reference signal affects the control signal (H_{ur} Figure 5.4 From: alphad To: deltae). Then this response gain would be lower for high frequencies.

Figure 5.5 shows gains for difference low-pass settings in the L1-controller. If the bandwidth of the low-pass filters $C_m(s)$ and $C_{um}(s)$ are increased, which means that matrix K diagonal elements are increased, the input load rejection is improved ($H_{y\sigma}$ in Figure 5.5). The high noise gain is increased if bandwidths in low-pass filters are increased (H_{yn} and H_{un} in Figure 5.5), so there is a trade-off between load rejection and noise gain to be performed by choosing elements in K.

Open-loop controller frequency response

Open controller dynamics are presented in Figure 5.6 corresponding to an L1-controller and a linear state feedback of (5.7). Responses are plotted from demanded angle of attack, alphad, from measured angle of attack, alpham, and finally from measured pitch angular rate, qm. Outputs are to demanded control surfaces deltae.

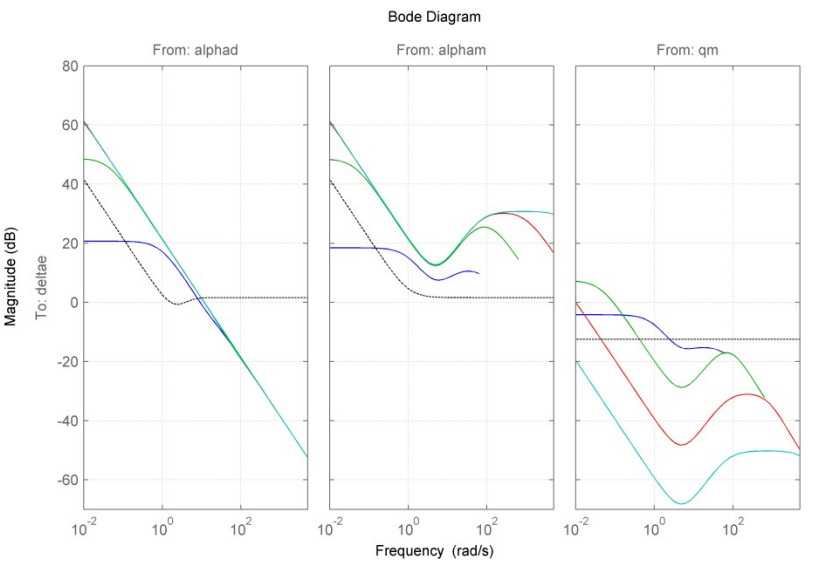

Figure 5.6 Bode magnitudes for open-loop controllers. Solid lines are L1-controllers for sampling periods T_s = [1/10, 1/100, 1/1000, 1/10000] s with the corresponding gains for state feedback control (dashed line).

Responses for L1-control exclude effects from the direct reference signal gain and the state feedback gain; they correspond to only the last two terms in (4.1). This is done in order to enlighten differences between the two control laws. For the L1-controller, four curves are shown for different sampling period T_s. The green curves correspond to a nominal setting of 1/100 s, blue present a sampling period 10 times larger than the nominal (1/10 s). The red and cyan curves present shorter sampling periods of 1/1000 s and 1/10000 s respectively. State feedback controller responses are dashed in Figure 5.6.

State feedback controller responses are dashed in Figure 5.6; they correspond to all terms in (4.2).

Comments on open-loop controller response

The augmented L1-controller path uses a higher gain from both reference signal and from outputs. High-frequency gains from measured angle of attack alpham for L1-control are increased as T_s is reduced. Feedback from pitch angular rate qm is reduced significantly as T_s is reduced

This rate gain is remarkable; there will be practically no feedback from angular velocity q from the L1-controller. If an L1-controller with unmatched compensation is implemented, this means that feedback will be done from states that are controlled, which corresponds to the signal $y = Cx$. So L1-methodology is stating that if there are unmatched errors, feedback should mainly use signals corresponding to the control objective. On the other hand there is derivation from alpham around 10 rad/s (bode gain slope of +1), so the L1-controller is extracting pitch angular rate information from the angle of attack, instead of using rate information directly from qm. The low gain from rate feedback and alpha derivation effects are reduced if separate matched and unmatched low-pass filters are designed and tuned as in (3.79).

Open-loop gain singular values frequency responses

The total system consisting of pitch and roll-yaw controller and aircraft dynamics has three inputs and three outputs so a singular values frequency response is a relevant observation, both for open-loop gain at output and at input. Open-loop gain singular values for a roll-pitch-yaw controller as in Figure 5.7 are presented.

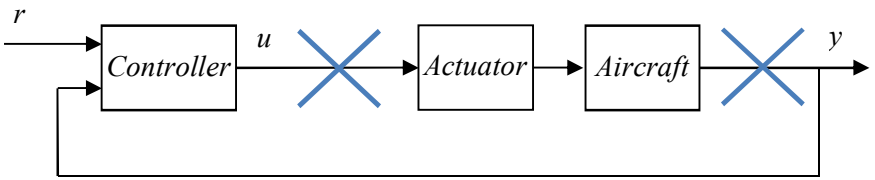

Figure 5.7 Open-loop gain analysis is performed by breaking the loop at the input and at the output.

Reference elements in r and corresponding outputs y are roll rate p, angle of attack α and angle of sideslip β. The control signal u has three roll-pitch-yaw control surface deflection demands generated from the linear state feedback augmented by the L1-controller. Diagrams are presented in Figure 5.8 (open-loop gain at input for varying T_s), Figure 5.9(open-loop gain at output for varying T_s) and Figure 5.10 (open-loop gain at input for varying K).

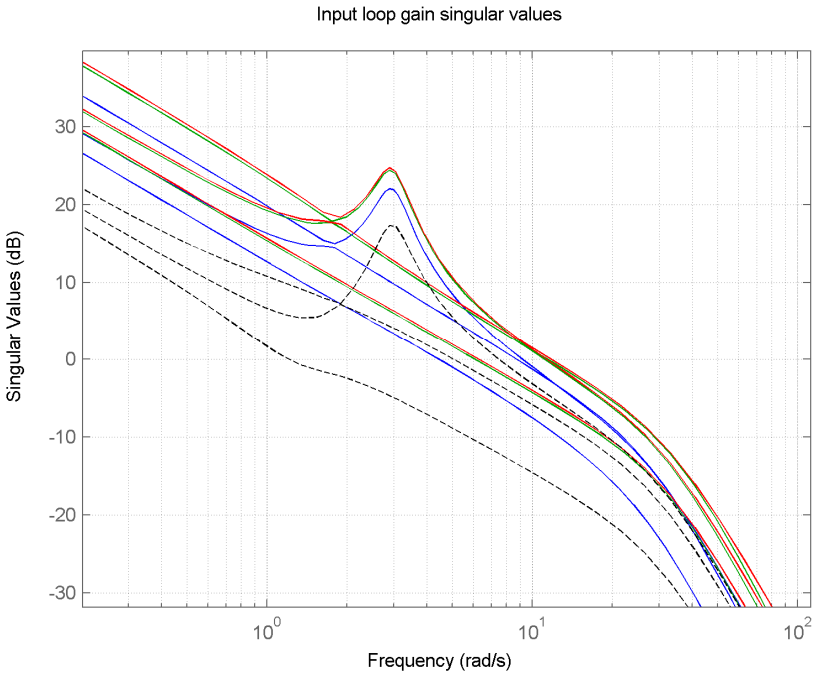

Figure 5.8 Input open-loop gain singular values for (5.6) dashed and (5.7) solid. Solid lines are L1-controllers for various T_s = [1/10, 1/100, 1/1000] s.

Dashed lines in Figure 5.8-Figure 5.10 correspond to a linear state feedback controller with integral action as in (5.6), solid lines correspond to an augmented L1-controller as in (5.7). Roll is of highest magnitude, followed by pitch and yaw in descending order.

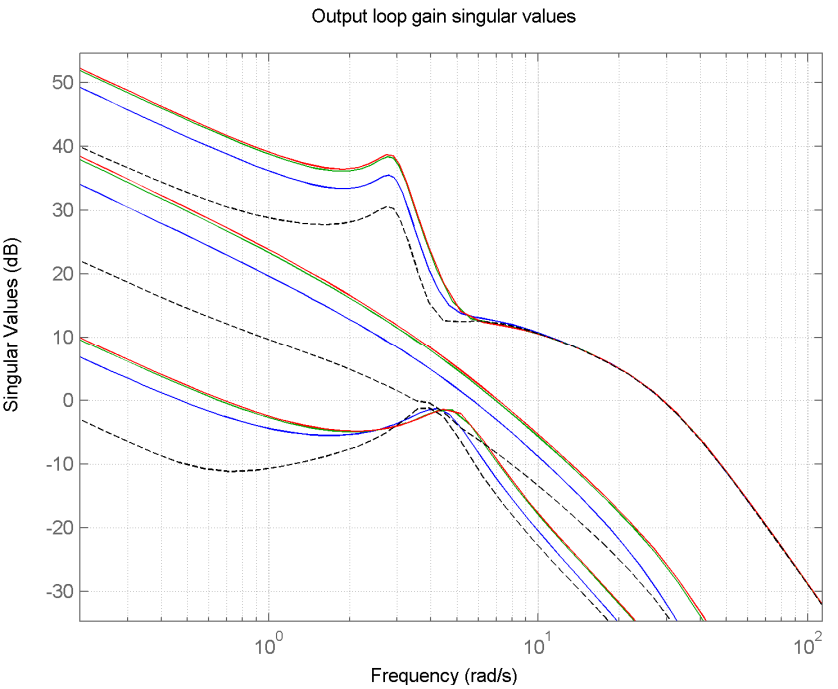

Figure 5.9 Output open-loop gain singular values for (5.6) dashed and (5.7) solid. Solid lines are L1-controllers for various T_s = [1/10, 1/100, 1/1000] s.

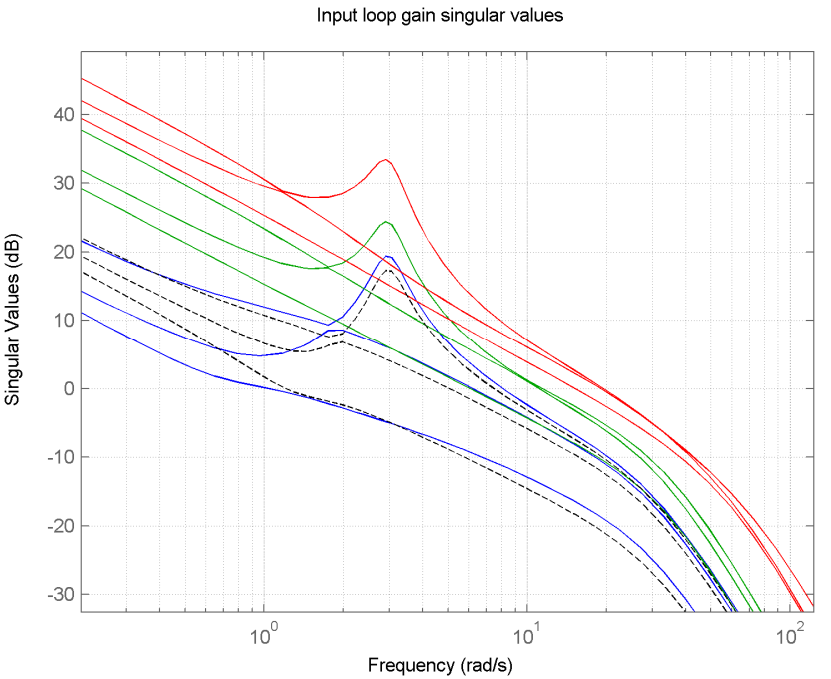

Figure 5.10 Singular values for input open-loop gain dynamics. Solid lines are L1-controllers as low-pass bandwidth is $K/10$, K and $10K$.

Comments on open-loop gain singular values diagram

When L1-control was augmented and tuned to the aircraft using Monte-Carlo simulations in Section 3.5, input open-loop unity gain crossover frequency (where the gain is unity) was generally increased (green lines compared to dashed in Figure 5.8). Also it can be noted that input open-loop gain singular values were clustered (magnitude of singular values were made equal) so that they cover a smaller interval close to the crossover frequency. This clustering of singular values can be recognized from robust linear MIMO-controller design as in [11]. With a low sampling rate (10 Hz), the collection of singular values was achieved to a lower degree (blue curves in Figure 5.8) than for higher sampling rates.

The output open-loop gain singular values of Figure 5.9 shows a moderate increase in unity gain crossover frequency for the L1-controller compared to the state feedback but there is no cluster of singular values. If the bandwidth of low-pass filters $C(s)$ were increased, which means that the diagonal elements in matrix K are increased, the crossover frequency

increases in Figure 5.10, where red curves correspond to a K ten times larger than the nominal K and blue curves are one tenth of the nominal.

Closed-loop system singular values frequency responses

Since input load disturbance attenuation and output noise gain to the control signal are interesting for an L1-controler, these frequency responses are analyzed for a roll-pitch-yaw system. The same block diagram as in Figure 5.3 is analyzed but this time for a three channel system.

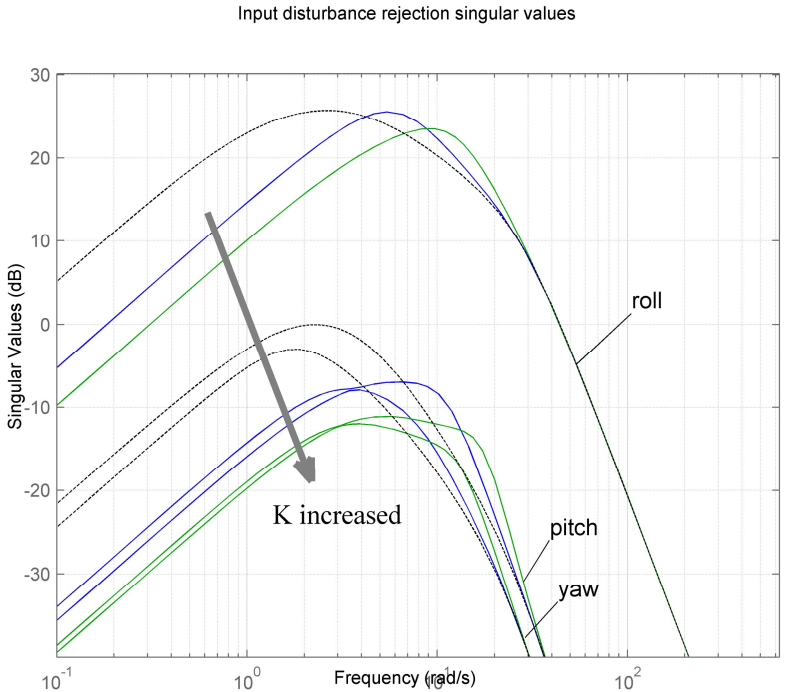

Figure 5.11 Input disturbance attenuation from σ to output y, (5.6) dashed and (5.7) solid, as low-pass filter bandwidth in (5.7) is K and $2K$.

Figure 5.11 shows how input load disturbance σ is attenuated to the output y. In Figure 5.11 one K value that results in a $C(s)$ with a bandwidth corresponding to the bandwidth that was tuned using simulations and another K that corresponds to twice that value. The input load attenuation is higher for the L1-controller than the state feedback and input load attenuation increases with K.

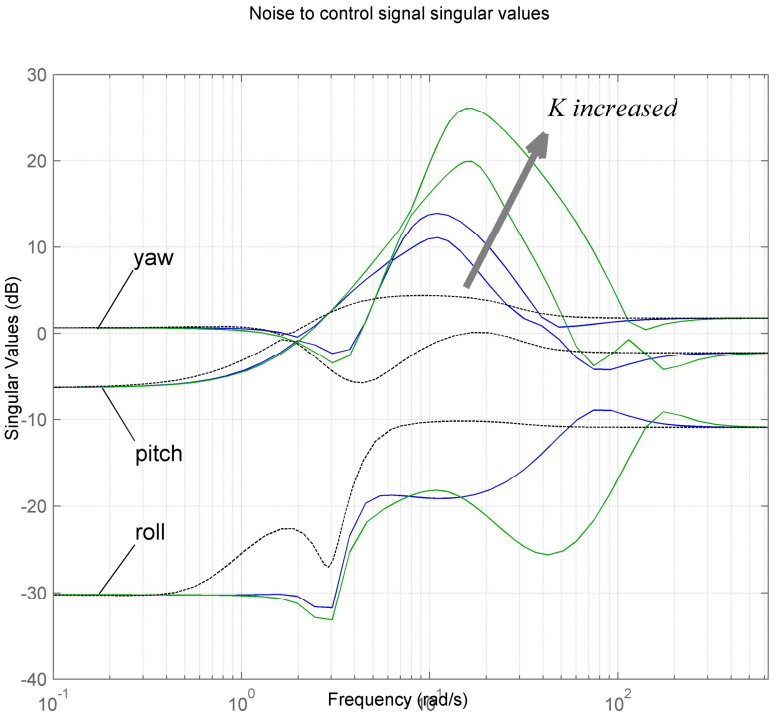

Figure 5.12 Disturbance and noise feedthrough from n to control signal u, for (5.6) dashed and (5.7) solid, as low-pass filter bandwidth in (5.7) is K and $2K$.

Figure 5.12 shows how output disturbance or measurement noise n propagates to the control signal u for the same variations as in Figure 5.11. The L1-controller feeds more noise through $C(s)$ to the control signal than the state feedback.

The choice of bandwidth K of the low-pass filter is a tradeoff between load disturbance attenuation and injection of measurement noise. A low value gives less disturbance attenuation with low noise injection. Increasing the bandwidth improves load disturbance attenuation but more measurement noise is injected causing large actuator demands. This noise injection will be damped by actuator and flight dynamics but could cause actuator wear and undesired excitation of the aircraft.

6 Discussion

Currently there is an on-going debate on the relationship among MRAC and L1 adaptive control. Robustness issues related to the input low-pass filter of L1-controllers are controversial. In this work the focus is on application of an L1-controller to aerospace products. Results from linear analysis and simulations performed in a detailed model are presented and analyzed in order to judge the suitability for aircraft and missiles. As an example, if L1-controllers should be considered as using fast *adaptation* or fast *estimation* is of less importance to industry. It is however crucial to know what to expect from L1-controllers in aeronautic applications.

Listed below are questions that were stated at the start of the project, together with answers as a piecewise constant L1-controller was augmented to a linear state feedback in an aerial vehicle:

- Could an adaptive controller replace gain scheduling or reduce number of scheduling points?

Higher robust performance will be the case so it is possible to use less scheduling points. L1-control does not identify slowly varying parameters such as airspeed and altitude separately, so there are probably better methods that identify those quantities.

- Will adaptive control increase safety by failure compensation (such as from structural damage)?

Higher robust performance will counteract damage effects to a higher degree. No estimation of physical parameters corresponding to the actual damage will be accomplished with L1-control.

- Can an adaptive control be used as a backup mode (limp home)?

Higher robust performance will increase possibility to cover a large flight envelope; Master thesis at SAAB has indicated that two controllers (cruise and landing configuration) would cover full envelope.

- Could adaptive control ”fix” performance and keep robustness in problem areas?

Depends on the problem area, high robust performance is promising. However if the problem is due to time delays, noise or actuator saturation,

L1-control would require careful design and tuning to improve the situation.

- Could rapid prototyping be addressed with adaptive control?

Not fully covered but improved results when compared to linear state feedback. Dynamics corresponding to four different aerial vehicles were tested and once the nonlinear design elements were included, it was easy to tune a controller to each configuration.

- Will Controller Clearance be easier with adaptive control?

Little advantage compared to other methods, L1-controller proofs state that an increase in low-pass filter bandwidth guarantee stability which in practice is not acceptable.

7 Conclusions and Future Work

An L1 adaptive controller of piecewise constant type was applied to a model of a fighter aircraft and results are presented from the design work when augmenting the L1-controller to a typical linear state feedback.

In the design process of an L1-controller, the desired closed-loop response is defined by a reference system dynamics and low-pass filters are tuned to balance performance and robustness. The idea of estimating input disturbances and using low-pass filtered versions of these disturbance estimates as the control signal is intuitive. In the L1-controller used in this application, a five-state reference system is designed and five parameters for first-order low-pass filters are tuned, for simultaneous roll-pitch-yaw control.

The augmentation of an L1-controller to the aerial vehicle achieves larger input disturbance attenuation than what a typical linear state feedback controller accomplishes in aeronautical applications. The L1-controller input disturbance estimation and compensation is suitable for aerial vehicles. Forces and moments disturbing the desired motion are quickly estimated and compensated for using counteracting control surface demands within the control channel bandwidth. The L1-controller input disturbance estimation and compensation in aeronautical applications focus on keeping the angular acceleration and angular velocity correct. Since angle of attack/sideslip over a short period of time is integrated angular velocity, also the control objectives will be catered to.

The L1-controller requires low-pass filters which have to be carefully tuned to balance performance and robustness to deviation that does not fit into the theory. The final choice requires manual tuning [6], systematic methods resulting in filter order and shape would be desirable. When a standard L1-controller is used to control an aerial vehicle with long periods of rate saturated actuators, it is hard to tune the controller. Including a model of the actuator, with rate limits, in the state predictor of the L1-controller makes tuning easier. This way it is possible to design physically-

based nonlinear internal models in the state predictor which will make the controller reduce effects that can be compensated for and leave other without control effort.

In this work, the implication of the sampling period in the piecewise constant L1-controller has been analyzed. To sample as fast as possible is equivalent to increasing a gain in a continuous-time equivalent to the piecewise constant L1-controller. This insight will make online controller design easier to implement in software since the sampling rate can be fixed and a parameter corresponding to a gain in the controller can be tuned. The results are similar to that of [35].

Some L1 adaptive controllers are linear time invariant as long as projection operators are inactive. Comparisons of linear L1-controllers were made to the type of internal model controller which is known as a disturbance observer. They share a lot of characteristics such that they can be seen as estimating and compensating for disturbances at the plant input by using inverse dynamics. L1-controllers focus on the desired reference dynamics while disturbance observers use the nominal plant dynamics. The use of desired reference inverses makes L1-controllers suitable for augmentation to a baseline controller.

By using the desired dynamics reference system inverse, L1-controllers accomplish both reference following and disturbance attenuation, without identifying if deviation comes from model error or an external disturbance from outside the plant. However, if the L1-controller is augmented to a feedback controller that make the plant dynamics nominally behave like the reference system dynamics (such as linear state feedback, possibly aided by feedforward from reference), better reference following is achieved since then only truly unknown factors will have to be compensated. The high gain in L1-controllers can be seen as a measure to approximate a reference system inverse better as the gain is increased.

A feedforward design that is applicable to aerial vehicles was designed and tested. It uses the nonlinear state equations and also uses the same reference system dynamics as the adaptive controllers. The created design makes it possible to apply nonlinear feedforward compensations so that linear dynamics nominally will be left to handle for the controllers.

One of the key concerns when dealing with feedforward is that nominal values of parameters need to be used. This concern comes from the circumstance that *variance* in parameters can be large. However, even though large variation around nominal values in parameters can be at hand, it is useful to incorporate the *mean* value of a parameter into the system, in

this design it is done by feedforward and variance effects will be dealt with by an adaptive controller

The method proposed here designs a structure suitable for use of adaptive control for aerial vehicles. Reference systems and feedforward signals have been tested for both fighter aircraft and missiles together with L1 adaptive control methodology. This design has the following benefits:

- Fundamentals of the flight dynamics are used to create reference systems that scale to the present conditions. This takes less effort than use of for example gain-scheduling and several controllers for combinations of airspeed and altitude.
- Feedforward and feedback that make the dynamics act like the linear reference system puts the adaptive controller in a better position of reducing truly unknown factors such as disturbances and deviations from nominal assumptions. It is a good idea to augment a baseline controller with an adaptive controller [34].

Compared to state feedback, the L1-controller augmentation increases the unity gain crossover frequency of the open-loop frequency response, thereby reducing robustness to time delays. Time delays are compensated for in this design by using prediction in a state observer. This prediction was found to be a suitable alternative to reducing bandwidths in controller low-pass filters or delaying input to the L1-controller state predictor. An L1-controller augmentation increase sensor noise gain to the control signal, in this application control signal noise levels are tolerable. Control objectives (angle of attack/sideslip) become excited by noise and since this is undesired, a state observer should be tuned to reduce this noise when used with an L1-controller.

L1-controllers of piecewise constant type have been found to add value for control of a fighter aircraft. Augmentation to a linear state feedback controller shows that nominal performance is maintained while improved robustness to perturbations is achieved. This comes at the cost of higher controller noise gain and the need for models of time delays and actuator rate limits in the controller.

For real-time implementation it is important to have understanding of the fundamental parts that are needed for exploiting L1 adaptive control benefits. Analysis of alternative equivalent structures gives options in how to implement the controller in a real-time application where it has to fit into a larger software structure. Mapping of control methods to each other also make it possible to use benefits from L1 adaptive control gradually. It will be possible to blend in design features such as a reference system inverse as a modification to standard aeronautical feedback laws. It is also

possible to gradually add nonlinearities in the state predictor. Such options could be important when compromises are needed to get clearance in use of new control designs in live aerospace products.

The L1-controller and the design rules corresponding to this thesis were tested as a feasibility study [39] for the backup mode of a SAAB fighter. The backup mode is a controller design that is used when the airspeed and altitude is unknown. It has to cover a large part of the envelope without gain-scheduling. The controller was evaluated using a pilot-in-the-loop simulated environment and using desktop simulations. The results were promising; an intended envelope was covered without any scheduling. There were issues at the low-speed boundary of the envelope, indicating that some kind of scheduling still could be required to cover the full envelope. Such an option would be use of one controller with the landing gear retracted and another for landing configuration.

The following benefits and deficiencies have been noted as an L1-controller was applied to an aerial vehicle.

Pros:

- Can be augmented to an existing controller to increase performance and robustness
- Points out a set of LTI-controllers, suitable for flying, that is not easily found by more traditional aerospace control methods
- Reference system is an intuitive design element that allows for a physical interpretation of how the controller works
- Nonlinearities corresponding to physical effects can be added so that the controller acts on relevant deviations and ignore others

Cons:

- Noise controller excitation is high, the control objective will be affected
- Sensitive to some kinds of deviation, such as rate saturation and noise
- Textbook recommendations is not suitable for real-time implementation
- Need to use some clever solutions (corresponding to e.g. actuator rate limits) outside the standard theory to get a controller that is easy to tune to aerospace application

When it comes to future work the following should be considered:

The concept of available bandwidth in the control channel is probably not fully understood. Are different bandwidths available to angular rates when compared to angles? Could better results be achieved if the L1-

controller parameter estimates are split into terms corresponding to different physical effects and a low-pass filter for each term is tuned?

An L1-controller that is augmented and tuned to give better robust performance generally increases crossover frequency in the open-loop response. Will this excite undesired structural bending modes in the aerial vehicle and become a limiting factor to the augmentation benefits?

Noise excitation from sensors and turbulence to the L1-controller output and to the control objective could limit the possible benefits. Noise reduction, both to the control signal and through the plant is needed. Are actuator wear and pilot ride comfort limiting factors in a final design of an L1-controller?

In flight applications matched signals correspond to moments that change rate and unmatched signals correspond to forces that change angles. Would it be possible to utilize this physical fact by designing an inner rate L1-controller augmented by an angle L1-controller?

Bibliography

[1] R. C. Nelson, *Flight stability and automatic control*, McGraw Hill, New York, 1998.

[2] R. F. Stengel, *Flight dynamics*, Princeton University Press, Princeton, NJ, 2004.

[3] B. Etkin, *Dynamics of atmospheric flight*, John Wiley & Sons, Inc., New York, 1972.

[4] B. L. Stevens and F. L. Lewis, *Aircraft control and simulation*, John Wiley & Sons, Inc, New York, 2003.

[5] K. J. Åström and B. Wittenmark, *Adaptive control*, Dover Publications, Inc., Mineola, 2008.

[6] N. Hovakimyan and C. Cao, *L1 Adaptive Control Theory*, SIAM, Philadelphia, 2010.

[7] T. Leman, E. Xargai, G. Dellerud, N. Hovakimyan and Thomas Wendel, "L1 adaptive control augmentation system for the X-48B aircraft", in *Proc. AIAA GNC Conference*, Chicago, IL, Aug. 2009, AIAA-2009-5619.

[8] B. D. O. Anderson and A. Dehghani, "Challenges of adaptive control – past, permanent and future", *Annual reviews in control*, 2008 32(2), pp.123-135.

[9] P. Zarchan, *Tactical and strategic missile guidance*, Fourth edition, AIAA Inc., Reston, 2002.

[10] Government publication, “Application of multivariable control theory to aircraft control laws, Multivariable control design guidelines”, Honeywell Inc., MN, 1996.

[11] D. Bates and I. Postlethwaite, *Robust Multivariable Control of Aerospace Systems*, DUP Science, Delft, 2002.

[12] O. Härkegård and T. Glad, “Vector backstepping for flight control”, in *Proc. AIAA GNC Conference*, Hilton Head, SC, Aug. 2007, AIAA-2007-6421.

[13] O. Härkegård, “Modifying L1 adaptive control for augmented angle of attack control”, in *Proc. AIAA GNC Conference*, Chicago, IL, Aug. 2009 AIAA-2009-6071.

[14] E. Kharisov, K. K. K. Kim, X. Wang and N. Hovakimyan, “Limiting Behaviour of L1 Adaptive Controllers”, in *Proc. AIAA GNC Conference*, Portland, OR, Aug. 2011, AIAA-2011-6441.

[15] K. van Heusden and G. A. Dumont, “Analysis of L1 adaptive output feedback control; equivalent LTI controllers”, in *Proc. 16th IFAC Symposium on System Identification*, pp.1472-1477, Belgium, 2012.

[16] P.J. Hacksel and S.E. Salcudean, “Estimation of Environment Forces and Rigid-Body Velocities using Observers”, *Robotics and Automation*, vol.2 pp.931-936, 1994.

[17] K. Kancko, K. Onishi and K. Komoriya, “A design method for manipulator control based on disturbance observer”, *Int. Conf. on Intelligent Robots and Systems* 2, pp.1405-1412, 1994.

[18] A. Šabanović, K. Ohnishi, *Motion Control Systems*, John Wiley & Sons (Asia) Ltd Pte, Clementi Loop, Singapore, Chapter 4: Disturbance observer, 2011.

[19] K.J. Åström and B. Wittenmark, *Computer Controlled Systems*, Prentice Hall, Upper Saddle River, 1984.

[20] M. Fliess, J. Lévine, P. Martin and P. Roughon, "A Lie-Bäcklund approach to equivalence and flatness of nonlinear systems", *IEEE Transactions on Automatic. Control*, vol. 44, no 5, May 1999, pp.922-937.

[21] V. Hagenmeyer and E. Delaleau, "Exact feedforward linearization based on differential flatness", *Int. J. Control*, Vol. 76, 2003.

[22] T. Glad and L. Ljung, *Control Theory: Multivariable and Nonlinear Methods*, Taylor & Francis, London, 2000.

[23] Z. T. Dydek, A. M. Annaswamy and E. Lavretsky, "Adaptive Control and the NASA X-15-3 Flight Revisited", *IEEE Control Systems Magazine*, vol. 30, no. 3, pp.32-48, June 2010.

[24] E. Xargai, N. Hovakimyan, V. Dobrokhodov, R.B. Statnikov, I. Kaminer, C. Cao, I. M. Gregory, "L1 Adaptive Flight Control System Systematic Design and Verification and Validation of Control Metrics", in *Proc. AIAA GNC Conference*, Toronto, Canada, Aug. 2010, AIAA-2010-7773.

[25] I. M. Gregory, E. Xargay, C. Cao, and N. Hovakimyan, "Flight test of L1 adaptive controller on the NASA AirSTAR flight test vehicle", in *Proc. AIAA GNC Conference*, Toronto, Canada, Aug. 2010, AIAA-2010-8015.

[26] F. Peter, F. Holzapfel, "L1 Adaptive Augmentation of a Missile Autopilot", in *Proc. AIAA GNC Conference*, Minneapolis, MN, Aug. 2012, AIAA-2012-4832.

[27] K.J. Åström and T. Hägglund, *Advanced PID Control*, ISA Society, Research Triangle Park, NC, 2006.

[28] P. Seiler, A. Dorobantu and G. Balas, "Robustness Analysis of an L1 Adaptive Controller", in *Proc. AIAA GNC Conference*, Minneapolis, MN, Aug. 2010, AIAA-2010-8407.

[29] N. Hovakimyan, C. Cao, E. Kharisov, E. Xargai, I. M. Gregory, "L1 Adaptive Control for Safety-Critical Systems", *IEEE Control Systems Magazine*, vol. 31, no. 5, Oct. 2011, pp. 54-104.

[30] B. J. Griffin, J. J. Burken, E. Xargai, "L1 Adaptive Control Augmentation System with Application to X-29 Lateral/Directional Dynamics: A MIMO Approach", in *Proc. AIAA GNC Conference*, Toronto, Canada, Aug. 2010, AIAA-2010-7687.

[31] G. Stein, "Respect the unstable", *IEEE Control Systems Magazine*, vol. 23, no. 4, Aug. 2003, pp.12-25.

[32] H.K. Khalil, *Nonlinear Systems*, Prentice-Hall, 3rd ed., New Jersey, 2002.

[33] M. Krstić, I. Kanellakopoulos and P. Kokotović, *Nonlinear and Adaptive Control Design*, John Wiley & Sons, New York, 1995.

[34] E. Lavretsky, K. A. Wise, *Robust and Adaptive Control with Aerospace Applications*, Springer, London, 2012.

[35] Z. Li, N. Hovakimyan, "L1 Adaptive Controller for MIMO Systems with Unmatched Uncertainties using Modified Piecewise Constant Adaptive Law", in *Proc. IEEE Conference on Decision and Control* (CDC2012), Maui, HI, Dec 2012.

[36] A. Pettersson, K. J. Åström, A. Robertsson and R. Johansson, "Augmenting L1 adaptive control of piecewise constant type to a fighter aircraft. Performance and robustness evaluation for rapid maneuvering", in *Proc. AIAA GNC Conference*, Minneapolis, MN, Aug. 2012, AIAA-2012-4757.

[37] A. Pettersson, K. J. Åström, A. Robertsson and R. Johansson, "Analysis of Linear L1 Adaptive Control Architectures for Aerospace Applications", in *Proc. IEEE Conference on Decision and Control* (CDC2012), Maui, HI, Dec 2012.

[38] A. Pettersson, K. J. Åström, A. Robertsson and R. Johansson, "Nonlinear Feedforward and Reference Systems for Adaptive Flight Control", accepted for *AIAA GNC Conference*, Boston, MA, Aug. 2013.

[39] A. Myleus, L1 adaptive control of a generic fighter aircraft, Master of Science Thesis, Royal Institute of Technology Stockholm, 2013, Report TRITA-MAT-E 2013:12.

Appendix

Nomenclature for frequently used quantities:

$\bar{v}$	body velocity vector, with vector elements u, v and w
$\bar{\omega}$	body angular velocity vector, with vector elements p, q and r
V	airspeed
α	angle of attack
β	angle of sideslip
Φ, θ, Ψ	roll, pitch and yaw Euler angles for expressing body attitude
m, I_i	mass and mass inertia tensor
$\bar{F}$, $\bar{M}$	force and moment acting on body
ρ	density of air
g	gravitational constant
p_s	static air pressure
q_d	dynamic air pressure
S, b, c	aerodynamic reference area and reference lengths
C_T, C_C, C_N	aerodynamic force coefficients in body x, y and z-axis
C_l, C_m, C_n	aerodynamic moment coefficients in body x, y and z-axis
δ_a, δ_e, δ_r	control inputs, aileron, elevator, rudder
τ_s	rise time in first-order system
ω_0	natural frequency in second-order system
ζ	damping in second-order system
A_m, B_m, C	state space matrices of the desired dynamics
L	linear state feedback gain
$H_m(s)$	desired transfer function from plant input to output
K_g	steady state inverse of desired plant input to output gain
$C(s)$	low-pass filter transfer function
$D(s)$	design factor in low-pass filter transfer function
K	low-pass filter bandwidth parameter
T_s	sampling period in piecewise constant controller
T_d	time delay in sensors and controller

Aerodynamics model used in simulations:

$$C_C = C_{C_\beta}\beta + C_{C\delta_r}\delta_r\left(1 + C_{\delta|\delta|}|\delta_r|\right) + C_{C\delta_a}\delta_a\left(1 + C_{\delta|\delta|}|\delta_a|\right)$$
$$+ \frac{b}{2V}\left(C_{C_p}p + C_{C_r}r + C_{C_{\dot\beta}}\dot\beta\right)$$
$$C_N = C_{N_0} + C_{N_\alpha}\alpha + C_{N\delta_e}\delta_e\left(1 + C_{\delta|\delta|}|\delta_e|\right) + \frac{c}{2V}\left(C_{N_q}q + C_{N_{\dot\alpha}}\dot\alpha\right)$$
$$C_l = C_{l_\beta}\beta + C_{l\delta_a}\delta_a\left(1 + C_{\delta|\delta|}|\delta_a|\right) + C_{l\delta_r}\delta_r\left(1 + C_{\delta|\delta|}|\delta_r|\right)$$
$$+ \frac{b}{2V}\left(C_{l_p}p + C_{l_r}r\right) + C_{l_{\alpha\beta}}\alpha\beta + C_{l_{\alpha|\alpha|\beta}}\alpha|\alpha|\beta$$
$$C_m = C_{m_0} + C_{m_\alpha}\alpha + C_{m\delta_e}\delta_e\left(1 + C_{\delta|\delta|}|\delta_e|\right)$$
$$+ \frac{c}{2V}\left(C_{m_q}q + C_{m_{\dot\alpha}}\dot\alpha\right) + C_{m_{\alpha|\alpha|}}\alpha|\alpha| + C_{m_{\alpha\beta}}\alpha\beta$$
$$C_n = C_{n_\beta}\beta + C_{n\delta_r}\delta_r\left(1 + C_{\delta|\delta|}|\delta_r|\right) + C_{n\delta_a}\delta_a\left(1 + C_{\delta|\delta|}|\delta_a|\right)$$
$$+ \frac{b}{2V}\left(C_{n_p}p + C_{n_r}r + C_{n_{\dot\beta}}\dot\beta\right) + C_{n_{\beta|\beta|}}\beta|\beta| + C_{n_{\alpha\beta}}\alpha\beta$$

Aircraft parameters used in controller analysis and in simulations:

Parameter	*Value*	*Unit*	*Uncertainty*
b	10	m	-
c	5	m	-
S	45	m^2	-
m	10000	kg	5%
I_x	20000	kgm^2	5%
I_y	80000	kgm^2	5%
I_z	100000	kgm^2	5%
I_{xz}	2500	kgm^2	5%
C_T	0.02	-	20%
C_{N_0}	-0.01	-	20%
C_{N_α}	3.3	-	20%
$C_{N\delta_e}$	0.5	-	20%
C_{N_q}	4	-	20%
$C_{N_{\dot\alpha}}$	2	-	20%
C_{m_0}	-0.01	-	20%
C_{m_α}	0.2	-	20%
$C_{m\delta_e}$	-0.3	-	20%
C_{m_q}	-1.8	-	20%
$C_{m_{\dot\alpha}}$	-0.6	-	20%

C_{l_β}	-0.1	-	20%
$C_{l\delta_a}$	0.2	-	20%
$C_{l\delta_r}$	0.02	-	20%
C_{l_p}	-0.3	-	20%
C_{l_r}	0.1	-	20%
C_{C_β}	0.8	-	20%
$C_{C\delta_r}$	-0.2	-	20%
$C_{C\delta_a}$	0.1	-	20%
C_{C_r}	-0.5	-	20%
$C_{C_{\dot{\beta}}}$	0.4	-	20%
C_{n_β}	0.1	-	20%
$C_{n\delta_r}$	-0.1	-	20%
$C_{n\delta_a}$	0.05	-	20%
C_{n_r}	-0.3	-	20%
C_{n_p}	-0.05	-	20%
$C_{n_{\dot{\beta}}}$	0.02	-	20%
$C_{\delta\|\delta\|}$	-0.2	-	20%
$C_{l_{\alpha\beta}}$	-1	-	20%
$C_{l_{\alpha\|\alpha\|\beta}}$	2	-	20%
$C_{m_{\alpha\|\alpha\|}}$	0.01	-	20%
$C_{m_{\alpha\beta}}$	-0.3	-	20%
$C_{n_{\beta\|\beta\|}}$	-0.01	-	20%
$C_{n_{\alpha\beta}}$	-0.1	-	20%
ω_{0a}	30	rad/s	10%
ζ_a	0.7	-	10%
δ_{max}	30	º	5%
$\dot{\delta}_{max}$	60	º/s	10%
$\ddot{\delta}_{max}$	10000	º/s^2	10%
T_d	0.02	s	10%
T_0	288.15	K	5%
p_{s_0}	10100	Pa	2%
L_H	0.0065	K/m	2%

Linear Pitch dynamics, full expressions:

Including linear aerodynamic resistance to change in angle of attack.

$$\begin{pmatrix}\dot{\alpha}\\ \dot{q}\end{pmatrix}=\begin{pmatrix}1+\frac{q_d Sc}{2mV^2}C_{N_{\dot{\alpha}}} & 0\\ -\frac{q_d Sc^2}{2I_y V}C_{m_{\dot{\alpha}}} & 1\end{pmatrix}^{-1}\left(\begin{pmatrix}-\frac{q_d S}{mV}C_{N_\alpha} & 1-\frac{q_d Sc}{2mV^2}C_{N_q}\\ \frac{q_d Sc}{I_y}C_{m_\alpha} & \frac{q_d Sc^2}{2I_y V}C_{m_q}\end{pmatrix}\begin{pmatrix}\alpha\\ q\end{pmatrix}+\begin{pmatrix}-\frac{q_d S}{mV}C_{N\delta_e}\\ \frac{q_d Sc}{I_y}C_{m\delta_e}\end{pmatrix}\delta_e\right)$$

Linear Roll-Yaw dynamics, full expressions:

Including linear aerodynamic resistance to change in angle of sideslip.

$$\begin{pmatrix}\dot{p}\\ \dot{\beta}\\ \dot{r}\end{pmatrix}=\begin{pmatrix}1 & 0 & 0\\ 0 & 1+\frac{q_d Sb}{2mV^2}C_{C_\beta} & 0\\ 0 & -\frac{q_d Sb^2}{2I_z V}C_{n_\beta} & 1\end{pmatrix}^{-1}\left(A_y\begin{pmatrix}p\\ \beta\\ r\end{pmatrix}+B_y\begin{pmatrix}\delta_a\\ \delta_r\end{pmatrix}\right)$$

State observer equations:

An observer using state space matrices as a function of airspeed and (relatively small) nonlinear elements.

$$\begin{pmatrix}\dot{\hat{\alpha}}\\ \dot{\hat{q}}\\ \dot{\hat{p}}\\ \dot{\hat{\beta}}\\ \dot{\hat{r}}\end{pmatrix}=\begin{pmatrix}A_p(V) & 0\\ 0 & A_y(V)\end{pmatrix}\begin{pmatrix}\hat{\alpha}\\ \hat{q}\\ \hat{p}\\ \hat{\beta}\\ \hat{r}\end{pmatrix}+\begin{pmatrix}B_p(V) & 0\\ 0 & B_y(V)\end{pmatrix}\begin{pmatrix}\delta_e\\ \delta_a\\ \delta_r\end{pmatrix}$$

$$+\begin{pmatrix}-(\hat{p}\cos\hat{\alpha}+\hat{r}\sin\hat{\alpha})\tan\hat{\beta}\\ \frac{I_z-I_x}{I_y}\hat{p}\hat{r}+\frac{I_{xz}}{I_y}(\hat{r}^2-\hat{p}^2)\\ \frac{I_y-I_z}{I_x}\hat{q}\hat{r}+\frac{I_{xz}(I_x-I_y+I_z)}{I_x I_z}\hat{p}\hat{q}\\ \hat{p}\sin\hat{\alpha}+\hat{r}(1-\cos\hat{\alpha})\\ \frac{I_x-I_y}{I_z}\hat{p}\hat{q}-\frac{I_{xz}(I_x-I_y+I_z)}{I_x I_z}\hat{q}\hat{r}\end{pmatrix}+K_0\left(y_m-\begin{pmatrix}\hat{\alpha}\\ \hat{q}\\ \hat{p}\\ \hat{\beta}\\ \hat{r}\end{pmatrix}\right)$$

$$\hat{y}=\begin{pmatrix}\hat{\alpha}\\ \hat{q}\\ \hat{p}\\ \hat{\beta}\\ \hat{r}\end{pmatrix}+T_d\begin{pmatrix}\dot{\hat{\alpha}}\\ \dot{\hat{q}}\\ \dot{\hat{p}}\\ \dot{\hat{\beta}}\\ \dot{\hat{r}}\end{pmatrix}$$

Terminology used:

Aerospace	Involves vehicles moving in air or space
Aeronautical	Involves vehicles flying through air
Aerial vehicle	Aircraft or Missile
Aircraft	Involves fixed winged vehicles
Missile	Slender body aerial vehicle